OFFICIAL JOURNAL OF THE SCIENTIFIC SOCIETY OF
ANATOMISTS, HISTOLOGISTS, EMBRYOLOGISTS AND
TOPOGRAPHIC ANATOMISTS OF UKRAINE

DOI: 10.31393
ISSN 1818-1295
eISSN 2616-6194

ВІСНИК МОРФОЛОГІЇ
REPORTS OF MORPHOLOGY

Vol. 28, №1, 2022

Scientific peer-reviewed journal in the fields of normal and pathological anatomy, histology, cytology and embryology, topographical anatomy and operative surgery, biomedical anthropology, ecology, molecular biology, biology of development

Published since 1993
Periodicity: 4 times a year

Vinnytsya • 2022

ВІСНИК МОРФОЛОГІЇ - REPORTS OF MORPHOLOGY

Founded by the "Scientific Society of Anatomists, Histologists, Embryologists, and Topographic Anatomists of Ukraine" and National Pyrogov Memorial Medical University, Vinnytsya in 1993

Certificate of state registration КВ №9310 from 02.11.2004

Professional scientific publication of Ukraine in the field of medical sciences in specialties 221, 222, 228, 229
According to the list of professional scientific publications of Ukraine, approved by the order of the Ministry of Education and Science of Ukraine No. 1188 of 24.09.2020
Professional scientific publication of Ukraine in the field of biological sciences in specialty 091
According to the list of professional scientific publications of Ukraine, approved by the order of the Ministry of Education and Science of Ukraine No. 1471 of 26.11.2020

Approved by the Academic Council of National Pyrogov Memorial Medical University, Vinnytsya, protocol №5 from 27.01.2022.

Indexation: CrossRef, Index Copernicus, Google Schoolar Metrics, National Library of Ukraine Vernadsky

Address editors and publisher:
Pyrogov Str. 56,
Vinnytsya, Ukraine - 21018
Tel.: +38 (0432) 553959
E-mail: nila@vnmu.edu.ua

Computer page-proofs - Klopotovska L.O.
Translator - Gunas V.I.
Technical support - Levenchuk S.S., Parashuk O.I.
Scientific editing - editorship

The site of the magazine - https://morphology-journal.com

CONTENT

DOI: 10.31393/morphology-journal-2022-28(1)-01 Reports of Morphology, Vol. 28, №1, Pages 5-10

ISSN 1818-1295 eISSN 2616-6194

REPORTS OF MORPHOLOGY

Official Journal of the Scientific Society of Anatomists, Histologists, Embryologists and Topographic Anatomists of Ukraine

journal homepage: https://morphology-journal.com

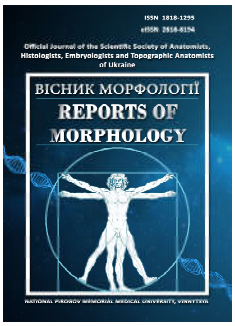

The role of neutrophilic granulocytes in the development of acute lung injury in experimental diabetes mellitus

Zaiats L.M., Fedorchenko Yu.V.
Ivano-Frankivsk National Medical University, Ivano-Frankivsk, Ukraine

ARTICLE INFO
Received: 3 November 2021
Accepted: 15 December 2021

UDC: 616.24+616.092.9+616.379-008.64

CORRESPONDING AUTHOR
e-mail: patfisiology@ifnmu.edu.ua
Zaiats L.M.

CONFLICT OF INTEREST
The authors have no conflicts of interest to declare.

FUNDING
Not applicable.

Diabetes mellitus takes one of the first places in the structure of endocrine diseases. Among the complications of diabetes are sufficiently described nephro- and retinopathy, neuropathy, damage to the cardiovascular system. However, changes in the respiratory system and, in particular, the state of the endothelium of the pulmonary hemocapillaries and the morphofunctional state of neutrophilic granulocytes remain poorly understood. The aim of this study was to determine the role of neutrophilic granulocytes in the pathogenesis of acute lung injury in experimental diabetes mellitus. The experiments were performed on 88 white male Wistar rats weighing 170-210 g. The animals were divided into three groups: 1 - intact (n=10); 2 - control (n=40); 3 - experimental (n=38) with a model of diabetes mellitus, which was reproduced by intraperitoneal administration of streptozotocin company "Sigma" (USA), diluted in 0.1 M citrate buffer with pH 4.5, at a rate of 60 mg/kg body weight. An equivalent dose of 0.1 M citrate buffer solution with a pH of 4.5 was intraperitoneally administered to the control group of animals. Pulmonary tissue collection for electron microscopic examination was performed under thiopental anesthesia 14, 28, 42, 70 days after streptozotocin administration. Pieces of lung tissue were fixed in 2.5% glutaraldehyde solution, followed by fixation in 1% osmium tetroxide solution. After dehydration, the material was poured into epon-araldite. Sections obtained on an ultramicrotome "Tesla BS-490" were studied in an electron microscope "PEM-125K". It was found that in the early stages of diabetes mellitus (14-28 days) there is a violation of the rheological properties of blood, as evidenced by erythrocyte aggregates, excessive accumulation of neutrophils, their adhesion and aggregation in the hemocapillaries of the alveolar wall. With the extension of the experiment (42-70 days) there is a progressive violation of the ultrastructural organization of hemocapillaries of the alveolar wall and pronounced changes in the rheological properties of blood. Erythrocyte sludges and leuco-platelet aggregates are determined in the lumen of microvessels. Increased permeability of hemocapillaries of the alveolar wall leads to the emigration of neutrophilic granulocytes into the interstitium and the lumen of the alveoli with the development of interstitial and intraalveolar edema. Thus, streptozotocin-induced diabetes is accompanied by the development of acute lung damage in the pathogenesis of which the leading role belongs to neutrophilic granulocytes. The nature and severity of changes in the lungs depends on the duration of exposure to hyperglycemia.

Keywords: *neutrophilic granulocytes, hemocapillaries, lungs, diabetes mellitus.*

Introduction

Today, diabetes mellitus (DM) occupies one of the first places in the structure of endocrine diseases [4, 18]. According to the scientific literature in recent years, there has been a steady increase in the number of patients with diabetes [1, 8, 22, 23, 27]. According to the WHO, by 2030 the number of patients with diabetes will reach 438 million (6-8% of the adult population), with more than 90% are people with type 2 diabetes [7, 15]. The severity of this problem is determined not only by the significant prevalence of diabetes in the population, but also the rapid development of complications that lead to reduced quality of life, early disability and premature death [10, 21, 24]. According to literature sources, among the complications of diabetes today are sufficiently described nephro- and

retinopathy, neuropathy, as well as damage to the cardiovascular system [2, 5, 9, 19, 27]. However, one of the little-studied aspects of modern diabetology is changes in the respiratory system. There is now growing evidence that the lungs are one of the target organs for diabetic microangiopathy in patients with diabetes, as they have a huge, well-developed microvascular network [20, 30].

Experimental and clinical studies indicate that the development of acute lung injury (ALI) due to pathogenic factors is damage to the endothelium of pulmonary hemocapillaries, alveolar epithelium and pronounced changes in the functional state of neutrophilic granulocytes (NG) [6, 11, 13, 14, 25].

The aim of the study: to determine the role of neutrophilic granulocytes in the pathogenesis of acute lung injury in experimental diabetes mellitus.

Materials and methods

The experiments were performed on 88 white male Wistar rats weighing 170-210 g, which were kept on a standard diet with free access to water. Animals were divided into three groups: 1 - intact (n=10); 2 - control (n=40); 3 - experimental (n=38) with a model of diabetes mellitus, which was reproduced by intraperitoneal administration of streptozotocin company "Sigma" (USA), diluted in 0.1 M citrate buffer with pH 4.5, at a rate of 60 mg/kg body weight. An equivalent dose of 0.1 M citrate buffer solution with a pH of 4.5 was intraperitoneally administered to the control group of animals.

Pulmonary tissue collection for electron microscopic examination was performed under thiopental anesthesia 14, 28, 42, 70 days after streptozotocin administration. Pieces of lung tissue were fixed in 2.5% glutaraldehyde solution, followed by fixation in 1% osmium tetroxide solution. After dehydration, the material was poured into epon-araldite. Sections obtained on an ultramicrotome "Tesla BS-490" were studied in an electron microscope "PEM-125K". All studies were performed under thiopentalone sodium analgesia at a rate of 60 mg/kg body weight.

Animal husbandry and research were conducted in accordance with the provisions of the "European Convention for the Protection of Vertebrate Animals Used for Experimental and Other Scientific Purposes" (Strasbourg, 1986), the Law of Ukraine on the "Protection of Animals from Cruelty" (2006) and the "General Ethical Principles of Experiments on animals" approved by the Fifth National Congress on Bioethics (Kyiv, 2013). **The Commission on Bioethics** of Ivano-Frankivsk National Medical University believes that the research does not contradict the basic bioethical standards (Minutes № 106/19 of 07.02.2019).

Results

Analysis of the results of ultrastructural studies showed that 14 days after modeling of streptozotocin diabetes mellitus in some hemocapillaries of the alveolar wall there

Fig. 1. Adhesion of neutrophilic granulocytes to the endothelium of the hemocapillary wall of the alveoli 14 days after the start of the experiment. 1 - neutrophilic granulocyte; 2 - lumen of the alveoli. Electronic microphotography. x8000.

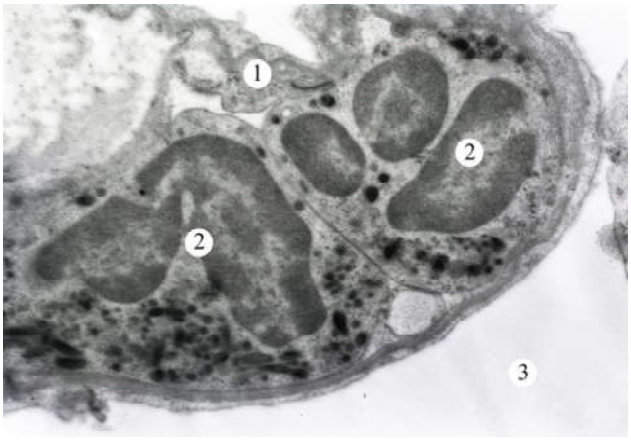

Fig. 2. Adhesion and aggregation of neutrophilic granulocytes in the hemocapillaries of the interalveolar septum 28 days after the start of the experiment. 1 - peripheral part of the endothelial cell; 2 - neutrophilic granulocyte; 3 - lumen of the alveoli. Electronic microphotography x6400.

are erythrocyte aggregates and adhesion of NG (Fig. 1). The nuclei of endothelial cells of such hemocapillaries with a matrix of low electron-optical density and contain marginally located chromatin. The perinuclear space is expanded. Mitochondria are enlarged in size with disoriented cristae. Tanks and tubules of the Golgi apparatus (GA) and granular endoplasmic reticulum (GER) are expanded with weakly osmophilic content inside. However, it should be noted that at this stage of the experiment the submicroscopic structure of many hemocapillaries does not differ from the ultrastructural organization of hemocapillaries of intact animals. Nuclei of endothelial cells of oval shape with a matrix of medium electron-optical density. The nucleolemma has wavy contours and forms shallow intussusception. In the cytoplasm of cells are mainly found mitochondria with a matrix of moderate electron-optical density. In the perinuclear zone, GA is visualized, represented by flattened

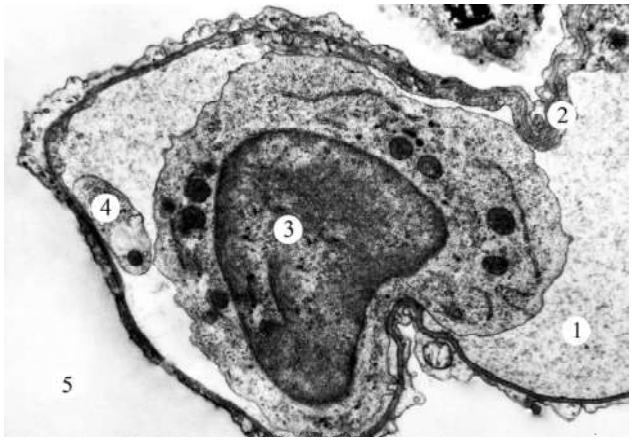

Fig. 3. Ultrastructural manifestations of adhesion and aggregation of neutrophilic granulocytes and platelets in hemocapillaries of the alveolar wall 42 days after the start of the experiment. 1 - hemocapillary lumen; 2 - peripheral part of the endothelial cell; 3 - neutrophilic granulocyte; 4 - platelet; 5 - lumen of the alveoli. Electronic microphotography. x6400.

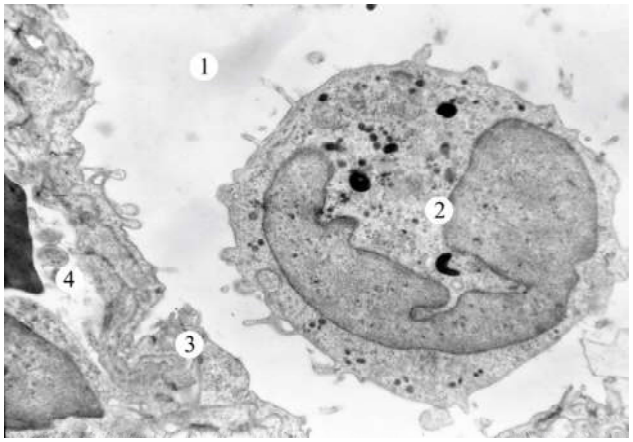

Fig. 4. Submicroscopic changes of the respiratory lungs 70 days after the start of the experiment. 1 - lumen of the alveoli; 2 - neutrophilic granulocyte; 3 - peripheral part of the endothelial cell; 4 - lumen of the hemocapillary. Electronic microphotography. x6400.

tanks and bubbles. GER channels are slightly expanded. Well-defined ribosomes are observed on the outer surface of GER membranes. An increased number of micropinocytic vesicles is detected in the peripheral parts of endotheliocytes. In some hemocapillaries on a lumenal plasmalemma separate microvilli are observed. Basal membrane in most hemocapillaries without significant structural changes. interndothelial junctions are preserved.

28 days after the start of the experiment in the lumen of the hemocapillaries of the alveolar wall there is an increased amount of NG, their adhesion and aggregation (Fig. 2).

Nuclei of some endothelial cells with a matrix of low electron-optical density and marginal localization of chromatin granules. Mitochondria of various sizes and shapes with an enlightened matrix and single crystals. The constituent components of GA and GER are expanded. In the peripheral parts of endotheliocytes, a large number of micropinocytic vesicles and vacuoles are detected, which are localized along both the lumenal and basal edges of the cytoplasm. The basement membrane is unevenly thickened.

In 42 days from the beginning of modeling of a diabetes mellitus in a lumen of hemocapillaries of an alveolar wall besides adhesion and aggregation of NG thrombo-leukocyte aggregates are noted (Fig. 3). However, it should be noted the presence in the hemocapillaries of individual neutrophils with devastated azurophilic granules. The nuclei of endothelial cells are enlarged in size with a matrix of low electron-optical density. Chromatin granules are placed along the inner surface of the nucleolemma or grouped into individual lumps. The perinuclear space is expanded. Destruction of cristae is observed in mitochondria. GA is represented by expanded tanks and vacuoles. GER tubules in many endotheliocytes are vacuolated and fragmented with a reduced number of ribosomes on the membranes of the latter. The basement membrane is in most cases of low electron-optical density. In some endotheliocytes on the lumenal surface of the plasmalemma its fan-shaped protrusions are observed.

With increasing duration of the study (70 days) there is a progressive violation of the ultrastructural organization of hemocapillaries of the alveolar wall. Characteristic of this stage of the study is the presence in the lumen of hemocapillaries adhesion and aggregation of leukocytes and platelets, erythrocyte aggregates and degranulated NG. As a result of endothelial edema and aggregation of blood cells, the lumen of some hemocapillaries is closed or sharply narrowed. In some hemocapillaries there are violations of the integrity of the lumenal membrane of endothelial cells, and sometimes their desquamation into the lumen of microvessels with the exposure of the basement membrane. The basement membrane of hemocapillaries is thickened for a long time with fuzzy contours. Interstitial tissue of interalveolar septa is expanded due to edema and infiltration of NG. At this stage of the study there is also a violation of interendothelial contacts, which leads to the release of NG into the interstitial tissue and alveoli (Fig. 4) with the development of interstitial and intraalveolar edema.

Discussion

The results of the study showed that in the early period of development of streptozotocin diabetes (14-28 days) in the hemocapillaries of the alveolar wall there is a violation of the rheological properties of blood, as indicated by excessive accumulation of NG, their aggregation and adhesion. According to the literature [14], the increased number of neutrophils in the pulmonary hemocapillaries is a key link in the development of inflammation in the lung tissue. It is proved that the adhesive property of NG increases under the action of inflammatory mediators [29]. In this case, endothelial cells produce leukocyte adhesion

molecules (ELAM, VCAM, ICAM-1), which function as specific receptors for polymorphonuclear leukocytes. However, not only has the endothelium promoted increased cell adhesion, but leukocytes and platelets also show increased surface expression of proteins such as the integrin CD11b/CD18, which act as binding proteins for molecule adhesion [30]. The interaction of ICAM-1 and CD11b/CD18 has been shown to play an important role in the accumulation of NG in the lungs. Adhesion of leukocytes to the endothelium is the cause of the formation and release of oxygen radicals, secretory degranulation (proteases, lysosomal polycationic proteins), which have a direct damaging effect on endothelial cells [9]. The devastation of NG granules, especially azurophilic, took place in our studies for 42-70 days of the experiment.

According to electron microscopic studies, a characteristic feature of neutrophils is the presence of cytoplasmic granules. According to the literature, there are three types of granules: primary or azurophilic, secondary or specific, and tertiary or secretory vesicles [3, 28]. Azurophilic granules are electronically dense and larger in size. They contain acid hydrolases, cathepsin C, bactericidal proteins (defensins, sergocidins, catemicidins), myeloperoxidase and neutrophil elastase. The latter can directly destroy the interndothelial junctions, breaking down surface proteins, which leads to increased vascular permeability [17, 25, 28]. Increased permeability of the endothelium of hemocapillaries of the alveolar wall is accompanied by the release of NG into the interstitium and lumen of the alveoli. Emigration of neutrophilic granulocytes into the lumen of the alveoli was observed by us on the 42-70th day of the experiment. The results of our studies are consistent with the data of a number of authors who indicate the important role of activated NG in the development of ALI in other pathological conditions [12, 14, 16, 26, 31].

Conclusion

1. Streptozotocin-induced diabetes is accompanied by the development of acute lung damage in the pathogenesis of which the leading role belongs to neutrophilic granulocytes.

2. The nature and severity of changes depends on the duration of exposure to hyperglycemia.

References

[1] Bingyan, C., Rui, L., Huanhuan, T., Yanjia, M., Xiaogang, H., Ning, J., & Yueying, W. (2016). Effect on glycemia in rats with type 2 diabetes induced by streptozotocin: low-frequency electro-pulse needling stimulated Weiwanxiashu (EX-B 3) and Zusanli (ST 36). *Journal of Traditional Chinese Medicine,* 6(36), 768-778. doi: 10.1016/s0254-6272(17)30013-4

[2] Blyshchak, N.B. (2012). Діабетичні ангіопатії [Diabetic angiopathy]. *Клінічна анатомія та оперативна хірургія - Clinical Anatomy and Operative Surgery*, 2(11), 74-77.

[3] Borregaard, N. (2010). Neutrophils, from marrow to microbes. *Immunity,* 5(33), 657-670. doi: 10.1016/j.immuni.2010.11.011

[4] Bukhtiiarova, I.P., Shchokina, K.H., Drohovoz, S.M., & Ishchenko, O.M. (2015). Антиоксидантна дія ралейкіну на моделі стрептозотоцинового діабету в щурів [Antioxidant effect of raleukin in a model of streptozotocin diabetes in rats]. *Фармакологія та лікарська токсикологія - Pharmacology and Drug Toxicology,* 6(46), 47-52.

[5] Cameron, F.J., & Wherrett, D.K. (2015). Care of diabetes in children and adolescents: controversies, changes, and consensus. *The Lancet,* 385(9982), 2096-2106. doi: 10.1016/S0140-6736(15)60971-0

[6] Hloba, Ye.V., Zelinska, N.B., & Shevchenko, I.Yu. (2017). Моногенний діабет в Україні: гени, фенотип, лікування [Monogenic diabetes in Ukraine: genes, phenotype, treatment]. *Клінічна ендокринологія та ендокринна хірургія - Clinical Endocrinology and Endocrine Surgery,* 3(59), 41-49.

[7] Ivankiv, Y.I., Oleshchuk, O.M., Dacko, T.V., & Fedoniuk, L.Y. (2016). Особливості показників прооксидантно-антиоксидантного гомеостазу, вуглеводного обміну та морфологічні зміни печінки за умов введення мелатоніну при експериментальному діабеті 2 типу [Features of indicators of prooxidant-antioxidant homeostasis, carbohydrate metabolism and morphological changes of the liver under the conditions of melatonin administration in experimental type 2 diabetes]. *Вісник морфології - Reports of Morphology,* 2(22), 253-258.

[8] Khromov, O.S., Dobrelia, N.V., Parshikov, O.V., & Boytsova, L.V. (2020). Influence of type 2 diabetes mellitus on the development of hypoxic pulmonary vasoconstriction. *Фармакологія та лікарська токсикологія - Pharmacology and Drug Toxicology,* 14(5), 324-336. doi: 10.33250/14.05.324

[9] Liu, Q., Wang, S., & Cai, L. (2014). Diabetic cardiomyopathy and its mechanisms: role of oxidative stress and damage. *Journal of Diabetes Investigation,* 5(6), 623-634. doi: 10.1111/jdi.12250

[10] Lukashevych, P.Yu., Orlenko, V.L., & Tronko, M.D. (2017). Сучасні підходи до забезпечення цукрознижувальною терапією хворих на цукровий діабет в Україні [Modern approaches to providing antidiabetic therapy to patients with diabetes in Ukraine]. *Ендокринологія - Endocrinology,* 1(22), 45-50.

[11] Marushchak, M.I. (2012). Встановлення кореляційних зв'язків між рівнем активних форм кисню, вмістом нейтрофільних гранулоцитів та газовим складом крові при експериментальному гострому ураженні легень [Establishing correlations between the level of reactive oxygen species, the content of neutrophilic granulocytes and blood gas composition in experimental acute lung injury]. *Науковий вісник Ужгородського університету, серія "Медицина" - Scientific Bulletin of Uzhgorod University, series "Medicine"*, 1(43), 9-12.

[12] Muzdubaeva, B.T. (2016). Патогенез острого респираторного дистресс-синдрома при сепсисе [Pathogenesis of acute respiratory distress syndrome in sepsis]. *Вестник Казахского Национального медицинского университета - Bulletin of the Kazakh National Medical University,* (1), 49-50.

[13] Orel, Yu.M. (2015). Участь нейтрофільних гранулоцитів у розвитку морфологічних змін у легенях при гострому їх пошкодженні в експерименті [Participation of neutrophilic granulocytes in the development of morphological changes in the lungs with acute damage in the experiment]. *Шпитальна хірургія. Журнал імені ЛЯ Ковльчука - Hospital Surgery. Magazine named after L.Ya.Kovlchuk,* (1), 43-45.

[14] Perl, M., Hohmann, C., Denk, S., Kellermann, P., Lu, D., Braumuller,

S., ... Huber-Lang, M.S. (2012). Role of activated neutrophils in chest trauma-induced septic acute lung injury. *Shock,* 38(1), 98-106. doi: 10.1097/SHK.0b013e31825be6a

[15] Polozova, L.G. (2013). Терапия сахарного диабета 2-го типа: эффективность, доказанная временем [Therapy for type 2 diabetes mellitus: time-proven effectiveness]. *Международный эндокринологический журнал - International Journal of Endocrinology,* 4(52), 57-62.

[16] Robb, C.T., Regan, K.H., Dorward, D.A., & Rossi, A.G. (2016). Key mechanisms governing resolution of lung inflammation. In: *Seminars in Immunopathology,* 38(4), 425-448. Springer Berlin Heidelberg. doi: 10.1007/s00281-016-0560-6

[17] Roychaudhuri, R., Hergrueter, A.H., Polverino, F., Laucho-Contreras, M.E., Gupta, K., Borregaard, N., & Owen, C.A. (2014). ADAM9 is a novel product of polymorphonuclear neutrophils: regulation of expression and contributions to extracellular matrix protein degradation during acute lung injury. *The Journal of Immunology,* 193(5), 2469-2482. doi: 10.4049/jimmunol.1303370

[18] Shchegol, I.M. (2019). Цукровий діабет [Diabetes]. *Медсестринство - Nursing,* (1), 52-54. doi: 10.11603/2411-1597.2019.1.9989

[19] Sohuiko, Yu.R., Lohash, M.V., Sohuiko, R.R., & Vilkhova, O.V. (2015). Основні молекулярні механізми розвитку діабетичних ускладнень [The main molecular mechanisms of diabetic complications]. *Світ медицини та біології - World of Medicine and Biology*, 2(49), 217-219.

[20] Sudy, R., Schranc, A., Fodor, G.H., Tolnai, J., Babik, B., & Petek, F. (2020). Lung volume dependence of respiratory function in rodent models of diabetes mellitus. *Respiratory Research,* 21(1), 1-12. doi: 10.1186/s12931-020-01334-y

[21] Sytnyk, I.M., & Khaitovych, M.V. (2015). Застосування антиоксидантів за цукрового діабету I типу [The use of antioxidants in type I diabetes]. *Фармакологія та лікарська токсикологія - Pharmacology and Drug Toxicology*, 6(46), 3-11.

[22] Tkachenko, V.I. (2014). Аналіз поширеності та захворюваності на цукровий діабет серед населення світу та України за 2003-2013 рр. [Analysis of the prevalence and incidence of diabetes among the population of the world and Ukraine for 2003-2013]. *Ліки України - Medicines of Ukraine,* 4(21), 55-59.

[23] Tkachenko, V.I., Vydyborets, N.V., & Kovalenko, O.F. (2014). Аналіз поширеності та захворюваності на цукровий діабет і його ускладнення серед населення України та у Київській області за 2004-2013 рр. [Analysis of the prevalence and incidence of diabetes and its complications among the population of Ukraine and in Kyiv region for 2004-2013]. *Здобутки клінічної і експериментальної медицини - Achievements of Clinical and Experimental Medicine*, (2), 177-182.

[24] Tsytovskyi, M.N. (2017). Статистичний, клінічний та морфологічний аспекти впливу цукрового діабету на стан серцево-судинної системи [Statistical, clinical and morphological aspects of the impact of diabetes on the state of the cardiovascular system]. *Науковий вісник Ужгородського університету, серія "Медицина" - Scientific Bulletin of Uzhgorod University, series "Medicine",* 1(55), 168-176.

[25] Wen, Z., Fan, L., Li, Y., Zou, Z., Scott, M.J., Xiao, G., ... Fan, J. (2014). Neutrophils counteract autophagy-mediated anti-inflammatory mechanisms in alveolar macrophage: role in posthemorrhagic shock acute lung inflammation. *The Journal of Immunology,* 193(9), 4623-4633. doi: 10.4049/jimmunol.1400899

[26] Whitsett, J.A., & Weaver, T.E. (2015). Alveolar development and disease. *American Journal of Respiratory Cell and Molecular Biology,* 53(1), 1-7. doi: 10.1165/rcmb.2015-0125PS

[27] Zahaiko, A.L., Briukhanova, T.O., & Shkapo, A.I. (2015). Модулюючий вплив сибутраміну на зміни метаболізму, зумовлені експериментальною інсулінорезистентністю в щурів [Modulating effect of sibutramine on metabolic changes due to experimental insulin resistance in rats]. *Фармакологія та лікарська токсикологія - Pharmacology and Drug Toxicology,* 3(44), 62-69.

[28] Zak, K.P. (2016). Роль нейтрофильных лейкоцитов в патогенезе сахарного диабета 1-го типа у человека (аналитический обзор с включением собственных данных) [The role of neutrophilic leukocytes in the pathogenesis of type 1 diabetes mellitus in humans (analytical review including own data)]. *Международный эндокринологический журнал - International Journal of Endocrinology,* 2(74), 130-139.

[29] Zemans, R.L., Colgan, S.P., & Downey, G.P. (2009). Transepithelial migration of neutrophils: mechanisms and implications for acute lung injury. *American Journal of Respiratory Cell and Molecular Biology,* 40(5), 519-535. doi: 10.1165/rcmb.2008-0348TR

[30] Zheng, H., Wu, J., Jin, Z., & Yan, L.J. (2017). Potential biochemical mechanisms of lung injury in diabetes. *Aging and Disease,* 8(1), 7-16. doi: 10.14336/AD.2016.0627

[31] Zordynova, K.A., Sadykova, Sh.S., Sailanova, D.K., Hulamova, H.M., Kudabaev, E.Sh., & Zhanaev, A.Zh. (2017). Современная диагностика и терапия острого респираторного дистресс синдрома у взрослых [Modern diagnostics and therapy of acute respiratory distress syndrome in adults]. *Вестник Казахского Национального медицинского университета - Bulletin of the Kazakh National Medical University,* (2), 31-37.

РОЛЬ НЕЙТРОФІЛЬНИХ ГРАНУЛОЦИТІВ У РОЗВИТКУ ГОСТРОГО УШКОДЖЕННЯ ЛЕГЕНЬ ПРИ ЕКСПЕРИМЕНТАЛЬНОМУ ЦУКРОВОМУ ДІАБЕТІ

Заяць Л.М., Федорченко Ю.В.

Цукровий діабет займає одне із перших місць у структурі ендокринних захворювань. Серед ускладнень цукрового діабету достатньо описані нефро- та ретинопатії, нейропатії, ушкодження серцево-судинної системи. Проте, маловивченими залишаються зміни зі сторони респіраторної системи і, зокрема, стану ендотелію легеневих гемокапілярів і морфофункціонального стану нейтрофільних гранулоцитів. Мета роботи - з'ясувати роль нейтрофільних гранулоцитів крові у патогенезі гострого ушкодження легень при експериментальному цукровому діабеті. Експерименти виконані на 88 білих щурах-самцях лінії Вістар масою 170-210 г. Тварини були розділені на три групи: 1 - інтактна (n=10); 2 - контрольна (n=40); 3 - експериментальна (n=38) з моделлю цукрового діабету, котрий відтворювали шляхом внутрішньоочеревинного введення стрептозотоцину фірми "Sigma" (США), розведеного в 0,1 М цитратному буфері з pH 4,5, із розрахунку 60 мг/кг маси тіла. Контрольній групі тварин внутрішньоочеревинно вводили еквівалентну дозу 0,1 М цитратного буферного розчину з pH 4,5. Забір легеневої тканини для електронно-мікроскопічного дослідження проводили під тіопенталовим наркозом через 14, 28, 42, 70 діб після введення стрептозотоцину. Шматочки легеневої тканини фіксували у 2,5% розчині

глютаральдегіду з подальшою дофіксацією в 1% розчині чотириокису осмію. Після дегідратації матеріал заливали в епон-аралдіт. Зрізи, отримані на ультрамікротомі "Tesla BS-490", вивчали в електронному мікроскопі "ПЕМ-125К". Встановлено, що вже у ранні терміни розвитку цукрового діабету (14-28 діб) спостерігається порушення реологічних властивостей крові, про що свідчать еритроцитарні агрегати, надмірна акумуляція нейтрофільних гранулоцитів, їх адгезія та агрегація в гемокапілярах альвеолярної стінки. Із продовженням терміну експерименту (42-70 діб) відмічається прогресуюче порушення ультраструктурної організації гемокапілярів стінки альвеоли та виражені зміни реологічних властивостей крові. У просвіті мікросудин визначаються еритроцитарні сладжі та лейкотромбоцитарні агрегати. Збільшення проникності гемокапілярів стінки альвеоли призводить до еміграції нейтрофільних гранулоцитів до інтерстицію й просвіту альвеоли з подальшим розвитком інтерстиційного та внутрішньоальвеолярного набряків. Таким чином, стрептозотоциніндукований діабет супроводжується розвитком гострого ушкодження легень у патогенезі котрого провідна роль належить нейтрофільним гранулоцитам крові. Характер і вираженість змін у легенях залежить від тривалості впливу гіперглікемії.

Ключові слова: *нейтрофільні гранулоцити, гемокапіляри, легені, цукровий діабет.*

DOI: 10.31393/morphology-journal-2022-28(1)-02 Reports of Morphology, Vol. 28, №1, Pages 11-16

ISSN 1818-1295 eISSN 2616-6194

REPORTS OF MORPHOLOGY

Official Journal of the Scientific Society of Anatomists, Histologists, Embryologists and Topographic Anatomists of Ukraine

journal homepage: https://morphology-journal.com

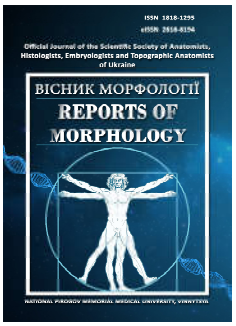

Discriminant models of possibilities occurrence and features of the course of different forms of eczema in men depending on the characteristics of anthropometric indicators

Al-Omary Ala'a Osama Ahmad[1], Vadzyuk S. N.[2], Shkolnikov V. S.[1], Prokopenko S. V.[1], Gunas I. V.[1]

[1]National Pirogov Memorial Medical University, Vinnytsya, Ukraine
[2]I. Horbachevsky Ternopil National Medical University, Ternopil, Ukraine

ARTICLE INFO
Received: 11 November 2021
Accepted: 17 December 2021

UDC: 616.521-07:616-071.2+159.922

CORRESPONDING AUTHOR
e-mail: alaaalomari33@yahoo.com
Al-Omary Ala'a Osama Ahmad

CONFLICT OF INTEREST
The authors have no conflicts of interest to declare.

FUNDING
Not applicable.

Eczema is a skin disease with a multifaceted clinical picture, numerous forms of manifestation and course and, last but not least, a life-modifying pathology that often requires lifestyle changes and reduces its quality. Identifying prognostic signs to predict the occurrence and severity of this disease is a priority for modern science. The purpose of the study is to build and analyze discriminant models of the possibility of occurrence and features of course of different forms of eczema in Ukrainian men of the first mature age depending on the characteristics of anthropometric parameters of the body. For men aged 22 to 35 years with true (n=34, including 16 mild and 18 severe) and microbial (n=38, including 28 mild and 10 severe) eczema, anthropometric examination according to the scheme of Bunak V.V. performed. Diagnosis of eczema was performed according to the nomenclature of ICD-10. The control group according to anthropometric data consisted of 82 practically healthy men of the same age, who were selected from the database of the research center of National Pirogov Memorial Medical University, Vinnytsya. Construction of discriminant models of the possibility of occurrence and features of the course of different forms of eczema depending on the anthropometric parameters of the body was carried out in the license package "Statistica 5.5". It was found that the distribution of sick men on the truth of mild and severe eczema and microbial eczema of mild and severe course is possible only reliable interpretation of the obtained classification indicators between healthy and groups of patients (correct function in 76.0% of cases, statistics Wilks' Lambda = 0.074); when dividing sick men only into truth and microbial eczema - a reliable interpretation of the obtained classification indicators both between healthy and sick, and between sick truth and microbial eczema is possible (function is correct in 87.7% of cases, Wilks' Lambda statistics = 0.088); in the distribution of sick men only for mild or severe eczema - possible reliable interpretation of the obtained classification indicators between healthy and sick men, and between patients with mild or severe eczema only a slight tendency to interpret the obtained classification indicators (correct function in 84.4% of cases, statistics Wilks' Lambda = 0.088). In all cases, the constructed discriminant equations most often include the thickness of skin and fat folds (62.5%, 57.1% and 71.4%, respectively) and body diameters (37.5%, 42.9% and 28.6%, respectively). The obtained results confirm the prospects of using anthropometric research methods to predict the possibilities and features of eczema course and occurrence.

Keywords: *eczema, anthropometric body parameters, discriminant analysis, men.*

Introduction

Eczema, or atopic dermatitis, is a disease that has plagued mankind for a long time. From the point of view of dermatology, it is a chronic inflammatory skin disease that has a recurrent nature and manifests itself in the form of various elements of the rash with severe itching. Quite often this disease is associated with allergic rhinitis and asthma (known as the atopic triad) [22].

However, despite the seemingly simple clinic, eczema is the product of a complex of interaction of both genetic factors inside the person and the action of the environment

on it from the outside. The skin is a human barrier that primarily performs a protective function, and according to genetic studies of biopsy material of the skin, it is a violation of this, the main function is the key to understanding the mechanisms of origin and onset of this disease [4].

The immediate cause of such increased attention to dermatological disease is not only not fully identified mechanisms of occurrence and treatment, but the widespread prevalence of this pathology. Deckers I. A. and co-authors [9] performed a large-scale study of literature sources in the period 1990-2010 on the epidemiological situation of atopic dermatitis. 2464 scientific sources were analyzed, from which 69 studies were selected, covering countries in Asia, Africa, Europe, the Americas and Oceania. Disappointing conclusions of this analysis were the data on the increase, which was heterogeneous on different continents (a sharp increase in Africa and a slight increase in Asia), the number of cases of atopic dermatitis among children.

Data from studies in Italy indicate the prevalence of eczema at 8.1 % (95 % CI: 7.6-8.7 %) (more patients regionally belonged to residents of central and southern Italy). About 60 % of patients had the onset of the disease in adulthood; It was also found that the predominance of patients is female, older people living in the area with nearby industrial enterprises and heavy traffic [17].

Among the population of Sweden, the prevalence of eczema is 40.7 %. As in Italy, the disease was mostly observed among women and people living in urban settlements with pollution from dust, automobile gases and industrial vapors. In addition, the family history and association of eczema with allergic rhinitis and asthma were clearly traced [18].

In the United States, the prevalence of eczema varies from state to state and ranges from 8.7 to 18.1 %, reaching the highest rates on the East Coast of the United States. Similarly, to previous studies, living in large cities is a significant factor in the occurrence of the disease with a chance factor of 1.67 (95 % confidence interval 1.19-2.35, P=0.008). There is also a higher prevalence of eczema among blacks (odds ratio 1.70, P=0.005) [20].

In addition to physical discomfort, patients with eczema also have psychological health problems. A study by Hon K. L. and others found that patients with atopic dermatitis had higher symptoms of stress and depression. Thus, symptoms of depression were found in 21 % of patients, symptoms of anxiety in 33 %, and symptoms of stress in 23 % of patients. Statistical analysis of the data showed that these symptoms correlated with low quality of life in patients (partial correlations 0.40-0.49; p<0.001). Interestingly, according to the results of the study, only 6 % of patients sought help from a psychologist [11].

The same trend is confirmed in another study, where signs of anxiety were found in 20 % and signs of depression in 14 % of patients. At the same time, worse indicators were found in women compared to men [3].

No less important element that indicates the severity of the problem of this disease is the material cost of the disease. Given its chronic and recurrent nature, this component must be considered. According to a German study, the annual cost of eczema averages 8,799 euros, of which 70 % are indirect costs [10].

Given all these data, researchers are looking for effective but simple and cheap methods of early detection, predicting the occurrence of this disease, predicting the severity and form of its course. One of the promising areas that is already being studied by scientists is the constitutional approach to identifying specific and reliable anthropometric markers of eczema [8], so it is appropriate to conduct a similar type of study using the Ukrainian population.

The purpose of the study is to build and analyze discriminant models of the possibility of occurrence and features of course of different forms of eczema in Ukrainian men of the first mature age depending on the characteristics of anthropometric parameters of the body.

Materials and methods

On the basis of the Military Medical Clinical Center of the Central Region and the Department of Dermatology and Venereal Diseases with a course of postgraduate education National Pirogov Memorial Medical University, Vinnytsya, men aged 22 to 35 years with the truth (n=34, including 16 with mild and 18 with severe course) and microbial (n=38, including 28 with mild and 10 with severe course) eczema, anthropometric examination was performed according to the scheme of Bunak V. V. [6].

The diagnosis of eczema was performed according to the nomenclature ICD-10 (https://zakononline.com.ua/documents/show/116857_531218).

As the control was used anthropometric data of 82 practically healthy men of the same age group, which were selected from the database of the research center National Pirogov Memorial Medical University, Vinnytsya.

Construction of discriminant models of the possibility of occurrence and features of the course of different forms of eczema depending on the anthropometric parameters of the body was carried out in the license package "Statistica 5.5".

Results

When dividing sick men into true eczema of mild and severe course and microbial eczema of mild and severe course, taking into account the structure and size of the body, the discriminant function is correct in 76.0% of cases. It was found that between healthy and sick men discriminant variables are shoulder width, transverse mid-chest diameter, skinfold thickness (SFT) on the back of the shoulder, SFT on the side, SFT on thigh, intercristal distance, SFT on the forearm and SFT at the lower angle of the shoulder blade, among whose greatest contribution to discrimination is shoulder width. In general, the totality of all anthropometric variables has a pronounced (Wilks' Lambda statistics=0.074; p<0.001) discrimination between healthy

and sick men with different forms of eczema.

The determined coefficients of classification discriminant functions make it possible to determine the classification index (Df), which allows to classify anthropo-somatotymphological indicators as "typical" for healthy or patients with different forms of eczema of different courses of men. In the form of equations, the definition of the indicator Df is given, where reference to healthy men is possible at the value of Df close to 197.7; to men with true eczema of mild course - at a value of Df close to 177.1; to men with true eczema of severe course - with a Df value close to 186.7; to men with mild microbial eczema - at a Df value close to 170.4; to men with severe microbial eczema - with a Df value close to 174.6:

Df (*for healthy men*) = shoulder width x 6.122 - transverse middle thoracic diameter x 1.450 + SFT on the back of the shoulder x 1.183 - SFT on the side x 1.996 + SFT on the thigh x 0.302 + intercristal distance x 6.711 + SFT on the forearm x 0.783 - SFT at the lower angle of the scapula x 1.051 - 197.7;

Df (*for men with true eczema of mild course*) = shoulder width 3.759 - transverse middle thoracic diameter x 0.234 - SFT on the back of the shoulder x 1.335 - SFT on the side x 1.050 - SFT on the thigh x 0.259 + intercristal distance x 7.986 + SFT on the forearm x 3.308 - SFT at the lower angle of the scapula x 1.719 - 177.1;

Df (*for men with true severe eczema*) = shoulder width x 4.017 - transverse middle thoracic diameter x 0.202 - SFT on the back of the shoulder x 1.186 - SFT on the side x 0.885 - SFT on the thigh x 0.446 + intercristal distance x 7.975 + SFT on the forearm x 3.045 - SFT at the lower angle of the scapula x 1.782 - 186.7;

Df (*for men with microbial eczema of mild course*) = shoulder width x 3.885 - transverse middle thoracic diameter 0.087 - SFT on the back of the shoulder x 1.271 - SFT on the side x 0.820 - SFT on the thigh x 0.221 + intercristal distance x 7.414 + SFT on the forearm x 3.000 - SFT at the lower angle of the scapula x 1.703 - 170.4;

Df (*for men with severe microbial eczema*) = shoulder width x 4.069 - transverse middle thoracic diameter x 0.110 - SFT on the back of the shoulder x 0.989 - SFT on the side x 0.701 - SFT on the thigh x 0.382 + intercristal distance x 7.336 + SFT on the forearm x 2.273 - SFT at the lower angle of the scapula x 1.696 - 174.6;

where (here and hereafter), transverse dimensions - in cm; SFT dimensions - in mm.

The statistical significance of all discriminant functions was determined using the criterion χ^2. It is established that taking into account anthropo-somatotypological indicators, a reliable interpretation of the obtained classification indicators is possible only between healthy and sick men.

When sick men are divided only into *truth and microbial eczema*, the discriminant function is correct in 87.7 % of cases. It was found that between healthy and sick men discriminant variables are shoulder width, transverse mid-chest diameter, SFT on the back of the shoulder, SFT on the side, SFT on thigh, intercristal distance and SFT on shin, among which the greatest contribution to discrimination is shoulder width. In general, the totality of all anthropometric variables has a pronounced (Wilks' Lambda statistics=0.088; $p<0.001$) discrimination between healthy and true men and patients with microbial eczema.

In the form of equations, the definition of the indicator Df is given, where reference to healthy men is possible at the value of Df close to 192.7; to men with true eczema - with a Df value close to 170.0; to men with microbial eczema - with a Df value close to 161.7:

Df (*for healthy men*) = shoulder width x 6.038 - transverse middle thoracic diameter x 1.668 + SFT on the back of the shoulder x 1.291 - SFT on the side x 2.779 + SFT on the thigh x 0.035 + intercristal distance x 6.416 + SFT on the shin x0.957 - 192.7;

Df (*for men with true eczema*) = shoulder width x 3.949 - transverse middle thoracic diameter x 0.532 - SFT on the back of the shoulder x 0.436 - SFT on the side x 2.210 - SFT on the thigh x 1.149 + intercristal distance x 7.310 + SFT on the shin x 2.039 - 170.0;

Df (*for men with microbial eczema*) = shoulder width x 3.927 - transverse middle thoracic diameter x 0.412 - SFT on the back of the shoulder x 0.425 - SFT on the side x 1.994 - SFT on the thigh x 0.945 + intercristal distance x 6.868 + SFT on the shin x 1.800 - 161.7.

Using the criterion χ^2, it is established that taking into account anthropo-somatotypological indicators, a reliable interpretation of the obtained classification indicators is possible not only between healthy and sick men, but also between men with various forms of eczema.

At distribution of sick men only on *eczema of mild or severe course*, discriminant function is correct in 84.4 % of cases. It was found that between healthy and sick men discriminant variables are shoulder width, transverse mid-chest diameter, SFT on the back of the shoulder, SFT on the side, SFT on thigh, SFT on the forearm and SFT at the lower angle of the shoulder blade, among which the greatest contribution to discrimination is width shoulders. In general, the set of all anthropometric variables has a pronounced (Wilks' Lambda statistics=0.088; $p<0.001$) discrimination between healthy and mild to severe eczema patients.

In the form of equations, the definition of the indicator Df is given, where reference to healthy men is possible at the value of Df close to 154.4; to men with mild eczema - with a Df value close to 114.7; to men with severe eczema - with a Df value close to 122.7:

Df (*for healthy men*) = shoulder width x 7.040 + transverse middle thoracic diameter x 0.673 + SFT on the back of the shoulder x 1.917 - SFT on the side x 1.110 + SFT on the thigh x 0.453 - SFT on the forearm x 2.141 - SFT at the lower angle of the scapula x 0.547 - 154.4;

Df (*for men with mild eczema*) = shoulder width x 4.817 + transverse middle thoracic diameter x 2.302 - SFT on the back of the shoulder x 0.513 + SFT on the side x 0.105 - SFT on the thigh x 0.062 - SFT on the forearm x 0.124 - SFT at the

lower angle of the scapula x 1.134 - 114.7;

Df (*for men with severe eczema*) = shoulder width x 5.060 + transverse middle thoracic diameter x 2.294 - SFT on the back of the shoulder x 0.306 + SFT on the side x 0.227 - SFT on the thigh x 0.254 - SFT on the forearm x 0.579 - SFT at the lower angle of the scapula x 1.185 - 122.7.

Using the criterion χ^2, it is established that taking into account anthropo-somatotypological indicators it is possible to reliably interpret the obtained classification indicators between healthy and sick men, and between men with mild or severe eczema there is only a slight tendency to interpret the obtained classification indicators.

Discussion

Thus, when dividing sick men into *true eczema of mild and severe course and microbial eczema of mild and severe course*, it was found that possible reliable ($p<0.001$) interpretation of the obtained classification indicators only between healthy and groups of sick men (discriminant function is correct in 76.0 % cases, statistics Wilks' Lambda=0.074); when dividing sick men only *into truth and microbial eczema* - a reliable interpretation of the obtained classification indicators is possible not only between healthy and sick ($p<0.001$), but also between patients with various forms of eczema ($p<0.05$) men (discriminant function is correct in 87.7 % cases, statistics Wilks' Lambda=0.088); in the distribution of sick men only on eczema of *mild or severe course* - possible reliable ($p<0.001$) interpretation of the obtained classification indicators between healthy and sick men, and between patients with eczema of mild or severe course - only a slight trend ($p=0.088$) the possibility of interpretation of the obtained classification indicators (discriminant function is correct in 84.4 % of cases, Wilks' Lambda statistics=0.088).

Discriminant models in the distribution of patients with *true eczema of mild and severe course and microbial eczema of mild and severe course* include body diameters (37.5 %) and SFT (62.5 %); in the distribution of sick men only for *truth and microbial eczema* - body diameters (42.9 %) and SFT (57.1 %); in the distribution of sick men only on eczema of *mild or severe course* - also body diameters (28.6 %) and SFT (71.4 %). Moreover, the greatest contribution to discrimination between groups of healthy and sick (regardless of the division into groups of patients) men makes the width of the shoulders. The obtained results (percentage of inclusion in the models of torso and pelvic diameters) indicate a higher genetic predisposition [16] of the form, rather than the course of this multifactorial disease.

Data from foreign studies on the study of constitutional markers in skin diseases are very encouraging [12]. Egyptian researchers found a statistically significant difference between waist circumference and diastolic blood pressure, which can be used to predict the severity of acne [1].

5249 cases of rosacea in American women were analyzed. It was found that the higher risk of this pathology in persons with elevated values of body mass index and waist circumference and thighs ($p_{trend}<0.0001$) [14].

At the same time, Iranian scientists, when examining adolescents with acne, found no significant correlations with such indicators as body mass index, waist circumference, systolic and diastolic pressure, sugar levels, total cholesterol ($P>0.05$) [19].

Studies concerning the study of atopic dermatitis strongly suggest the existence of a relationship between anthropometric parameters and the risk of disease [12]. Thus, a massive review of literature sources, covering a total of 90 thousand people, showed that elevated human body mass index is associated with an increased risk of atopic dermatitis [2]. In another publication, which analyzed the data of 30 studies, this information is also confirmed, but a significant correlation was found in studies conducted on populations in North America and Asia, but not in Europe [23].

Budu-Aggrey A. and co-authors [5] found that an increase in body mass index increases the risk of eczema (8 % 5 units higher than BMI; OR=1.02 (1.00 to 1.03) per 1 kg/m^2; $p=0.09$).

Changes in body mass index at the age of 1 to 4 years and high physical activity in combination with changes in body weight index at the age of 6-10 years are positively correlated with the risk of atopic dermatitis at 10.8 years [7].

A group of scientists led by Hu Y. [13] found a relationship between the risk of atopic dermatitis and the index of body mass index, waist circumference, the percentage of body fat. This connection was especially seen in young women. Another study in the United States also found an association between obesity and the risk of eczema in children [21].

The study, which covered 266 people from Harbin (PRC), found that all components of the atopic triad also correlated positively with elevated body mass index values (OR=3.2, 95 % CI: 1.8, 5.7). For atopic dermatitis in particular OR=2.7, 95 % CI: 1.2, 6.3 [15].

The results obtained during our study, as well as data from the scientific literature, confirm the prospects of using anthropometric research methods to predict the possibility and features of various multifactorial diseases, including eczema.

Conclusion

1. Developed on the basis of anthropometric parameters of the body reliable discriminant models allow with a high probability to predict only the possibility of occurrence and form of eczema in men.

2. The composition of the constructed discriminant equations in all groups of men (in the distribution of patients with true eczema of mild and severe course and microbial eczema of mild and severe course; in the distribution of patients only for true and microbial eczema; in the distribution of patients with only eczema of mild or severe course) most often include SFT (62.5 %, 57.1 % and 71.4 %, respectively) and body diameters (37.5 %, 42.9 % and 28.6 %, respectively).

3. Shoulder width makes the largest contribution to discrimination in all groups of men.

References

[1] Ahmed, G. I., Yousef, A. E., & Salah El-Din, E. (2020). Evaluation of the Association between Acne Vulgaris and Metabolic Syndrome in Adolescents at Zagazig University Hospitals. *The Egyptian Journal of Hospital Medicine,* 81(3), 1628-1633. doi: 10.21608/EJHM.2020.116811

[2] Ali, Z., Suppli Ulrik, C., Agner, T., & Thomsen, S. F. (2018). Is atopic dermatitis associated with obesity? A systematic review of observational studies. *Journal of the European Academy of Dermatology and Venereology,* 32(8), 1246-1255. doi: 10.1111/jdv.14879

[3] Boehm, D., Schmid?Ott, G., Finkeldey, F., John, S. M., Dwinger, C., Werfel, T., ... & Breuer, K. (2012). Anxiety, depression and impaired health?related quality of life in patients with occupational hand eczema. *Contact dermatitis*, 67(4), 184-192. doi: 10.1111/j.1600-0536.2012.02062.x

[4] Brown, S. J. (2017). Molecular mechanisms in atopic eczema: insights gained from genetic studies. *The Journal of pathology,* 241(2), 140-145. doi: 10.1002/path.4810

[5] Budu-Aggrey, A., Brumpton, B., Tyrrell, J., Watkins, S., Modalsli, E. H., Celis-Morales, C., ... & Paternoster, L. (2018). Evidence of a common causal relationship between body mass index and inflammatory skin disease: a Mendelian Randomization study. *bioRxiv*, 265629. doi: 10.1101/265629

[6] Bunak, V. V. (1941). *Antropometriia [Anthropometry].* M.: Narkompros RSFSR - M.: People's Commissariat of the RSFSR.

[7] Byberg, K. K., Eide, G. E., Forman, M. R., Juliusson, P. B., & Øymar, K. (2016). Body mass index and physical activity in early childhood are associated with atopic sensitization, atopic dermatitis and asthma in later childhood. *Clinical and translational allergy,* 6(1), 1-9. doi: 10.1186/s13601-016-0124-9

[8] Choon, S. E., Ngim, C. F., Premaa, S., Tey, K. W., & Nalini, M. N. (2016). Clinico-epidemiological profile, including body mass index of Malaysian children with psoriasis. *Med J Malaysia,* 71(4), 171-176.

[9] Deckers, I. A., McLean, S., Linssen, S., Mommers, M., Van Schayck, C. P., & Sheikh, A. (2012). Investigating international time trends in the incidence and prevalence of atopic eczema 1990-2010: a systematic review of epidemiological studies. *PloS one,* 7(7), e39803. doi: 10.1371/journal.pone.0039803

[10] Diepgen, T. L., Scheidt, R., Weisshaar, E., John, S. M., & Hieke, K. (2013). Cost of illness from occupational hand eczema in Germany. *Contact Dermatitis*, 69(2), 99-106. doi: 10.1111/cod.12038

[11] Hon, K. L., Pong, N. H., Poon, T. C., Chan, D. F., Leung, T. F., Lai, K. Y., ... & Luk, N. M. (2015). Quality of life and psychosocial issues are important outcome measures in eczema treatment. *Journal of Dermatological Treatment,* 26(1), 83-89. doi: 10.3109/09546634.2013.873762

[12] Hu, Y., Zhu, Y., Lian, N., Chen, M., Bartke, A., & Yuan, R. (2019). Metabolic syndrome and skin diseases. *Frontiers in endocrinology,* 10, 788. doi: 10.3389/fendo.2019.00788

[13] Lee, J. H., Do Han, K., mi Jung, H., Youn, Y. H., Lee, J. Y., Park, Y. G., ... & Park, Y. M. (2016). Association between obesity, abdominal obesity, and adiposity and the prevalence of atopic dermatitis in young Korean adults: the Korea national health and nutrition examination survey 2008-2010. *Allergy, asthma & immunology research,* 8(2), 107-114. doi: 10.4168/aair.2016.8.2.107

[14] Li, S., Cho, E., Drucker, A. M., Qureshi, A. A., & Li, W. Q. (2017). Obesity and risk for incident rosacea in US women. *Journal of the American Academy of Dermatology,* 77(6), 1083-1087. doi: 10.1016/j.jaad.2017.08.032

[15] Luo, X., Xiang, J., Dong, X., Cai, F., Suo, J., Wang, Z., & Liu, M. (2013). Association between obesity and atopic disorders in Chinese adults: an individually matched case-control study. *BMC public health,* 13(1), 1-5. doi: 10.1186/1471-2458-13-12

[16] Nikityuk, B. A., Moroz, V. M., & Nikityuk, D. B. (1998). *Теория и практика интегративной антропологии. Очерки [Theory and practice of integrative anthropology. Essays].* Киев-Винница, "Здоров'я" - Kiev-Vinnitsa, "Zdorov'ya".

[17] Pesce, G., Marcon, A., Carosso, A., Antonicelli, L., Cazzoletti, L., Ferrari, M., ... & De Marco, R. (2015). Adult eczema in Italy: prevalence and associations with environmental factors. *Journal of the European Academy of Dermatology and Venereology,* 29(6), 1180-1187. doi: 10.1111/jdv.12784

[18] Rönmark, E. P., Ekerljung, L., Lötvall, J., Wennergren, G., Rönmark, E., Toren, K., & Lundback, B. (2012). Eczema among adults: prevalence, risk factors and relation to airway diseases. Results from a large-scale population survey in Sweden. *British Journal of Dermatology*, 166(6), 1301-1308. doi: 10.1111/j.1365-2133.2012.10904.x

[19] Shariatpanahi, G., Hashemi, R., Asadabadi, M., Shirzadi, N., Sadat Haddadi, N., & Shakoei, S. (2020). Association between metabolic syndrome and acne in teenage girls: a cross-sectional study. *Iranian Journal of Dermatology,* 23(3), 85-90. doi: 10.22034/IJD.2020.111544

[20] Shaw, T. E., Currie, G. P., Koudelka, C. W., & Simpson, E. L. (2011). Eczema prevalence in the United States: data from the 2003 National Survey of Children's Health. *Journal of Investigative Dermatology*, 131(1), 67-73. doi: 10.1038/jid.2010.251

[21] Silverberg, J. I. (2011). Role of childhood obesity in atopic dermatitis. *Expert Review of Dermatology*, 6(6), 635-642. doi: 10.1586/edm.11.68

[22] Sohn, A., Frankel, A., Patel, R. V., & Goldenberg, G. (2011). Eczema. Mount Sinai Journal of Medicine: A Journal of Translational and Personalized Medicine, 78(5), 730-739. doi: 10.1002/msj.20289

[23] Zhang, A., & Silverberg, J. I. (2015). Association of atopic dermatitis with being overweight and obese: a systematic review and metaanalysis. *Journal of the American Academy of Dermatology*, 72(4), 606-616. doi: 10.1016/j.jaad.2014.12.013

ДИСКРИМІНАНТНІ МОДЕЛІ МОЖЛИВОСТІ ВИНИКНЕННЯ ТА ОСОБЛИВОСТЕЙ ПЕРЕБІГУ РІЗНИХ ФОРМ ЕКЗЕМИ У ЧОЛОВІКІВ В ЗАЛЕЖНОСТІ ВІД ОСОБЛИВОСТЕЙ АНТРОПОМЕТРИЧНИХ ПОКАЗНИКІВ

Аль-Омарі Ала'а Осама Ахмад, Вадзюк С.Н., Школьніков В.С., Прокопенко С.В., Гунас І.В.

Екзема є захворюванням шкіри з багатогранною клінічною картиною, численними формами прояву та перебігу і, що не менш важливо, такою патологією, котра модифікує життя людини та часто вимагає зміни способу життя із пониженням його якості. Виявлення прогностичних ознак для прогнозування виникнення та тяжкості перебігу даного захворювання є першочерговою задачею для сучасної науки. Мета дослідження - побудувати та провести аналіз дискримінантних моделей можливості виникнення та особливостей перебігу різних форм екземи в українських чоловіків першого зрілого віку в залежності

від особливостей антропометричних параметрів тіла. Чоловікам, віком від 22 до 35 років, хворим на істинну (n=34, серед яких 16 із легким перебігом і 18 із тяжким перебігом) та мікробну (n=38, серед яких 28 із легким перебігом і 10 із тяжким перебігом) екзему, проведено антропометричне обстеження відповідно до схеми Бунака В.В. Встановлення діагнозу екземи проводили згідно номенклатури МКХ-10. Контрольну (за антропометричними даними) групу становили 82 практично здорових чоловіків аналогічного віку, котрі були відібрані з банку даних науково-дослідного центру Вінницького національного медичного університету ім. М.І.Пирогова. Побудова дискримінантних моделей можливості виникнення та особливостей перебігу різних форм екземи в залежності від антропометричних параметрів тіла проведена в ліцензійному пакеті "Statistica 5.5". Встановлено, що при розподілі хворих чоловіків на істинну екзему легкого і тяжкого перебігу та мікробну екзему легкого і тяжкого перебігу можлива лише достовірна інтерпретація отриманих показників класифікації між здоровими та групами хворих (функція коректна в 76.0% випадків, статистика Wilks' Lambda=0,074); при розподілі хворих чоловіків лише на істинну та мікробну екзему - можлива достовірна інтерпретація отриманих показників класифікації як між здоровими та хворими, так і між хворими на істинну та мікробну екзему (функція коректна в 87.7% випадків, статистика Wilks' Lambda=0.088); при розподілі хворих чоловіків лише на екзему легкого або тяжкого перебігу - можлива достовірна інтерпретація отриманих показників класифікації між здоровими та хворими чоловіками, а між хворими на екзему легкого або тяжкого перебігу лише незначна тенденція можливості інтерпретації отриманих показників класифікації (функція коректна у 84.4% випадків, статистика Wilks' Lambda = 0.088). До складу побудованих дискримінантних рівнянь в усіх випадках найбільш часто входять товщина шкірно-жирових складок (відповідно 62.5%, 57.1% і 71,4%) і діаметри тіла (відповідно 37.5%, 42.9% і 28.6%). Отримані результати підтверджують перспективність використання антропометричних методів дослідження для прогнозування можливостей виникнення та особливостей перебігу екземи.

Ключові слова: *екзема, антропометричні параметри тіла, дискримінантний аналіз, чоловіки.*

DOI: 10.31393/morphology-journal-2022-28(1)-03 Reports of Morphology, Vol. 28, №1, Pages 17-26

ISSN 1818-1295 eISSN 2616-6194

REPORTS OF MORPHOLOGY

Official Journal of the Scientific Society of Anatomists, Histologists, Embryologists and Topographic Anatomists of Ukraine

journal homepage: https://morphology-journal.com

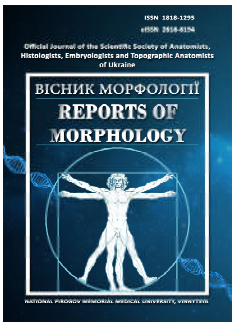

Fractal analysis of anatomical structures linear contours: modified Caliper method vs Box counting method

Maryenko N.I., Stepanenko O.Yu.
Kharkiv National Medical University, Kharkiv, Ukraine

ARTICLE INFO
Received: 19 November 2021
Accepted: 23 December 2021

UDC: 611:57.086:517:530.191

CORRESPONDING AUTHOR
e-mail: maryenko.n@gmail.com
Maryenko N.I.

CONFLICT OF INTEREST
The authors have no conflicts of interest to declare.

FUNDING
Not applicable.

Fractal analysis estimates the metric dimension and complexity of the spatial configuration of different anatomical structures. This allows the use of this mathematical method for morphometry in morphology and clinical medicine. Two methods of fractal analysis are most often used for fractal analysis of linear fractal objects: the Box counting method (Grid method) and the Caliper method (Richardson's method, Perimeter stepping method, Ruler method, Divider dimension, Compass dimension, Yard stick method). The aim of the research is a comparative analysis of two methods of fractal analysis - Box counting method and author's modification of Caliper method for fractal analysis of linear contours of anatomical structures. A fractal analysis of three linear fractals was performed: an artificial fractal - a Koch snowflake and two natural fractals - the outer contours of the pial surface of the human cerebellar vermis cortex and the cortex of the cerebral hemispheres. Fractal analysis was performed using the Box counting method and the author's modification of the Caliper method. The values of the fractal dimension of the artificial linear fractal (Koch snowflakes) obtained by the Caliper method coincide with the true value of the fractal dimension of this fractal, but the values of the fractal dimension obtained by the Box counting method do not match the true value of the fractal dimension. Therefore, fractal analysis of linear fractals using the Caliper method allows you to get more accurate results than the Box counting method. The values of the fractal dimension of artificial and natural fractals, calculated using the Box counting method, decrease with increasing image size and resolution; when using the Caliper method, fractal dimension values do not depend on these image parameters. The values of the fractal dimension of linear fractals, calculated using the Box counting method, increase with increasing width of the linear contour; the values calculated using the Caliper method do not depend on the contour line width. Thus, for the fractal analysis of linear fractals, preference should be given to the Caliper method and its modifications.

Keywords: *fractal analysis, morphometry, linear contour, Caliper, Box counting.*

Introduction

Fractal analysis has been increasingly used as a morphometric method in morphology and clinical medicine for the last few decades [3, 4]. This method of mathematical analysis provides a quantitative assessment of the metric dimension and complexity of the spatial configuration of different anatomical structures [12, 13]. Fractal analysis is based on fractal geometry, which characterizes the structure and spatial organization of fractals [12, 13, 14]. A fractal is a mathematical set or object characterized by self-repetition, self-similarity and large-scale invariance (part of the object partially or completely repeats the structure of the object as a whole, the structure of the object at different scales is similar) [1, 10, 12, 13, 14].

Fractals based on clear mathematical algorithms are called mathematical or artificial. Some natural objects (including the anatomical structures of the human body) have the properties of fractals, but their structure, unlike artificial fractals, is not mathematically regulated. Such structures are called natural fractals or quasi-fractals [12, 13, 14]. Artificial and natural fractals can be different in structure. Among the structures of the human body are often linear fractals, most often linear contours of various objects and structures, which in two-dimensional images are represented by curved or broken lines of different configurations (fibers, membrane cross-sections, outer and inner linear contours of various structures and

pathological cells, etc.). Fractal analysis of linear contours of anatomical structures (outer contour characterizing the surface of the anatomical structure or inner contour characterizing the inner surface of a hollow organ or cavity inside the anatomical structure) allows to quantify the features of their spatial configuration: the more complex the linear contour of the formation (for example, the contour has a wavy, twisted, broken configuration, etc.), the more complex is the spatial configuration of the anatomical structure as a whole.

Fractal properties of different objects can be quantified using fractal dimension (FD, fractal index). The fractal dimension determined on two-dimensional images can vary from 1 to 2 [5, 6, 12, 13, 14]. Box counting (Grid Method) is most often used for fractal analysis of linear objects in medicine and morphology due to its simplicity and versatility [2, 7, 8, 18, 21]. In addition, the classic method used for fractal analysis of linear contours is the Caliper method (Richardson's method, Perimeter stepping method, Ruler method, Divider dimension, Compass dimension, Yard stick method) [5, 6, 11, 17, 19, 20, 23, 24]. However, in medicine, due to routine and lack of accuracy, this method is used much less often than the method of counting squares [11, 23]. In some studies, both methods of fractal analysis (Box counting and Caliper) were used in different modifications [17, 19, 20, 24] and a comparative analysis of Box counting and other methods of fractal analysis was performed [5, 6].

We developed our own modification of the Caliper method, adapted for use in morphology as a morphometric method [15] and used it for fractal analysis of the linear contour of the cerebellum [16]. In this paper, a comparison of two methods of fractal analysis for the selection of optimal techniques for morphometric study of linear contours of anatomical structures.

The aim of the study is a comparative analysis of two methods of fractal analysis - Box counting method and the author's modification of the Caliper method for fractal analysis of linear contours of anatomical structures.

Materials and methods

The study was conducted in compliance with the basic bioethical provisions of the Council of Europe Convention on Human Rights and Biomedicine (April 4, 1997), the Helsinki Declaration of the World Medical Association on Ethical Principles for Human Scientific Research (1964-2008), as well as the order of the Ministry of Health of Ukraine №690 of 23.09.2009. **The conclusion of the Commission on Ethics and Bioethics** of Kharkiv National Medical University confirms that the study was conducted in compliance with human rights, in accordance with current legislation in Ukraine, meets international ethical requirements and does not violate ethical standards in science and standards for conducting biomedical research (minutes of the meeting of the Commission on Ethics and Bioethics of KhNMU №10 dated November 7, 2018).

Three linear fractal objects were chosen as objects for comparative analysis of two methods of fractal analysis (Fig. 1): artificial (mathematical) fractal - Koch snowflake, which is a classic example of a linear fractal [1, 10, 12, 13, 14] (the fourth iteration was chosen for the study), and two natural fractal objects - the outer contours of the pial surface of the human cerebellar cortex and the cortex of the cerebral hemispheres. The pial surface of the cerebral cortex and the surface of the brain are traditionally considered as a self-similar complex fractal structure [9], and its study is of great importance for clinical neuroscience [3, 4, 7, 8], so different areas of the cerebral cortex (namely - its external linear contours on two-dimensional MR images) were selected for the study.

For fractal analysis of the external linear contours of the cerebellar cortex and cerebral hemispheres, magnetic resonance (MR) tomograms of the brains of persons who did not have structural changes in the brain were used.

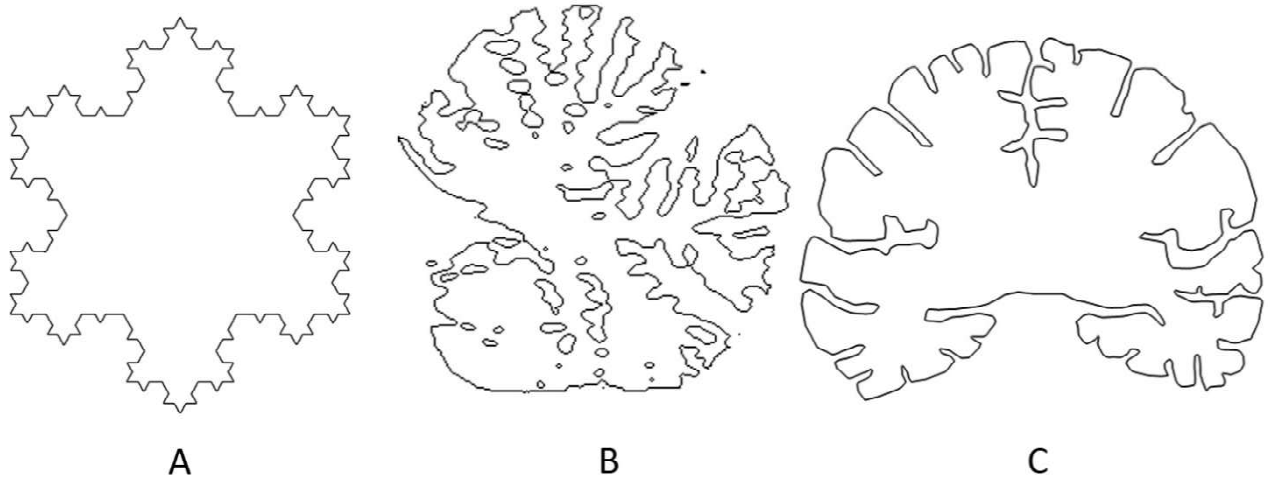

Fig. 1. Linear fractal objects used for fractal analysis: A - Koch snowflake, B - outer linear contour of the human cerebellar cortex, C - outer linear contour of the cortex of the human cerebral hemispheres.

Magnetic resonance imaging was performed using a magnetic resonance imaging with a magnetic induction value of 1.5 T. MR images of the cerebellum in sagittal projection were used for fractal analysis of the linear contour of the cerebellar vermis, and MR images in coronal projection were used to analyze the contour of the cerebral cortex.

Preliminary preparation of digital images for the two methods of fractal analysis (Caliper and Box counting) was performed in the same way. Adobe Photoshop CS5 created images with a resolution of 128 pixels per inch with the following dimensions: to study the contour of the cerebellum and Koch's snowflake, the image size was 128x128 pixels, the contour of large hemispheres - 512x400 pixels. A fragment of a digital MR image of the brain containing the structure under study, or a digital image of a Koch snowflake, was placed in the resulting rectangle. Subsequently, to determine the effect of scale and resolution on the fractal dimension, the image resolution was doubled (from 128 to 256 pixels per inch) and quadrupled (up to 512 pixels per inch), with linear image sizes varying in proportion to the resolution.

After preliminary preparation, fractal image analysis was performed. The methods of the two fractal analysis methods analyzed in this paper were described earlier: the Box counting method is a classic method used in the vast majority of studies using fractal analysis [2, 5, 6, 7, 8, 18, 21], the author's modification of the Caliper method described in our previous work [15] and used to study the cerebellum [16]. But we consider it expedient to give a general description of the two methods of fractal analysis in this paper to better understand the results.

Different methods of fractal analysis involve the use of fractal measurement units (fractal measurement units), which cover the object under study [5, 6, 12, 13, 14, 15, 18, 20, 21, 24]. Fractal measures can be linear segments, squares, cubes and other geometric shapes. The type of fractal measure is determined by the peculiarities of the method and the object under study. Fractal analysis always includes several stages, in which an iterative (repeated and uniform) change in the size of the fractal measure (S) is performed; most often it is a doubling or halving of the linear size of a fractal measure (for example, doubling or halving the length of a fractal linear segment or each side of a fractal square). At each stage of fractal analysis, the value of N is calculated - the minimum number of fractal measures that allow you to completely cover (cover, fit) the object under study. Then the natural logarithms of two numbers are calculated: N and 1/S - numbers, the inverse of the fractal measure (Ln (N) and Ln (1/S)). Then calculate the linear regression equation of the dependence of Ln(N) on Ln (1/S), the value of the fractal dimension is equal to the slope of the direct regression relative to the abscissa [5, 6, 12, 13, 14, 15, 16]. The value of the fractal dimension can be calculated by the formula:

$$FD = \frac{\Sigma\left(Ln\left(\frac{1}{S}\right) - \overline{Ln\left(\frac{1}{S}\right)}\right)\left(Ln(N) - \overline{Ln(N)}\right)}{\Sigma\left(Ln\left(\frac{1}{S}\right) - \overline{Ln\left(\frac{1}{S}\right)}\right)^2}$$

where FD is the fractal dimension, S is the relative size of the fractal measure, N is the number of fractal measures covering the structure under study (cited according to [16] with changes).

But, despite the similarities, the two methods of fractal analysis have fundamental differences.

Method of counting squares (Box counting). For fractal analysis with the help of the Box counting method an additional stage of preliminary image preparation is performed: with the help of a graphic editor a linear contour is selected and a line is drawn, which is necessary for further image analysis. Since the contour is studied, and not the structure as a whole, it is advisable to use the outline of the contour with a line of the minimum possible width, which for digital raster images is 1 pixel (Fig. 2). In addition, a 2-6 pixel-wide contour outline was used to determine the effect of linear contour width on fractal dimension values.

After delineation, the fractal analysis is performed according to the classical method of Box counting [5, 6]. A fractal grid is superimposed on the image, which divides the image into rectangles. In the first stage, the fractal grid lines divide each side of the image in half, and the size of the fractal measure (S) at this stage is 1/2. The size of the sides of the squares of the fractal grid decreases several times, so the value of S in the second stage is 1/4, the third - 1/8, the fourth - 1/16, the fifth - 1/32 (see Fig. 2). The fractal measure size for the Box counting method is also called box size (box edge size) [5, 6].

At each stage of fractal analysis, the number of fractal measures covering the contour (N) is determined by counting the number of squares containing fragments of the studied structure (in the study of delineated images - the contour of the studied structure) (see Fig. 2) [5, 6].

Fractal analysis using the method of Box counting in this study was performed automatically using the program Image J [22], the following values of S (box size) were selected: 1/2, 1/4, 1/8, 1/16, 1/32, 1/64, 1/128.

Caliper method. The classic version of the Caliper method uses a one-dimensional fractal measure - a linear segment. A linear object is covered with a broken line consisting of linear segments of a certain length and the number of these segments is counted (N). Then their length is increased or decreased twice and the number of fractal measures is counted again [5, 6, 12, 13, 14, 15, 20, 21, 24]. This method in the classic version is routine, because the calculation is done manually.

In our proposed author's modification of the Caliper method [15, 16], the analysis is performed automatically using Adobe Photoshop CS5. This technique includes the following steps. After preliminary preparation on the investigated image the linear contour by means of the tool "selection" is allocated. Unlike the method of counting squares, this method does not require outlining a line. After selection, the length of the contour in pixels (P) is measured using the tool "analysis" (Fig. 3) [15, 16].

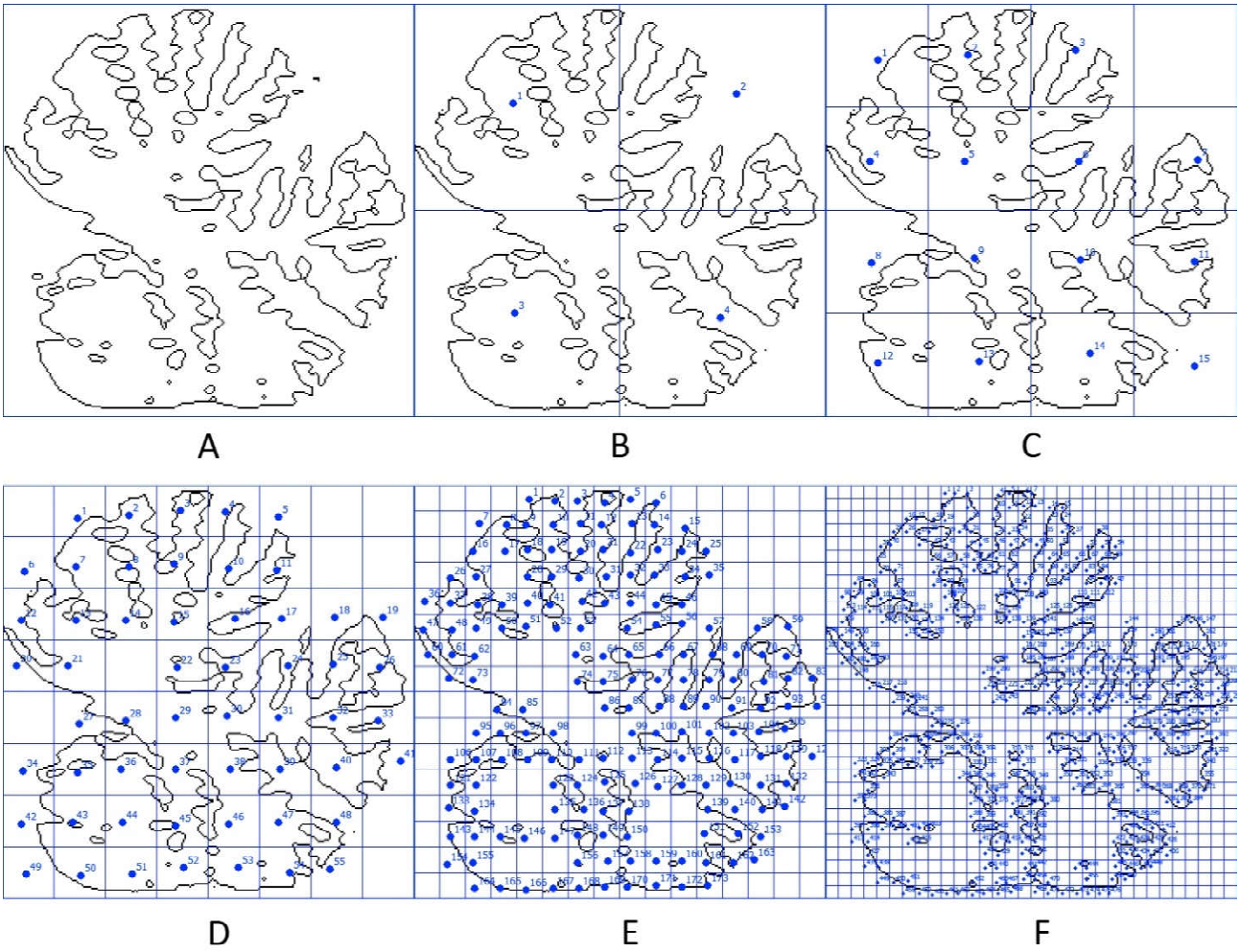

Fig. 2. Fractal analysis of the linear contour of the cerebellum using the method of Box counting. A - delineation of the linear contour of the object under study; B-F - stages of fractal analysis using a fractal grid: B - 1st stage of fractal analysis, S (box size) 1/2; C - 2nd stage of fractal analysis, S (box size) 1/4; D - 3rd stage of fractal analysis, S (box size) 1/8; E - 4th stage of fractal analysis, S (box size) 1/16; F - 5th stage of fractal analysis, S (box size) 1/32.

The minimum possible length of linear segments that can cover a linear contour on a digital bitmap image is 1 pixel. In the subsequent stages, as in the classic version of this method, the length of the linear segment is doubled several times. The modification developed by us allows to automate and simplify calculation by smoothing of a contour. Smoothing removes small bends from the contour that cannot be fractally covered with a radius larger than the radius of these bends. In the classical version of the Caliper method, those curves of the contour that have a radius less than the length of the fractal measure will not be covered by such linear segments. For example, if a contour has curves with a radius of 1 pixel, a fractal measure 2 pixels long will not cover those curves. Therefore, smoothing allows you to automatically modify the contour and get a result comparable to the classic version of the Caliper method. Gradual smoothing of the contour is performed starting from the second stage of fractal analysis using the tool "smoothing", followed by measuring the length of the contour after each smoothing. In the second stage, for images with a resolution of 128 pixels per inch, the anti-aliasing radius is 2 pixels, in the third stage - 4 pixels, in the fourth - 8 pixels, in the fifth - 16 pixels; the absolute length of the fractal segment (Sa) coincides with the smoothing radius and in the second stage of fractal analysis is 2 pixels, in the third - 4, in the fourth - 8 and in the fifth - 16 pixels (see Fig. 3) [15, 16].

When resizing an image, the smoothing radius and the absolute size of the fractal measure should be scaled in proportion to the change in resolution and image size. Fractional values that characterize the relative size of the fractal measure (S) do not depend on the image resolution and are in the first stage - 1/16, the second stage - 1/8, the third - 1/4, the fourth - 1/2, the fifth - 1. The number of fractal measures covering the studied contour (N) is defined as the ratio of P - contour length in pixels to S_a - the absolute size of the fractal measure in pixels: $N=P/S_a$ [15].

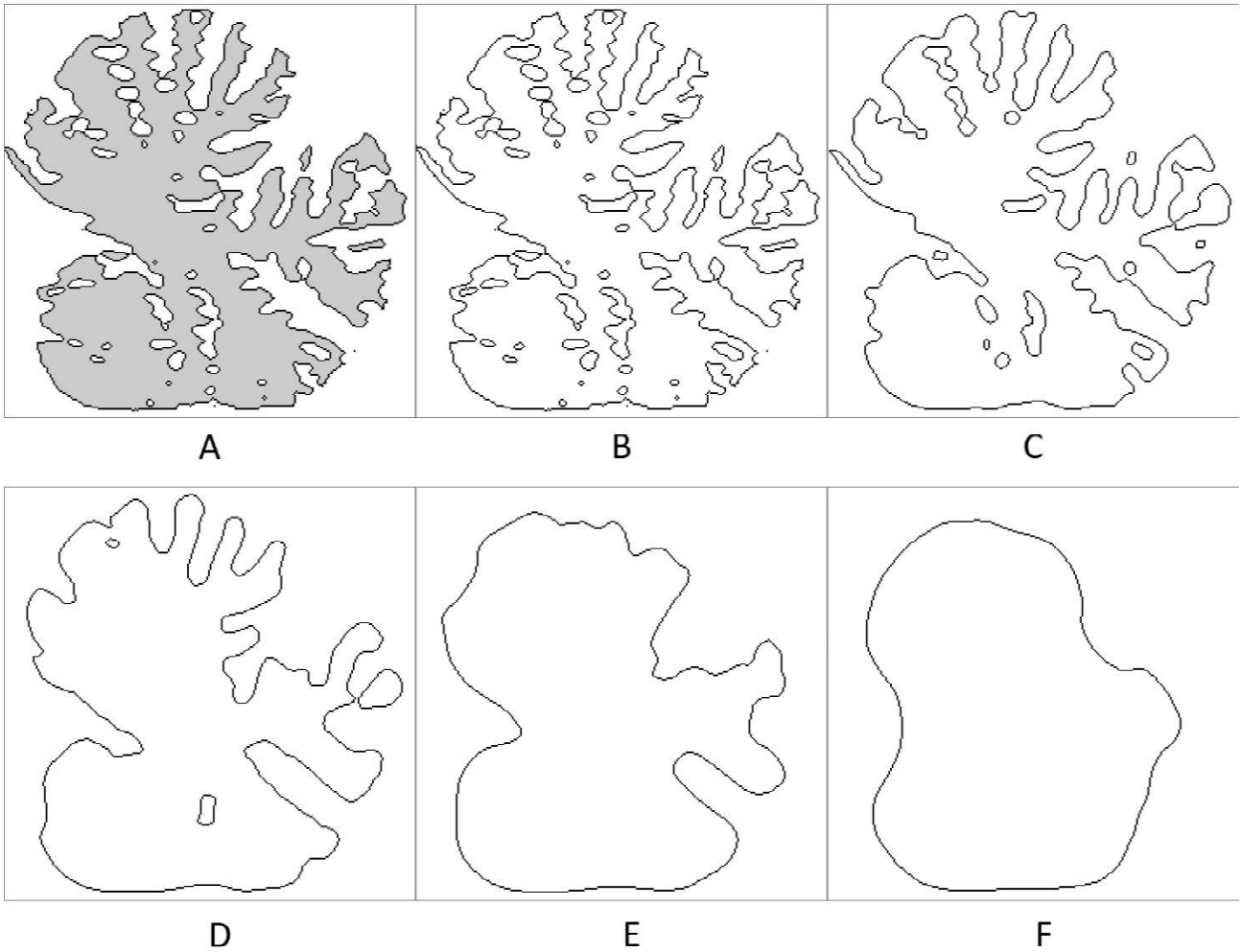

Fig. 3. Fractal analysis of the linear contour of the cerebellum using the Caliper method in the author's modification (described in [15]). A - selection of the linear contour of the object under study (contour delineation is used for clarity); B - 1st stage of fractal analysis, linear contour smoothing was not used, S=1; C-F - stages of fractal analysis using contour smoothing: C - 2nd stage of fractal analysis, S= 1/2; D - 3rd stage of fractal analysis, S=1/4; E - 4th stage of fractal analysis, S=1/8; F - 5th stage of fractal analysis, S=1/16. This modification was used by us for fractal analysis of the linear contour of the cerebellum [16].

Results

Initially, a fractal analysis of images with a resolution of 128 pixels per inch was performed. The values of the fractal dimension of the studied linear fractals, obtained using two methods of fractal analysis, did not match. Thus, the value of FD contour of the cerebellum, obtained using the method of Box counting, was 1.690, the method of Caliper - 1.501; the value of FD contour of the cortex of the cerebral hemispheres, obtained by the method of Box counting, was 1.125, the method of Caliper - 1.403. The values of the fractal dimension of these natural fractals are not known in advance, so in addition to these objects to validate the accuracy of measurements will be studied artificial fractal - Koch snowflake, the value of the fractal dimension of which is constant and therefore - known in advance (FD=Ln(4)/ Ln 3)≈1.26). The FD value of the Koch snowflake (fourth iteration) obtained using the Box counting method was 1.188, the Caliper method was 1.266. Therefore, the Caliper method in the study of images with a resolution of 128 pixels per inch allows to obtain a value of fractal dimension, which coincides with the true value of FD of the artificial linear fractal.

However, the resolution and size of the images used for analysis can vary significantly. Therefore, the influence of image size and resolution on fractal dimensional values was also studied. To do this, the same images were studied, but with three different resolution values: 128 pixels per inch (scale 1), 256 pixels per inch (scale 2) and 512 pixels per inch (scale 3) (Fig. 4). The dimensions of the images of the linear contour of the cerebellum and Koch's snowflake were 128x128 pixels (scale 1, small image size), 256x256 pixels (scale 2, medium size) and 512x512 pixels (scale 3, large size); the dimensions of the images with the linear contour of the cortex of the cerebral hemispheres were 512x400 pixels (scale 1, small image size), 1024x800 pixels (scale 2, medium size) and 2048x1600 pixels (scale

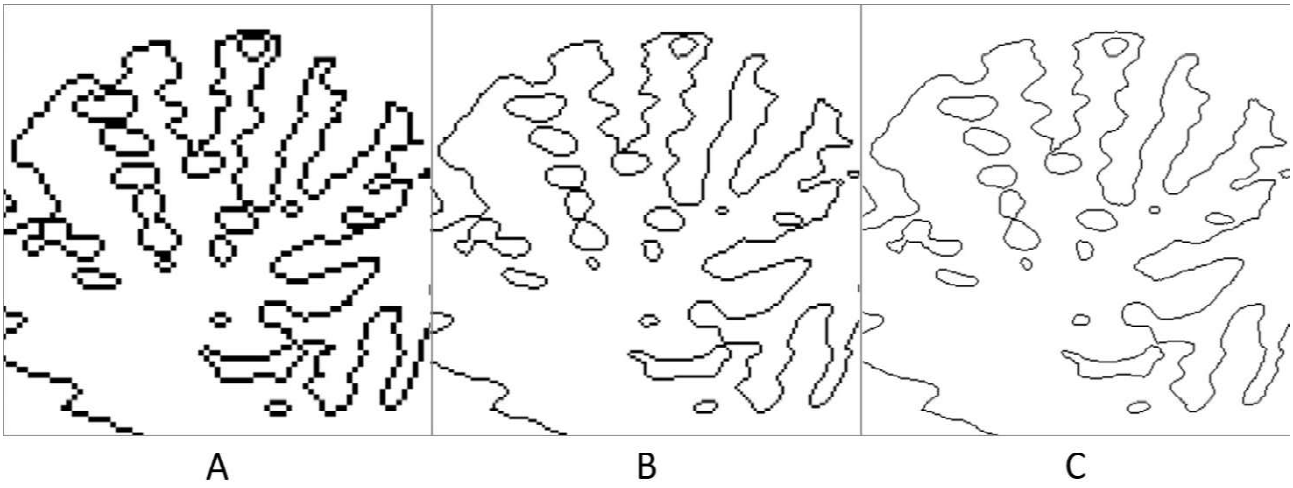

Fig. 4. Linear contour of the cerebellum in images with different resolutions: A - 128 pixels per inch, B - 256 pixels per inch, C - 512 pixels per inch. The outline of the line with the smallest possible value of width - 1 pixel is applied.

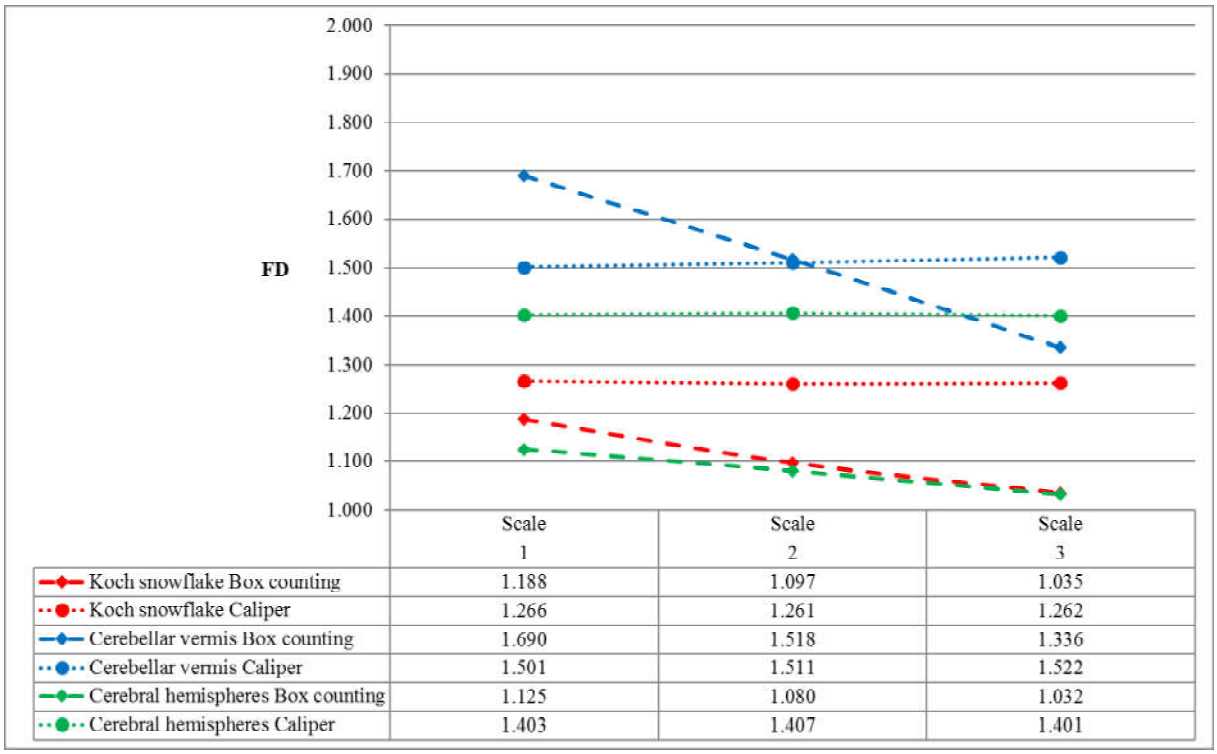

	Scale 1	Scale 2	Scale 3
Koch snowflake Box counting	1.188	1.097	1.035
Koch snowflake Caliper	1.266	1.261	1.262
Cerebellar vermis Box counting	1.690	1.518	1.336
Cerebellar vermis Caliper	1.501	1.511	1.522
Cerebral hemispheres Box counting	1.125	1.080	1.032
Cerebral hemispheres Caliper	1.403	1.407	1.401

Fig. 5. Fractal dimensional (FD) values determined on images with different resolutions and sizes using Caliper and Box counting methods. Scale 1 - resolution of 128 pixels per inch, scale 2 - resolution of 256 pixels per inch, and scale 3 - resolution of 512 pixels per inch.

3, large size). The smoothing radius values for the Caliper method and the absolute dimensions of the fractal measures for both fractal analysis methods changed in proportion to the change in the image resolution; the relative dimensions of fractal measures when scaling the image remained unchanged.

As can be seen from Figure 5, the FD values of the three studied fractals determined by the Box counting method decrease with increasing resolution and image size, and the FD values determined by the Caliper method remain virtually unchanged when these image parameters change. The FD values of the artificial fractal (Koch snowflakes) determined by the Caliper method on images of different sizes coincide with the true FD values of this fractal, in contrast to the FD values determined by the Box counting method. Therefore, the results obtained using the Caliper method are virtually independent of image size and resolution, which allows you to use this method to analyze linear contours on images of different sizes and with different resolutions.

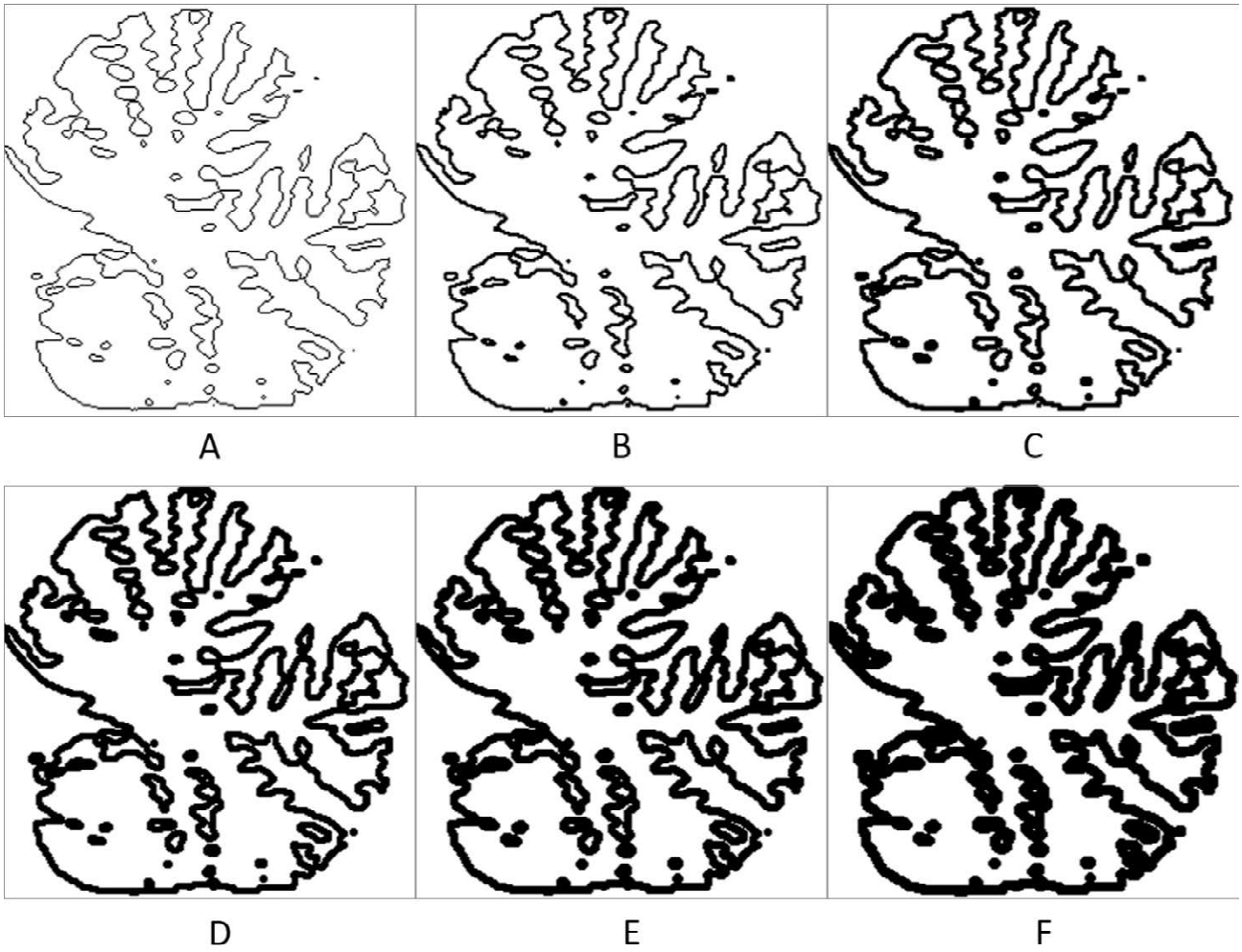

Fig. 6. Linear contour of the cerebellum, outline of the outer contour with a line of different width: A - 1 pixel; B - 2 pixels, C - 3 pixels, D - 4 pixels, E - 5 pixels, F - 6 pixels. Image resolution - 256 pixels per inch (image size 256x256 pixels).

The difference in fractal dimension values determined by the Box counting method on images of different sizes and resolutions is due to the different relative widths of the contour line. For all three values of the resolution it is necessary to outline the contour with a line, using the minimum possible value - 1 pixel. However, for a 128x128 pixel image, 1 pixel will be 1/128 of the square of the image, for a 256x256 pixel image, 1 pixel will be 1/256 side, and for a 512x512 pixel image, 1/512 (see Figure 4). Therefore, under the same absolute width of the contour, the relative width of the contour decreases with increasing image size, which causes a difference in the values of the fractal dimension.

The next step was to study the effect of the absolute width of the line used to delineate the contour on the value of the fractal dimension. Because the Caliper method does not provide contour delineation, the effect of line width on fractal dimension values has only been studied for the Box counting method. During the preliminary preparation of the images, contours were drawn with lines from 1 to 6 pixels wide (Fig. 6). For the contour of the cerebellum and the Koch snowflake, the average image size was selected (256x256 pixels, resolution 256 pixels per inch, scale 2), for the contour of cerebral hemispheres - small size (512x400 pixels, resolution 128 pixels per inch, scale 1).

As can be seen from Figure 7, as the contour width increases, the fractal dimension of the three objects studied increases. That is, the value of the fractal dimension determined by the method of Box counting is affected not only by the complexity of the spatial configuration of the linear fractal, but also the width of the linear contour.

Discussion

Taking into account the results of comparative analysis of two methods of fractal analysis of linear contours of artificial and natural linear fractals, we can conclude that the FD values determined by Box counting are significantly influenced by both relative and absolute line widths of the studied linear fractal. Our conclusions are consistent with the data of King R.D., etc.: when performing fractal analysis

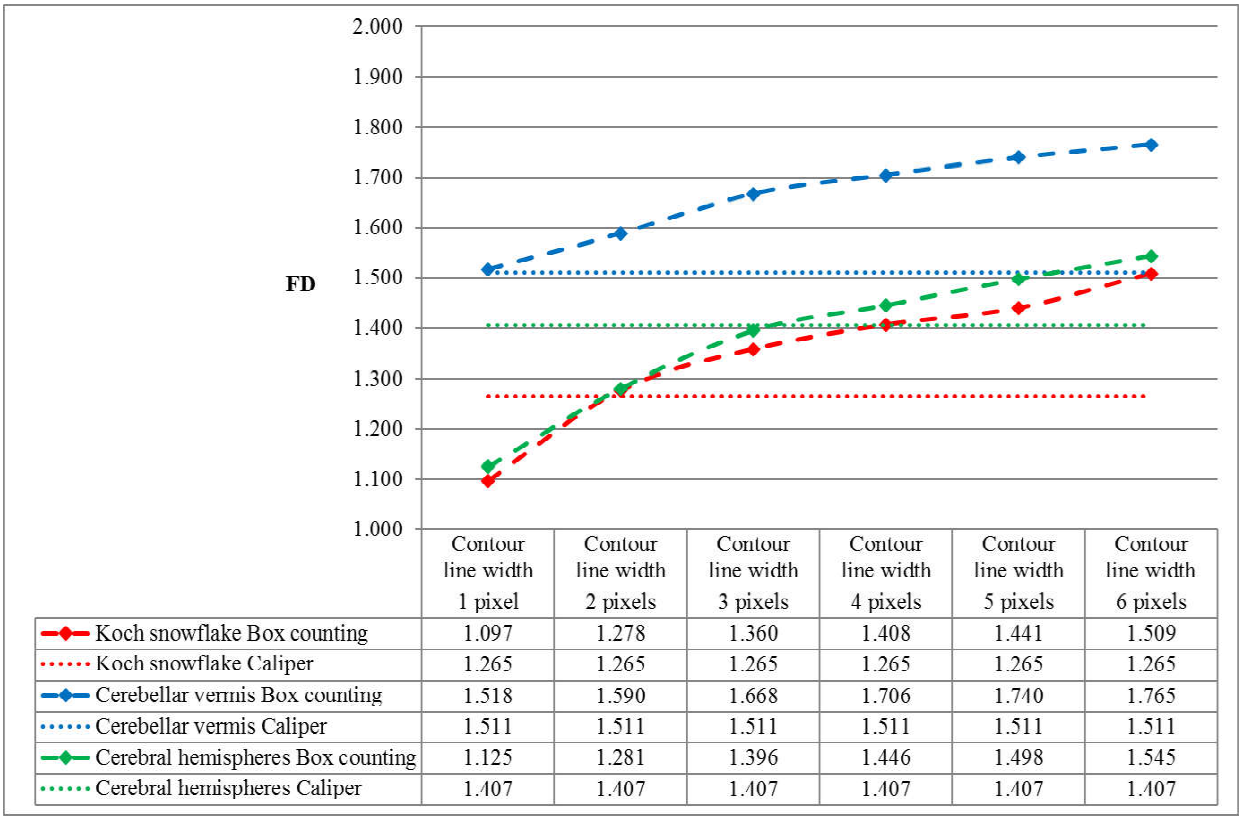

	Contour line width 1 pixel	Contour line width 2 pixels	Contour line width 3 pixels	Contour line width 4 pixels	Contour line width 5 pixels	Contour line width 6 pixels
Koch snowflake Box counting	1.097	1.278	1.360	1.408	1.441	1.509
Koch snowflake Caliper	1.265	1.265	1.265	1.265	1.265	1.265
Cerebellar vermis Box counting	1.518	1.590	1.668	1.706	1.740	1.765
Cerebellar vermis Caliper	1.511	1.511	1.511	1.511	1.511	1.511
Cerebral hemispheres Box counting	1.125	1.281	1.396	1.446	1.498	1.545
Cerebral hemispheres Caliper	1.407	1.407	1.407	1.407	1.407	1.407

Fig. 7. Fractal dimensional (FD) values determined on images with different linear contour widths using the Box counting method. For comparison, the FD values obtained using the Caliper method on images with identical size and resolution are given.

of the cerebral cortex using the method of Box counting, it was found that the thickness of the cortex has an effect on the value of FD, comparable to the effect of girification index, which characterizes the severity, complexity and number of convolutions of the cortex [8].

The method of Box counting in the two-dimensional version involves the use of a two-dimensional fractal measure - fractal squares. Therefore, the value of the fractal dimension is influenced not only by the length of the line, but also its width: the greater the width of the line, the more squares of the fractal grid this line will fall, the greater the value of the fractal dimension. Therefore, it is better to use the Box counting method to study objects that are close in configuration to the plane, or in cases where not only the length and complexity of the fractal line configuration but also its width must be taken into account. For example, atrophic changes in the cerebral cortex lead not only to smoothing the surface of the cortex, but also to reducing its thickness [7, 8].

Unlike the Box counting method, the Caliper method involves the use of a one-dimensional fractal measure that takes into account only one linear fractal size, namely its length. The width of the fractal line is not taken into account, which eliminates the effect of both the absolute width of the line and the relative width of the linear contour, which may differ in images of different sizes. Contour delineation is a necessary step in the preliminary preparation of images for the study of contours using the method of Box counting. But the images studied can have different quality, size and resolution, so the line width is difficult to standardize. The Caliper method does not require standardization of the image pre-algorithm and selection of the optimal line width, as contour delineation is not used. Therefore, the Caliper method is optimal for fractal analysis of linear fractals, especially in cases where you want to assess the complexity of the spatial configuration of the fractal line, leveling its width.

The two methods of fractal analysis analyzed in this work were used in our previous work to study the external linear contour of the cerebellum [16], fractal dimension values determined by two methods on 30 MR images of cerebellar vermis did not differ statistically significantly.

Both methods of fractal analysis in the classical version (Ruler (Caliper) and Box counting) were used to analyze the linear contours of benign and malignant breast tumors to interpret the results of mammography [17, 19], fractal dimension values obtained by two methods were close, but differed significantly in the contours of benign and malignant tumors, so both methods of fractal analysis allowed to reliably differentiate benign and malignant tumors.

In neuromorphological studies of the dendritic tree of neurons, a modified Richardson method (Caliper) was used in comparison with the Box counting method [20, 24].

In these studies, the dendritic tree of neurons was divided into linear segments and the analysis of each of the segments was performed by manual calculation, the fractal dimension of the dendritic tree as a whole was determined by the sum of measurements. The authors demonstrated that the Box counting method is sensitive to image orientation and to the presence or absence of skeletonization, and the Richardson method is independent of these factors and does not require the use of a grid for analysis [20]. The analysis of the dendritic tree of superficial and deep pyramidal neurons of the cerebral cortex of rats was performed; the fractal dimension of the dendritic tree of these neurons was statistically significantly different, but the level of statistical significance of the difference in FD values obtained by the modified Richardson method (Caliper) was significantly higher than the level of statistical significance of the difference in FD values obtained by Box counting [24].

Thus, taking into account the results of our research and the research of other scientists, we can conclude that the Caliper method is an effective method of mathematical image analysis in medicine, which has significant advantages in studying the linear contours of anatomical structures compared to the current Box counting method which is currently the most popular and used in the vast majority of studies.

Conclusion

1. Fractal analysis of linear fractals using the Caliper method allows to obtain values of fractal dimension that do not differ from the true value of the fractal dimension of artificial linear fractals; the values obtained using the Box counting method do not match the true values in some cases.

2. The values of the fractal dimension of linear fractals determined by the Caliper method do not depend on the size and resolution of the images. Fractal dimension values calculated using the Box counting method decrease as the image size and resolution increase.

3. The values of the fractal dimension of linear fractals, calculated using the method of Box counting, increase with increasing width of the linear contour; the values calculated using the Caliper method do not depend on the width of the contour line.

4. For fractal analysis of linear fractals (including linear contours of anatomical structures), preference should be given to the Caliper method and its modifications.

References

[1] Addison, P.S. (1997). *Fractals and chaos: an illustrated course.* CRC Press.

[2] Chikui, T., Tokumori, K., Yoshiura, K., Oobu, K., Nakamura, S., & Nakamura, K. (2005). Sonographic texture characterization of salivary gland tumors by fractal analyses. *Ultrasound in Medicine & Biology,* 31(10), 1297-1304. doi: 10.1016/j.ultrasmedbio.2005.05.012

[3] Di Ieva, A., Esteban, F.J., Grizzi, F., Klonowski, W., & Martin-Landrove, M. (2015). Fractals in the neurosciences, part II: clinical applications and future perspectives. *The Neuroscientist,* 21(1), 30-43. doi: 10.1177/1073858413513928

[4] Di Ieva, A., Grizzi, F., Jelinek, H., Pellionisz, A.J., & Losa, G.A. (2014). Fractals in the neurosciences, part I: general principles and basic neurosciences. *The Neuroscientist,* 20(4), 403-417. doi: 10.1177/1073858413513927

[5] Fernandez, E., & Jelinek, H.F. (2001) Use of fractal theory in neuroscience: methods, advantages, and potential problems. *Methods,* 24(4), 309-321. doi: 10.1006/meth.2001.1201

[6] Jelinek, H.F., & Fernandez, E. (1998). Neurons and fractals: how reliable and useful are calculations of fractal dimensions?. *Journal of Neuroscience Methods*, 81(1-2), 9-18. doi: 10.1016/s0165-0270(98)00021-1

[7] King, R.D., Brown, B., Hwang, M., Jeon, T., George, A.T., & Alzheimer's Disease Neuroimaging Initiative. (2010). Fractal dimension analysis of the cortical ribbon in mild Alzheimer's disease. *Neuroimage,* 53(2), 471-479. doi: 10.1016/j.neuroimage.2010.06.050

[8] King, R.D., George, A.T., Jeon, T., Hynan, L.S., Youn, T.S., Kennedy, D.N., Dickerson, B. & Alzheimer's Disease Neuroimaging Initiative. (2009). Characterization of Atrophic Changes in the Cerebral Cortex Using Fractal Dimensional Analysis. *Brain Imaging and Behavior,* 3(2), 154-166. doi: 10.1007/s11682-008-9057-9

[9] Kiselev, V.G., Hahn, K.R., & Auer, D.P. (2003). Is the brain cortex a fractal? *Neuroimage,* 20(3), 1765-1774. doi: 10.1016/s1053-8119(03)00380-x

[10] Lauwerier, H. (1991). *Fractals: endlessly repeated geometrical figures.* ICON Group International.

[11] Lee, K.I., Choi, S.C., Park, T.W., & You, D.S. (1999). Fractal dimension calculated from two types of region of interest. *Dento Maxillo Facial Radiology,* 28(5), 284-289. doi: 10.1038/sj/dmfr/4600458

[12] Mandelbrot, B. B. (1982). *The Fractal Geometry of Nature.* N.Y.: W.H.Freeman & Co.

[13] Mandelbrot, B.B. (1977). *Fractals - Form, Chance and Dimension.* San Francisco: W.H. Freeman & Co.

[14] Mandelbrot, B.B. (1967). How Long Is the Coast of Britain? Statistical Self-Similarity and Fractional Dimension. *Science, New Series,* 3775(156), 636-638.

[15] Maryenko, N.I., & Stepanenko, O.Yu. (2021). Fractal analysis as a method of morphometric study of linear anatomical objects: modified Caliper method. *Reports of Morphology,* 27(4), 28-34. doi: 10.31393/morphology-journal-2021-27(4)-04

[16] Maryenko, N.I., & Stepanenko, O.Yu. (2021). Fractal dimension of external linear contour of human cerebellum (magnetic resonance imaging study). *Reports of Morphology,* 27(2), 16-22. doi: 10.31393/morphology-journal-2021-27(2)-03

[17] Raguso, G., Ancona, A., Chieppa, L., L'abbate, S., Pepe, M.L., Mangieri, F. ... Rangayyan, R.M. (2010, January). Application of fractal analysis to mammography. In: *2010 Annual International Conference of the IEEE Engineering in Medicine and Biology* (pp. 3182-3185). IEEE. doi: 10.1109/IEMBS.2010.5627180

[18] Rajković, N., Krstonošić, B., & Milošević, N. (2017). Box-counting method of 2D neuronal image: method modification and quantitative analysis demonstrated on images from the monkey and human brain. *Computational and mathematical methods in medicine,* 2017, 8967902. doi: 10.1155/2017/8967902

[19] Rangayyan, R. M., & Nguyen, T. M. (2007). Fractal analysis of contours of breast masses in mammograms. *Journal of digital imaging,* 20(3), 223-237. doi: 10.1007/s10278-006-0860-9
[20] Ristanović, D., Stefanović, B.D., & Puskas, N. (2013). Fractal analysis of dendrites morphology using modified Richardson's and Box counting method. *Theoretical biology forum*, 106(1-2), 157-168.
[21] Ristanović, D., Stefanović, B. D., & Puskać, N. (2014). Fractal analysis of dendrite morphology of rotated neuronal pictures: the modified Box counting method. *Theoretical biology forum*, 107(1-2), 109-121.
[22] Schneider, C.A., Rasband, W.S., & Eliceiri, K.W. (2012). NIH Image to ImageJ: 25 years of image analysis. *Nature methods,* 9(7), 671-675. doi: 10.1038/nmeth.2089
[23] Shrout, M.K., Potter, B.J., & Hildebolt, C.F. (1997). The effect of image variations on fractal dimension calculations. *Oral Surgery, Oral Medicine, Oral Pathology, Oral Radiology, and Endodontics,* 84(1), 96-100. doi: 10.1016/s1079-2104(97)90303-6
[24] Zaletel, I., Ristanović, D., Stefanović, B.D., & Puskać, N. (2015). Modified Richardson's method versus the box-counting method in neuroscience. *Journal of Neuroscience Methods,* (242), 93-96. doi: 10.1016/j.jneumeth.2015.01.013

ФРАКТАЛЬНИЙ АНАЛІЗ ЛІНІЙНИХ КОНТУРІВ АНАТОМІЧНИХ СТРУКТУР: АВТОРСЬКА МОДИФІКАЦІЯ СПОСОБУ CALIPER ПОРІВНЯНО ЗІ СПОСОБОМ BOX COUNTING

Мар'єнко Н.І., Степаненко О.Ю.

Фрактальний аналіз дозволяє оцінити метричну розмірність та складність просторової конфігурації різних анатомічних структур, що дозволяє використовувати цей математичний метод для морфометрії у морфології та клінічній медицині. Для фрактального аналізу лінійних фрактальних об'єктів найчастіше використовують два способи фрактального аналізу: спосіб підрахунку квадратів (Box counting, Grid method) та спосіб Caliper (спосіб Річардсона, Perimeter stepping method, Ruler method, Divider dimension, Compass dimension, Yard stick method). Мета дослідження - порівняльний аналіз двох способів фрактального аналізу - способу Box counting та авторської модифікації способу Caliper для фрактального аналізу лінійних контурів анатомічних структур. Був проведений фрактальний аналіз трьох лінійних фракталів: штучного фракталу - сніжинки Коха та двох природніх фракталів - зовнішніх контурів піальної поверхні кори мозочка людини та кори великих півкуль головного мозку. Фрактальний аналіз проводився за допомогою способу Box counting та авторської модифікації способу Caliper. Значення фрактальної розмірності штучного лінійного фракталу (сніжинки Коха), отримані за допомогою способу Caliper, збігаються із істинним значенням фрактальної розмірності цього фракталу, але значення фрактальної розмірності, отримані за допомогою способу Box counting, із істинним значенням фрактальної розмірності не співпадають. Тому фрактальний аналіз лінійних фракталів за допомогою способу Caliper дозволяє отримати правдивіші результати, ніж спосіб Box counting. Значення фрактальної розмірності штучного та природних фракталів, обчислені за допомогою способу Box counting, зменшуються при збільшенні розміру та роздільної здатності зображення; при використанні способу Caliper значення фрактальної розмірності від цих параметрів зображення не залежать. Значення фрактальної розмірності лінійних фракталів, обчислені за допомогою способу Box counting, зростають при збільшенні ширини лінійного контуру; значення, обчислені за допомогою способу Caliper, не залежать від ширини лінії. Таким чином, для фрактального аналізу лінійних фракталів перевага має надаватися способу Caliper та його модифікаціям.

Ключові слова: *фрактальний аналіз, морфометрія, лінійний контур, Caliper, Box counting.*

DOI: 10.31393/morphology-journal-2022-28(1)-04 Reports of Morphology, Vol. 28, №1, Pages 27-33

ISSN 1818-1295 eISSN 2616-6194

REPORTS OF MORPHOLOGY

Official Journal of the Scientific Society of Anatomists, Histologists, Embryologists and Topographic Anatomists of Ukraine

journal homepage: https://morphology-journal.com

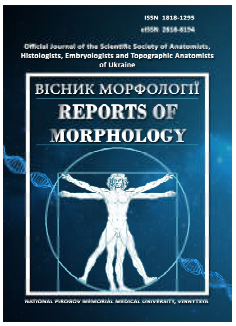

CT assessment of the height of the coronary arteries orifice location and the height of the aortic sinuses in women with structural changes in the coronary arteries

Pidvalna U. Ye.[1], Beshley D. M.[1,2,3], Mateshuk-Vatseba L. R.[1]

[1]Danylo Halytsky National Medical University of Lviv, Lviv, Ukraine
[2]Municipal Non-Profit Enterprise of the Lviv Regional Council "Lviv Regional Clinical Hospital", Lviv, Ukraine
[3]Ukrainian-Polish Heart Center "Lviv", Lviv, Ukraine

ARTICLE INFO
Received: 23 November 2021
Accepted: 27 December 2021

UDC: 611.132.2:616.132.2:616.132.11]-055.2-073.756.8

CORRESPONDING AUTHOR
e-mail: Uljaska.p@gmail.com
Pidvalna U.Ye.

CONFLICT OF INTEREST
The authors have no conflicts of interest to declare.

FUNDING
Not applicable.

The most common form of cardiovascular disease in Ukraine is coronary heart disease, which is characterized by damage to the coronary arteries. The height of the aortic sinuses and the height of the coronary arteries are assessed when planning interventional procedures and cardiac surgery. Computed tomography can verify structural changes in the coronary arteries and morphometrically evaluate the components of the aortic sac. The purpose of the study: to measure the height of the coronary arteries orifice; height of the aortic sinuses in women with structural changes of the coronary arteries using computed tomography and assess the interdependence of measurements with anthropometric indicators (age, height, weight, body mass index, body surface area). Computed tomography-angiography of the chest of females with coronary arteries were processed. Statistical analysis: Shapiro-Francia test (correctness of distribution), Student's t-test (comparison of the height of the coronary arteries and the height of the aortic sinuses); Pearson's linear correlation; Fisher's multifactorial regression analysis. The study found a direct correlation between height and measurability in women with coronary artery disease. The value of the growth rate was directly correlated with the height of the right aortic sinus (r=0.85, p=0.001), with the height of the lower edge of the right coronary artery orifice (r=0.74, p=0.01), the height of the upper edge of the left coronary artery orifice (r=0.67, p=0.03), the height of the upper edge of the right coronary artery orifice (r=0.67, p=0.03). It is proved that with increasing body surface area, the parameters of the right aortic sinus decrease: the inverse strong correlation r=-0.83, p=0.002. Significant direct relationships have been established between most of the measured components of the aortic root. Multifactor regression analysis showed a proven strong effect of anthropometric data and age on the height of the right aortic sinus: R=0.96, at p=0.009 (according to Fisher). This made it possible to build a model for predicting the height of the right aortic sinus depending on anthropometric and age parameters. Thus, in women with structural lesions of the coronary arteries, the increase in height correlates with an increase in the height of the right aortic sinus, the height of the coronary arteries orifice. An increase in body surface area correlates with a decrease in the height of the right aortic sinus in women with structural lesions of the coronary arteries.

Keywords: *coronary artery orifice, anatomy, computed tomography, aorta, measurements, aortic sinuses.*

Introduction

According to the World Health Organization, cardiovascular disease (CVD) is the leading cause of death worldwide [17]. The most common form of CVD in Ukraine is coronary heart disease among both men and women [15]. The quality of life of women in Ukraine due to CVD is much worse than in neighboring Europe and the United States [10].

Coronary heart disease (CHD) is characterized by damage to the coronary arteries. The main cause of coronary heart disease is atherosclerotic lesions of the

coronary arteries, followed by calcium deposition. Computed tomography allows to determine the density of deposited calcium and verify structural changes in the coronary arteries [6]. The right and left coronary arteries originate from the corresponding aortic sinuses. The height of the aortic sinuses and the height of the coronary arteries are important clinically when planning endovascular interventions [1, 4, 5].

The purpose of the study: to measure the height of the right and left coronary arteries orifice; height of the right, left and posterior aortic sinuses in women with structural changes of the coronary arteries using computed tomography and to assess the interdependence of measurements with anthropometric indicators.

Materials and methods

The research was conducted in accordance with the Declaration of Helsinki and the **Bioethics Commission** of the Danylo Halytsky Lviv National Medical University (№10 of 2021). All patients or officials provided informed consent to participate in the study.

The material of the study was computed tomography-angiography (CT) of the thoracic organs of females with coronary artery disease. Inclusion criteria: women over 18 years of age; structural changes of coronary arteries (coronary artery calcification; density measurement according to Hounsfield units (HU)); no history of coronary artery bypass grafting and coronary artery stenting. Exclusion criteria: females with congenital malformations or anomalies of the cardiovascular system; persons with damage to heart valves or heart vessels; history of cardiac surgery or endovascular interventions; artifacts; incomplete clinical data. Of the 143 surveys analyzed, 11 people met these criteria, which were further divided into 2 groups: 1 group with a height of less than 1.60 m (n=5), 2 group - with a height of more than 1.61 m (n=6). Clinical data used: age, height, body weight, based on which the body mass index (BMI) and body surface area (BSA) were calculated (according to Mosteller's formula).

The study was performed on a LightSpeed 64 VCT XT, GE (General Electric, USA) CT scanner according to a standard protocol. Contrast - Ultravist 470 (Bayer Healthcare, Germany). Analysis of the image and measurement of the height of the coronary arteries, the height of the aortic sinuses (Valsalva sinuses) was performed according to the instructions [2] at the appropriate station with licensed software (General Electric, USA). Data are given in millimeters. The measurements were performed independently by two doctors.

Statistical analysis: software R version 4.0.5 (R Core Team, 2021) based on the Windows XP operating system [13]. Correctness of distribution: Shapiro-Francia test. Comparison of mean values: Student's t-test. Correlation analysis: Pearson's linear correlation (r). Multifactor regression analysis: Fisher. Data presented: arithmetic mean ± standard deviation (M±SD), absolute figures. Significance level: $p<0.05$.

Results

According to the results of the analysis of CT of the chest of women with coronary artery disease, it was found that the largest value was the height of the posterior aortic sinus - 19.10±1.65 mm. Indicators of the height of the aortic sinuses and the height of the coronary arteries in women with structural lesions of the coronary arteries are presented in table 1. Visualization of the components of the aortic bulb and coronary arteries with structural lesions of the coronary arteries is presented in Figure 1.

A study of the correlation between anthropometric parameters and measured parameters in women with structural lesions of the coronary arteries showed a direct relationship between height and most indicators, indicating their growth with increasing height. In particular, the value of the growth rate directly correlated with the height of the right aortic sinus (r=0.85, p=0.001), with the height of the lower edge of the right coronary artery orifice (r=0.74, p=0.01), the height of the upper edge of the left coronary artery orifice (r=0.67, p=0.03), the height of the upper edge of the right coronary artery orifice (r=0.67, p=0.03) (Table 2).

It is proved that with the increase of the anthropometric index of BSA, the parameters of the height of the right aortic sinus decrease: the strong inverse correlation r=-0.83, p=0.002. There are also significant direct relationships between most of the measured components of the aortic root. In particular, the height of the posterior aortic sinus increased with increasing height of the left aortic sinus (r=0.80, p=0.003), the height of the lower edge of the left coronary artery orifice (r=0.71, p=0.01), the height of the lower edge of the right coronary artery orifice (r=0.70, p=0.02), the height of the upper edge of the left coronary artery orifice (r=0.67, p=0.02), the height of the upper edge of the right coronary artery orifice (r=0.64, p=0.03). The value of the height of the left aortic sinus was directly related, except for the height of the posterior aortic sinus, with the height of the lower edge of the left coronary artery orifice (r=0.80, p=0.003), with the height of the lower edge of the right coronary artery orifice (r=0.62, p=0.04) and with the height of the upper edge of the left coronary artery orifice (r=0.78, p=0.005). There is also a direct strong correlation between the height of the right aortic sinus and the height of the lower edge of the right coronary artery (r=0.76, p=0.01) and the medium strength relationship with the height of the upper edge of the right coronary artery orifice (r=0.63, p=0.04).

Table 1. Indicators of the height of the aortic sinuses and the height of the coronary arteries orifice in women with structural lesions of the coronary arteries (m±SD, mm).

Parameters	n=11
Height of the posterior aortic sinus	19.10±1.65
Height of the left aortic sinus	17.98±1.71
Height of the right aortic sinus	17.00±1.34
Height of the left coronary artery orifice	11.69±2.04
Height of the right coronary artery orifice	12.07±2.17

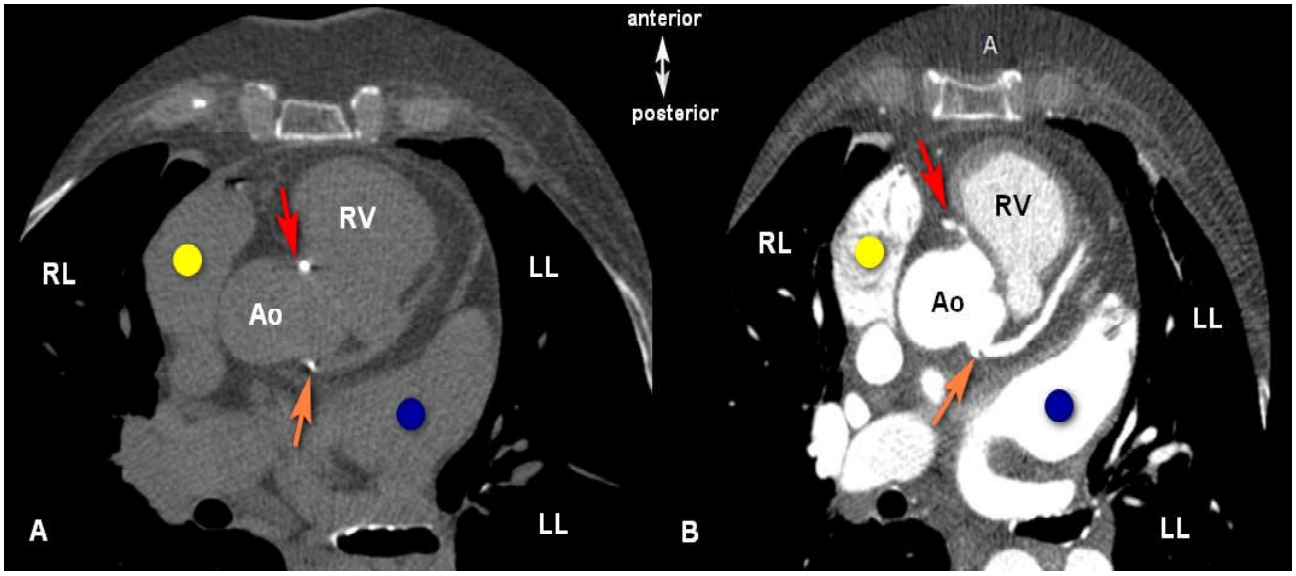

Fig. 1. Visualization of the components of the aortic bulb and coronary arteries in structural lesions of the coronary arteries. Image A, without and B, with the introduction of a contrast agent. Ascending aorta (*Ao*), right ventricle (*RV*), auricula atrii (*yellow circle*), left atrium (*blue circle*), right lung (*RL*), left lung (*LL*). A - calcium deposits in the projection of the right coronary artery (*red arrow*) and the left coronary artery (*orange arrow*). High calcium density is well visualized on examination without contrast. B - contrasting right coronary artery (*red arrow*) and left coronary artery (*orange arrow*). Chest computed tomography, axial section.

Table 2. Correlations (r) between coronary artery orifice height indicators and other studied parameters in women with coronary artery disease.

Indexes		Posterior AS	Left AS	Right AS	LCAI	RCAI	LCAu	RCAu
Age	r	-0.38	-0.19	-0.08	-0.37	-0.06	-0.40	-0.09
	p	*0.25*	*0.58*	*0.81*	*0.27*	*0.86*	*0.23*	*0.79*
Height	r	0.44	0.56	**0.85**	0.54	**0.74**	**0.67**	**0.67**
	p	*0.18*	*0.07*	***0.001***	*0.08*	***0.01***	***0.03***	***0.03***
Weight	r	0.03	-0.26	-0.58	0.01	-0.26	0.07	-0.01
	p	*0.94*	*0.44*	*0.06*	*0.98*	*0.43*	*0.84*	*0.97*
BMI	r	-0.16	-0.43	**-0.83**	-0.21	-0.53	-0.21	-0.30
	p	*0.64*	*0.18*	***0.002***	*0.54*	*0.09*	*0.54*	*0.38*
BSA	r	0.13	-0.14	-0.36	0.12	-0.07	0.24	0.17
	p	*0.70*	*0.68*	*0.28*	*0.72*	*0.84*	*0.49*	*0.62*
Left AS	r	**0.80**		0.53	**0.80**	**0.62**	**0.78**	0.57
	p	***0.003***		*0.10*	***0.003***	***0.04***	***0.005***	*0.07*
Posterior AS	r		**0.80**	0.36	**0.71**	**0.70**	**0.67**	**0.64**
	p		***0.003***	*0.28*	***0.01***	***0.02***	***0.02***	***0.03***
Right AS	r	0.36	0.53		0.42	**0.76**	0.45	**0.63**
	p	*0.28*	*0.10*		*0.20*	***0.01***	*0.16*	***0.04***
LCAI	r	**0.71**	**0.80**	0.42		0.49	**0.77**	0.47
	p	***0.01***	***0.003***	*0.20*		*0.13*	***0.01***	*0.14*
RCAI	r	**0.70**	**0.62**	**0.76**	0.49		0.45	**0.93**
	p	***0.02***	***0.04***	***0.01***	*0.13*		*0.17*	***0.001***
LCAu	r	**0.67**	**0.78**	0.45	**0.77**	0.45		0.47
	p	***0.02***	***0.005***	*0.16*	***0.01***	*0.17*		*0.15*

Continuation of table 2.

Indexes		Posterior AS	Left AS	Right AS	LCAl	RCAl	LCAu	RCAu
RCAu	r	**0.64**	0.57	**0.63**	0.47	**0.93**	0.47	
	p	***0.03***	*0.07*	***0.04***	*0.14*	***0.001***	*0.15*	

Notes: Posterior AS - posterior aortic sinus; Left AS - left aortic sinus; Right AS - right aortic sinus; LCAl - height of the lower edge of the left coronary artery orifice; LCAu - the height of the upper edge of the left coronary artery orifice; RCAl - the height of the lower edge of the right coronary artery orifice; RCAu - height of the upper edge of the right coronary artery orifice, BMI - body mass index; BSA - body surface area.

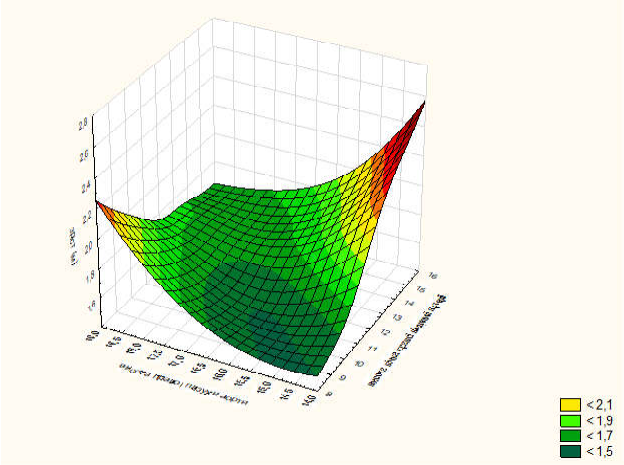

Fig. 2. Relationship between growth rates, right aortic sinus height and lower right margin coronary artery orifice height in women with coronary artery structural changes.

Table 3. The results of logistic regression calculations for predicting the size of the height of the right aortic sinus in women with structural changes of the coronary arteries.

Indicator	Symbol	Coefficient
Constant		-42.63
age	A1	-0.011
height	A2	11.05
weight	A3	-0.830
BMI	A4	0.616
BSA	A5	47.63

Notes: BMI - body mass index; BSA - body surface area.

The interdependence between the heights of the upper and lower edges of the coronary arteries is absolutely logical. In particular, the height of the lower edge of the left coronary artery orifice, in addition to the above connections, was also interdependent with the height of the upper edge of the left coronary artery orifice: strong direct connection (r=0.77, p=0.01), and the height of the lower edge of the right coronary artery with the height of the upper edge of the right coronary artery orifice: direct strong connection (r=0.93, p=0.001). A graphical representation of the relationship between height of person and height of the right aortic sinus and the height of the lower edge of the right coronary artery orifice is shown in Figure 2.

Multifactor regression analysis between independent predictors (anthropometric parameters and age) and dependent (aortic sinus height and coronary artery orifice height) in women with coronary artery structural changes showed a proven direct strong effect of anthropometric data and age on right aortic sinus height: R=0.96, at p=0.009 (according to Fisher) and a standard error of 0.53. The adjusted coefficient of multiple determination was R^2_{adj}=0.84, which indicates the proven effect of the complex of these independent predictors on the height of the right aortic sinus in 84% of cases. This made it possible to build a model for predicting the size of the right aortic sinus depending on anthropometric and age parameters. The necessary components are given in Table 3.

Taking into account the calculations, the linear equation of logistic regression relative to the predicted size of the height of the right aortic sinus in women with coronary artery disease will look like:

Height size = - 0.011 x A1 + 11.05 x A2 - 0.830 x A3 + 0.616 x A4 + 47.63 x A5 - 42.63

The average predicted value of the height of the right aortic sinus is 17.00±1.29 mm (minimum value 14.55 mm, maximum 18.98 mm), which coincides with the actual average value of 17.00±1.34 mm. The work of this logistic model was tested on the studied patients with different anthropometric and age parameters, which were selected from the general primary patient base. Below are two practical examples of the model.

Example №1. Patient №6 in the database: female, 63 years old, height 1.55 m, weight 110 kg, BMI 45.79 kg/m^2, BSA 2.18 m^2. According to the CT of the chest, the height of the right aortic sinus is 14.6 mm.

Substituting the patient's data, we obtain a linear equation:

Height size = -0.011 x 63 + 11.05 x 1.55 - 0.830 x 110 + 0.616 x 45.79 + 47.63 x 2.18 - 42.63 = 14.54 mm

Thus, the predicted value almost coincides with the actual value obtained by CT diagnosis.

Example №2. Patient №10 in the database: female, 70 years old, height 1.70 m, weight 85 kg, BMI 29.41 kg/m^2, BSA 2.00 m^2. According to the CT of the chest, the height of the right aortic sinus is 18.3 mm. Substituting the patient's data, we obtain a linear equation:

Height size = -0.011 x 70 + 11.05 x 1.70 - 0.830 x 85 + 0.616 x 29.41 + 47.63 x 2.00 - 42.63 = 18.20 mm

In this case, the predicted value is also very close to the actual value obtained by CT.

Thus, the use of this model may allow the rapid calculation of the size of the height of the right aortic sinus in women with structural changes in the coronary arteries when planning endovascular interventions or cardiac surgery. A

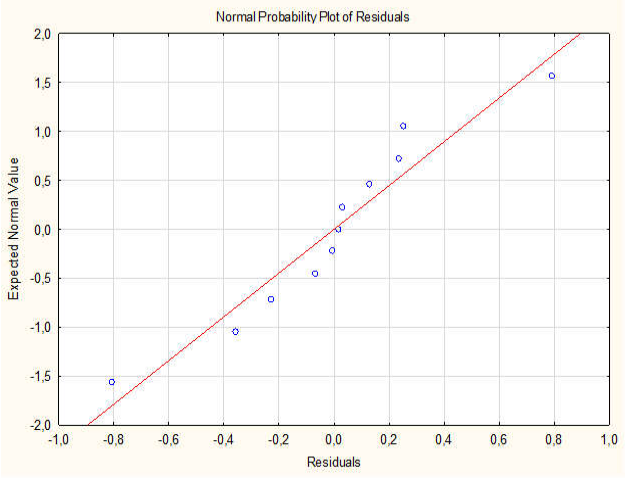

Fig. 3. Normal probability of influence of predictors on the predicted value of the height of the right aortic sinus in women with structural changes of the coronary arteries.

Table 4. Distribution of aortic sinus height and coronary artery orifice height (according to CT) in groups of women with structural changes of coronary arteries. Distribution by groups by height (M±SD, mm).

Indexes	1 group (women with height smaller than 1.60 m), n=5	2 group (women with height more than 1.61 m), n=6	p
Height of the posterior aortic sinus	18.06±1.85	19.97±0.87	0.06
Height of the left aortic sinus	16.68±1.49	19.07±0.97	0.013
Height of the right aortic sinus	15.78±0.78	18.02±0.63	0.001
The height of the lower edge of the left coronary artery orifice	10.55±2.39	12.65±1.15	0.11
The height of the lower edge of the right coronary artery orifice	10.07±1.21	13.73±0.96	0.0004
The height of the upper edge of the left coronary artery orifice	14.56±1.79	16.40±1.23	0.08
The height of the upper edge of the right coronary artery orifice	12.94±1.36	16.32±1.02	0.001

graphical representation of the normal probability of predictors influencing the predicted value of the right aortic sinus height is shown in Figure 3.

In comparing the dependence of other measured aortic parameters on anthropometric and age indicators by multifactorial regression analysis, no significant relationship was found between the studied data in women with structural changes of the coronary arteries: multiple correlation coefficient R = from 0.66 to 0.87, adjusted coefficient of multiple determination R^2_{adj} = from -0.13 to 0.51, at p>0.05 (according to Fisher).

A comparison of the height of the aortic sinuses and the height of the coronary arteries in women with structural changes in the coronary arteries by different growth groups showed that all studied parameters had a higher height in the second group (height over 1.61 m) compared to the first group (women's height less than 1.60 m). The height of the left aortic sinus was proved to be higher in the second group: 19.07±0.97 mm against 16.68±1.49 mm (p=0.013) in the first group; indicators of the height of the right aortic sinus: 18.02±0.63 mm against 15.78±0.78 mm (p=0.001); indicators of height of the lower edge of the right coronary artery orifice: 13.73±0.96 mm against 10.07±1.21 mm (p=0.0004), indicators of height of departure of the upper edge of the right coronary artery orifice: 16.32±1.02 mm against 12.94±1.36 mm (p=0.001) accordingly (Table 4). Other studied indicators were higher in the second group than in the first, but the difference was insignificant (p>0.05).

Discussion

In 2019, about 17.9 million people died from CVD. In low- and middle-income countries, including Ukraine, the proportion of CVD deaths is over 75% [17]. Analysis of the incidence rate from 1990 to 2019 shows a lack of positive dynamics [10]. Given the disappointing trend, steps are being taken to reduce the increase in morbidity and mortality due to CVD. According to the Resolution of the Ministry of Health and the National Academy of Medical Sciences of Ukraine, there is the State Program for Prevention, Treatment and Rehabilitation of Cardiovascular Diseases (2017-2021) (dated 15.07.2016 №711/61). In the Program of Medical Guarantees of the National Health Service of Ukraine, the treatment of acute myocardial infarction remains a priority.

Morphometric analysis of the components of the aortic bulb is taken into account when performing cardiac and cardiac surgical procedures. It is important to take into account anthropometric indicators. If the world data is sufficiently complete [3, 7, 8, 11], the relevant publications are just beginning to appear in Ukraine [9].

The study measured the height of the coronary arteries orifice and the height of the aortic sinuses in women with structural changes of the coronary arteries using computed tomography and evaluated the interdependence of measurements with anthropometric indicators. Using the correlation between anthropometric parameters (age, height, body weight, body mass index, body surface area) and measured parameters (height of the coronary arteries orifice and height of the right, left, posterior aortic sinuses) in women with structural lesions of the coronary arteries proved the presence of a direct relationship between growth and most of the studied indicators of the aortic bulb, which indicates their growth with increasing of height. In fact, higher height correlates with a lower risk of morbidity and mortality from cardiovascular disease [14, 18]. In contrast, an increase in body surface area correlates with a decrease in the height of the right aortic sinus (strong inverse correlation).

The use of multifactor regression analysis between independent predictors (anthropometric indicators and age) and dependent (aortic sinus height and coronary artery orifice height) in women with structural changes of coronary arteries showed a proven strong effect of anthropometric data and age on right aortic sinus height. Analysis of the

relationship between age and aortic bulb parameters varies between different study groups [3, 12, 16].

The proved influence of the complex of independent predictors on the height of the right aortic sinus made it possible to build a model for predicting the size of the right aortic sinus height depending on anthropometric and age parameters. This model can be used to quickly calculate the height of the right aortic sinus in women with structural changes in the coronary arteries when planning endovascular interventions or cardiac surgery.

Conclusion

In women with structural lesions of the coronary arteries, the increase in height correlates with an increase in the height of the right aortic sinus, the height of the upper edge of the left coronary artery orifice, the height of the upper and lower edges of the right coronary artery orifice. An increase in body surface area correlates with a decrease in the height of the right aortic sinus in women with structural lesions of the coronary arteries.

References

[1] Berdajs, D. A. (2016). Aortic root morphology: a paradigm for successful reconstruction. *Interactive cardiovascular and thoracic surgery*, 22(1), 85-91. doi: 10.1093/icvts/ivv290

[2] Blanke, P., Weir-McCall, J. R., Achenbach, S., Delgado, V., Hausleiter, J., Jilaihawi, H., ... & Leipsic, J. A. (2019). Computed tomography imaging in the context of transcatheter aortic valve implantation (TAVI)/transcatheter aortic valve replacement (TAVR) an expert consensus document of the Society of Cardiovascular Computed Tomography. *JACC: Cardiovascular Imaging,* 12(1), 1-24. doi: 10.1016/j.jcct.2018.11.008

[3] Forte, E., Punzo, B., Salvatore, M., Maffei, E., Nistri, S., Cavaliere, C., & Cademartiri, F. (2020). Low correlation between biometric parameters, cardiovascular risk factors and aortic dimensions by computed tomography coronary angiography. *Medicine,* 99(35). doi: 10.1097/MD.0000000000021891

[4] Heitkemper, M., Sivakumar, S., Hatoum, H., Dollery, J., Lilly, S. M., & Dasi, L. P. (2021). Simple 2-dimensional anatomic model to predict the risk of coronary obstruction during transcatheter aortic valve replacement. *The Journal of thoracic and cardiovascular surgery,* 162(4), 1075-1083. doi: 10.1016/j.jtcvs.2020.01.085

[5] Hennessey, B., Vera-Urquiza, R., Mejia-Renteria, H., Gonzalo, N., & Escaned, J. (2020). Contemporary use of coronary computed tomography angiography in the planning of percutaneous coronary intervention. *The International Journal of Cardiovascular Imaging,* 36(12), 2441-2459. doi: 10.1007/s10554-020-02052-8

[6] Jinnouchi, H., Sato, Y., Sakamoto, A., Cornelissen, A., Mori, M., Kawakami, R., ... & Finn, A. V. (2020). Calcium deposition within coronary atherosclerotic lesion: Implications for plaque stability. *Atherosclerosis,* 306, 85-95. doi: 10.1016/j.atherosclerosis.2020.05.017

[7] Merz, A. A., & Cheng, S. (2016). Sex differences in cardiovascular ageing. *Heart,* 102(11), 825-831. doi: 10.1136/heartjnl-2015-308769

[8] Nasr, A. Y., & El Tahlawi, M. (2018). Anatomical and radiological angiographic study of the coronary ostia in the adult human hearts and their clinical significance. *Anatomy & cell biology,* 51(3), 164-173. doi: 10.5115/acb.2018.51.3.164

[9] Pidvalna, U. Y., Beshley, D. M., Mirchuk, M. Z., & Mateshuk-Vatseba, L. R. (2021). Normal values of coronary arteries branching height in women. *Reports of Morphology,* 27(4), 41-46. doi: 10.31393/morphology-journal-2021-27(4)-06

[10] Roth, G. A., Mensah, G. A., Johnson, C. O., Addolorato, G., Ammirati, E., Baddour, L. M., ... & GBD-NHLBI-JACC Global Burden of Cardiovascular Diseases Writing Group. (2020). Global burden of cardiovascular diseases and risk factors, 1990-2019: update from the GBD 2019 study. *Journal of the American College of Cardiology,* 76(25), 2982-3021. doi: 10.1016/j.jacc.2020.11.010

[11] Silventoinen, K., Zdravkovic, S., Skytthe, A., McCarron, P., Herskind, A. M., Koskenvuo, M., ... & Kaprio, J. (2006). Association between height and coronary heart disease mortality: a prospective study of 35,000 twin pairs. *American Journal of Epidemiology*, 163(7), 615-621. doi: 10.1093/aje/kwj081

[12] Stolzmann, P., Knight, J., Desbiolles, L., Maier, W., Scheffel, H., Plass, A., ... & Alkadhi, H. (2009). Remodelling of the aortic root in severe tricuspid aortic stenosis: implications for transcatheter aortic valve implantation. *European radiology,* 19(6), 1316-1323. doi: 10.1007/s00330-009-1302-0

[13] Team, R. C. (2021). *R software (software environment for statistical computing and graphics), version 4.0.5.* Retrieved from https://www.r-project.org/

[14] Teraura, H., Suzuki, T., & Kotani, K. (2019). Association of taller stature with lower cardiovascular disease mortality in Asian people: a systematic review. *Journal of physiological anthropology,* 38(1), 1-5. doi: 10.1186/s40101-019-0197-y

[15] Vos, T., Lim, S. S., Abbafati, C., Abbas, K. M., Abbasi, M., Abbasifard, M., ... & Bhutta, Z. A. (2020). Global burden of 369 diseases and injuries in 204 countries and territories, 1990-2019: a systematic analysis for the Global Burden of Disease Study 2019. *The Lancet,* 396(10258), 1204-1222. doi: 10.1016/S0140-6736(20)30925-9

[16] Wang, X., Ren, X. S., An, Y. Q., Hou, Z. H., Yu, Y. T., Lu, B., & Wang, F. (2021). A Specific Assessment of the Normal Anatomy of the Aortic Root in Relation to Age and Gender. *International Journal of General Medicine,* 14, 2827-2837. doi: 10.2147/IJGM.S312439

[17] World Health Organization. (2017). Cardiovascular diseases. Retrieved from 17 May 2017 website: https://www.who.int/news-room/fact-sheets/detail/cardiovascular-diseases-(cvds)

[18] Yeboah, J., Blaha, M. J., Michos, E. D., Qureshi, W., Miedema, M., Flueckiger, P., ... & Bertoni, A. G. (2017). Adult height, prevalent coronary artery calcium score, and incident cardiovascular disease outcomes in a multiethnic cohort. *American journal of epidemiology,* 186(8), 935-943. doi: 10.1093/aje/kwx165

КТ ОЦІНКА ВИСОТИ ВІДХОДЖЕННЯ ВІЧОК ВІНЦЕВИХ АРТЕРІЙ ТА ВИСОТИ ПАЗУХ АОРТИ В ЖІНОК ПРИ СТРУКТУРНИХ ЗМІНАХ ВІНЦЕВИХ АРТЕРІЙ

Підвальна У. Є., Бешлей Д. М., Матешук-Вацеба Л. Р.

Найпоширенішою формою серцево-судинних захворювань в Україні є ішемічна хвороба серця, котра характеризується ураженням вінцевих артерій. Висота пазух аорти та висота відходження вічок вінцевих артерій оцінюється при плануванні інтервенційних процедур та кардіохірургічних операцій. Комп'ютерна томографія дозволяє верифікувати структурні зміни

вінцевих артерій та морфометрично оцінити складові цибулини аорти. Мета дослідження: провести вимірювання висоти відходження вічок вінцевих артерій; висоти пазух аорти в жінок при структурних змінах вінцевих артерій за допомогою комп'ютерної томографії та оцінити взаємозалежність замірів з антропометричними показниками (вік, зріст, маса, індекс маси тіла, площі поверхні тіла). Були оброблені зображення комп'ютерної томографії-ангіографії органів грудної клітки осіб жіночої статі з ураженням вінцевих артерій. Статистичний аналіз: тест Шапіро-Франсіа (правильність розподілу), t-критерій Стьюдента (порівняння висоти відходження вінцевих артерій та висоти пазух аорти); лінійна кореляція Пірсона; мультифакторний регресійний аналіз за Фішером. За результатами дослідження доведений прямий кореляційний зв'язок між зростом та вимірюваними показниками у жінок зі структурним ураженням вінцевих артерій. Значення показника зросту прямо корелювало з висотою правої пазухи аорти (r=0,85, p=0,001), з висотою нижнього краю вічка правої вінцевої артерії (r=0,74, p=0,01), висотою верхнього краю вічка лівої вінцевої артерії (r=0,67, p=0,03), висотою верхнього краю вічка правої вінцевої артерії (r=0,67, p=0,03). Доведено, що зі збільшенням показника площі поверхні тіла, параметри висоти правої пазухи аорти зменшуються: зворотній сильний кореляційний зв'язок r=-0,83, p=0,002. Встановлено суттєві прямі взаємозв'язки між більшістю показників вимірюваних складових кореня аорти. Мультифакторний регресійний аналіз показав доведений прямий сильний вплив антропометричних даних та віку на висоту правої пазухи аорти: R=0,96, при p=0,009 (за Фішером). Це дало змогу побудувати модель прогнозування розмірів висоти правої пазухи аорти залежно від антропометричних та вікових параметрів. Таким чином, у жінок зі структурним ураженням вінцевих артерій збільшення зросту корелює зі збільшенням висоти правої пазухи аорти, висоти відходження вічок вінцевих артерій. Збільшення показника площі поверхні тіла корелює зі зменшенням висоти правої пазухи аорти у жінок зі структурним ураженням вінцевих артерій.

Ключові слова: *вічка вінцевих артерій, анатомія, комп'ютерна томографія, аорта, вимірювання, пазухи аорти.*

DOI: 10.31393/morphology-journal-2022-28(1)-05 Reports of Morphology, Vol. 28, №1, Pages 34-41

ISSN 1818-1295 eISSN 2616-6194

REPORTS OF MORPHOLOGY

Official Journal of the Scientific Society of Anatomists, Histologists, Embryologists and Topographic Anatomists of Ukraine

journal homepage: https://morphology-journal.com

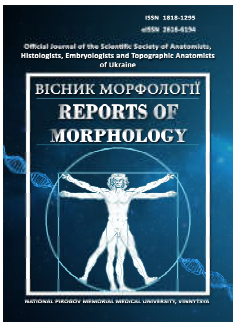

Investigation of the effect of TNF-α on damage to retinal pigment epithelial cells in age-related macular degeneration

Malachkova N.V., Mohammad Mashhour Mohammad Masa'deh
National Pirogov Memorial Medical University, Vinnytsia, Ukraine

ARTICLE INFO
Received: 26 November 2021
Accepted: 29 December 2021

UDC: 617.735:575.113

CORRESPONDING AUTHOR
e-mail: malachkovanataliia@gmail.com
Malachkova N.V.

CONFLICT OF INTEREST
The authors have no conflicts of interest to declare.

FUNDING
Not applicable.

Oxidative stress alters cellular homeostasis and elicits a cellular response that depends on the severity and type of damage: some cells activate defense mechanisms designed to ensure survival; the other, provided that the defense mechanisms are inhibited, triggers alternative signaling pathways that lead to apoptosis, necrosis, pyroptosis, autophagy, and so on. However, the exact cause of such damage and induction of oxidative stress, including the associated oxidative effects around pigment epithelial cells in the context of the onset and progression of age-related macular degeneration - one of the world's most common eye diseases with blindness, remains unclear. Therefore, in the course of the study we turned to key biogenetic points of regulation of inflammation and apoptosis, in particular TNF. The aim of the work is to shed light on the role of TNF as a genetic determinant that can initiate and influence the course of age-related macular degeneration. For this purpose, the main pathognomonic markers of the morphological structure of the macula were determined in 291 persons with age-related macular degeneration and in 105 persons without ophthalmic pathology, using optical coherence tomography to confirm or exclude the diagnosis of the disease. To detect polymorphism of the TNF gene, we used the method of real-time PCR diagnostics on the BioRad CFX 96 amplifier using LiTech reagents. Statistical processing of the results was performed using Hardy-Weinberg equilibrium, Kruskal-Wallis method, logistic regression analysis and construction of the ROC curve to determine the AUC range and sensitivity and specificity values. The study revealed a significant difference in the distribution of mutant genotypes between patients with both forms of AMD and the control group. There was also a statistically significant effect of mutant allele A on the development of both "dry" (OR = 3.40; 95.0 %; CI = 1.90-6.07, p<0.001) and "wet" form of AMD (OR = 4.78; 95.0 % CI 2.65-8.64, p<0.001), and in the analysis of mutant genotypes it was found that the GA genotype increases the chances of "dry" and "wet" forms of the disease by 3.13 and 4.74 times, respectively, while AA - 5 times, regardless of the form of the disease. confirms the influence of TNF gene polymorphism on the occurrence and progression of age-related macular degeneration. In the analysis of ROC-curves and AUC regions, it was found that all mutant genotypes have a significant effect on the occurrence of age-related macular degeneration (p<0.05). However, the obtained values of sensitivity and specificity, especially in the AA genotype in both "dry" (17.9 % and 95.8 %, respectively) and "wet" (18.2 % and 95.8 %, respectively) forms of age-related macular degeneration indicate a low chance of error-free confirmation of the diagnosis. a disease that may be associated with multifactorial disease and requires further research.

Keywords: *age-related macular degeneration, TNF-α, ROS, NOS, gene.*

Introduction

Age-related macular degeneration (AMD) is a common irreversible eye disease characterized by visual impairment in the elderly and is a major cause of blindness/vision loss in developed countries [3, 10]. The vast majority of modern classifiers agree with the division of AMD nosological units into "dry" form and "wet" form [4].

According to the European Consortium of Epidemiology of Eye Diseases, there is an increase in morbidity in the European population. Mathematical models indicate that if this rate of eye pathology persists, by 2040 the number of

people in Europe with early-onset age-related macular degeneration will range from 14.9 to 21.5 million, and with late-onset from 3.9 to 4.8 million [3]. The World Health Organization's World Report on Vision (2019) highlights the urgency of the problem - at least 2.2 billion people worldwide have impaired vision, where AMD ranks third in morbidity with 196 million people suffering from various forms of it, while yielding only to biopsy and presbyopia [21].

Numerous factors determine the risk of developing age-related macular degeneration, including both genetic and environmental factors. Oxidative stress and aging have a powerful effect, which resonate in terms of the pathogenesis of age-related macular degeneration [5]. Retinal pigment epithelial cells are the main target of pathological changes in age-related macular degeneration - they involve phagocytosis of photoreceptor outer segments (POS) and removal of cellular waste under physiological conditions. Age-related cumulative oxidative stimuli mediated by reactive oxygen species (ROS) and reactive nitrogen species (RNS) cause degeneration of pigment epithelial cells and incomplete POS lysis, leading to accumulation of cellular wastes [24]. The ubiquitin proteasome and the lysosomal/autophagic pathway are the two main proteolytic systems for removing damaged proteins and organelles, and their disruption due to deregulation of signaling pathways leads to the accumulation of lethal mutations or trigger apoptosis [11].

Cytokine tumor necrosis factor α (TNF-α) is one of the main regulators of the immune system that can affect apoptosis, cell proliferation and differentiation, local and systemic inflammation, immune response through its binding site - TNF receptor 1 type (TNFR1). It is known that TNFR1 can cause oxidative stress directly by activating enzymes that produce ROS and active forms of nitrogen RNS, involving the fundamental signaling pathways NFE2L2, PGC-1, p62, AMPK й PI3K/Akt/mTOR [8, 19, 24]. In addition, the activity of mTNF-α to reactogenic formulation is regulated by the matrix metalloproteinases MMP and the associated ADAM17 complex - metalloproteinases of this family themselves can cause remodeling of the extracellular matrix, particularly in the Bruch membrane [10]. Ways of regulation are really branched, but regularly return to the fight against pathological oxidants [9]. In turn, the TNF-R1 type 1 receptor activates a complex caspase cascade in the inflammatory cluster of signaling pathways, resulting in changes in NF-κB and p55 activity, thus retaining the ability to modulate proapoptotic effects at the systemic level via TNF-α. On the other hand, the TNF-R2 type 2 receptor simultaneously interacts with NF-κB and ROS-sensitive AP-1, indicating a significant role of oxidative stress in the development of deregulation of apoptosis, endothelial cell degeneration, where TNF-R2 is most expressed. Similarly, the heterodimeric redox transcription factor AP-1 is activated, which responds to the presence of reactive oxygen species around [14]. We see this as age-related macular degeneration, as TNF-α attracts the most likely triggers of pathology - cell cycle disruption, extracellular matrix rearrangement, and oxidative stress of cells in photosensitive cells under the influence of aging [15].

Therefore, *the aim of the study* was to shed light on the role of TNF as a genetic determinant capable of initiating and influencing the course of age-related macular degeneration.

Materials and methods

The study group included 291 middle-aged and elderly people with AMD (89 - with "dry" form, 97 - with "wet" form), the control group - 105 people without ophthalmic pathology in the anamnesis of the relevant age range.

The work adhered to the ethical principles of the Declaration of Helsinki of the World Medical Association (World Medical Association Declaration of Helsinki, 1964) [22]. Each subject was provided with all the details of medical procedures, given the opportunity to discuss any issues with health professionals, and then signed a detailed form of informed consent for the study. The scientific work was approved by the **Commission on Biomedical Ethics** of VNMU of the Ministry of Health of Ukraine in accordance with Protocol №6 of 17.09.20.

Optical coherence tomography of the macular area of the retina was used to determine the presence or absence of pathognomonic markers of the morphological structure of the macula that was characteristic of AMD. It was performed using a SOCT Copernicus optocoherent tomograph "Optopol" with the possibility of angiography (Poland) in 3D-Scan mode (sequential scanning of the entire retinal segment). To study the anatomical and topographic relationship between the layers and the thickness of the retina in the macular area and the analysis of the thickness of the macula in different departments, the parameter - ILM-RPE (internal limiting membrane-retinal pigmented epithelium; internal boundary membrane-retinal pigment epithelium) was used. When drusen were found, the AMD form was verified as "dry", while cystic edema of the neuroepithelium, transudative detachment of the pigment epithelium, chorioretinal vascular proliferation, and subretinal fibrosis were verified, AMD form was verified as "wet."

DNA was isolated from the buccal scraper using the Chelex® 100 kit from Bio-Rad according to the manufacturer's instructions. To detect the rs1800629 polymorphism of the TNF gene, real-time polymerase chain reaction (PCR) was used using a set of reagents according to the manufacturer's instructions (Litech, Russia). Amplification was performed on a Bio-Rad CFX96 thermal cycler (BioRad, USA).

Statistical processing of the results was performed using Statistica 10 (StatSoft, Inc., USA) and SPSS 23.0. To determine the frequencies of distribution of genotypes and alleles in the studied groups was determined using Hardy-Weinberg equilibrium. The Kruskal-Wallis ANOVA by Ranks

and Friedman ANOVA and Kendall Coeff criteria were used to compare categorical variables (genotypes) and to determine a significant difference in the distribution of genotypes between groups. of Concordance. In order to compare the distribution of values of qualitative features used H-criterion. The degree of association of mutant genotypes with the development of AMD was determined by logistic regression using odds ratios (OR) and 95 % confidence interval (±95 % CI; Confidence limit for means Interval - CI). To assess the adequacy of logistics models and the predictive ability of the diagnostic test used the method of analysis of curves of operational characteristics (ROC - Receiver Operating Characteristic curve analysis). For this purpose, the area under the ROC curve (AUC - Area under the ROC curve) was calculated. The model was considered adequate with a statistically significant difference in AUC from 0.5. Special formulas using 2x2 tables were also used to calculate the specificity and sensitivity of mutant genotypes.

Results

In the study, we analyzed the genotype distribution of the rs1800629 polymorphism of the TNF gene in both patients with "dry" and "wet" forms of age-related macular degeneration, as well as in patients of the control group. In particular, the influence of mutant genotypes and alleles on the development of the disease was determined.

After genetic testing as a result of statistical calculations by the Kruskal-Wallis method, high statistical significance of differences in the distribution of genotypes of rs1800629 polymorphism of the TNF gene in patients with "dry" and "wet" forms of age-related macular degeneration and control group (H = 29.57) at p<0.001, which was also found when comparing the genotype distribution of patients in the control group with "dry" form of AMD (H = 16.28) and "wet" (H = 26.42), respectively, at p<0.001 (Table 1).

By evaluating the data, it was found that the wild-type (GG) polymorphism rs1800629 of the TNF gene predominated among the control group (23.4 %), while in patients with "dry" (11.0 %) and "wet" (9.3 %) forms it was not widely represented. Mutant genotypes were mostly observed in patients with AMD, which previously indicates a possible association between pathology and SNP. Thus, the heterozygous variant was most important among people with "wet" (22.0 %) and "dry" (17.2 %) forms of the disease, while in the control group the subjects were distributed 1.9 and 1.5 times less than patients. Regarding the mutant AA genotype, the highest number of people was among the "dry" form of age-related macular degeneration (2.4 %), followed by the "wet" form (2.1 %), and the lowest - the control group (1.0 %).

The outlined results, together with the lack of statistical significance in the difference in the distribution of genotypes of patients between "dry" and "wet" forms (H = 0.77, p>0.05), may indicate that polymorphism rs1800629 TNF gene affects both disease development and its further progression.

The frequency of distribution of genotypes and alleles of the rs1800629 polymorphism of the TNF gene among patients with "dry" and "wet" forms of AMD and the control group was studied using Hardy-Weinberg analysis (Fig. 1).

As can be seen from the results of the analysis in Figure 1, the genotype distribution of the rs1800629 polymorphism of the TNF gene had significant differences between patients with AMD and the control group. The frequency of homozygous genotype for the main allele in the control group (GG) was 1.59 times lower compared to the "dry" form (0.410) and 1.76 times lower compared to the "wet" (0.370) compared to the control group (0.654). In contrast to the results of the wild-type distribution studied with the heterozygous variant, it was the lowest among the control group (0.309), which was 1.49 times less than patients with "dry" form (0.461) and 1.5 times less than patients with wet" form (0.477). The mutant genotype of the rs1800629 polymorphism of the TNF gene was represented by a small number of subjects (see Table 1), so the frequency of distribution changed insignificantly: it was greatest in the case of "wet" form of AMD (0.154), which was 4.3 times more than the control group (0.036), and in the "dry" form was 0.130. When estimating the frequency of allele distribution (Fig. 1) it was found that the mutant allele A was most observed in the "wet" form of AMD (0.39), in the "dry" - slightly less (0.360), while in the control group found 2 times and 1,88 times less, respectively (0.190). Regarding the wild-type allele (G), it was most common among the control group (0.810), while no significant difference was observed between patients - 0.640 in the

Table 1. Distribution of rs1800629 TNF gene polymorphism genotypes in patients with "dry" and "wet" forms of age-related macular degeneration and control group.

	GG (n, %)	GA (n, %)	AA (n, %)	H-criterion, p	H-criterion, p	H-criterion, p
"Dry" form	32 (11.0 %)	50 (17.2 %)	7 (2.4 %)	0.77*	16.28**	29.57^
"Wet" form	27 (9.3 %)	64 (22.0 %)	6 (2.1 %)		26.42**	
Control group	68 (23.4 %)	34 (11.7 %)	3 (1.0 %)	-	-	
Total (100 %)	127 (43.6 %)	148 (50.9 %)	16 (5.5 %)			

Notes: * - the level of significance of the H-criterion in the comparison of the "dry" form with the "wet" form, p>0.05, ** - the level of significance of the H-criterion compared to the control, p<0.001, ^ - the level of significance of the H-criterion in comparison with the studied groups, p<0.001.

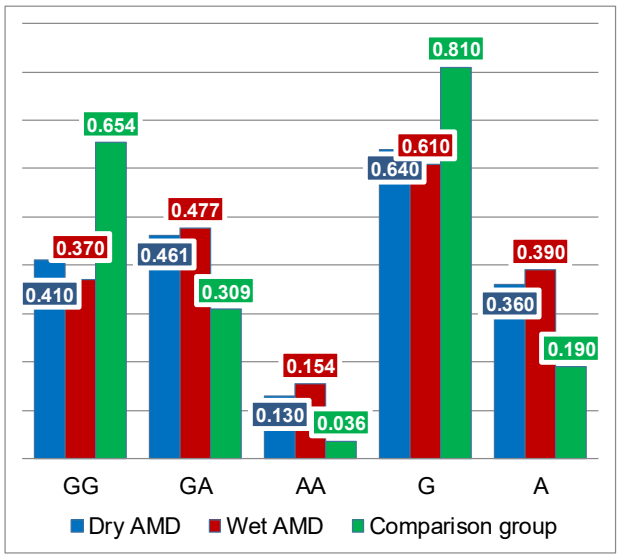

Fig. 1. Frequency of distribution of genotypes and alleles of rs1800629 polymorphism of TNF gene in patients with "dry" and "wet" forms of age-related macular degeneration and control group.

case of "dry" and 0.610 - "wet". As a result, it can be argued that mutant variants of the rs1800629 polymorphism of the TNF gene are associated with the development and progression of age-related macular degeneration, namely the AA genotype and the A allele may be associated with the "wet" form.

To determine the degree of association of genotypes of the rs1800629 polymorphism of the TNF gene with the development of "dry" and "wet" forms of AMD, a logistic regression method was performed, the results of which are presented in Table 2.

Logistic regression analysis revealed a direct statistically significant association between the presence of a heterozygous variant of the rs1800629 polymorphism of the TNF gene and the occurrence of age-related macular degeneration regardless of form at p<0.001. A high level of statistical significance was also found in the case of association of allele A with age-related macular degeneration of both "dry" and "wet" forms (p<0.001). A statistically significant association was found in the study of the correlation between mutant genotypes and disease with both forms at p<0.05 (see Table 2).

Table 2 shows that allele A increases the risk of "dry" form of AMD by 3.4 times (OR = 3.40; 95.0 % CI 1.90-6.07), and in the case of "wet" form the risk is even higher - 4.8 times (OR = 4.78; 95.0 % CI 2.65-8.64). When assessing the degree of association of mutant genotypes of the rs1800629 polymorphism of the TNF gene with the development of the disease, it was found that homozygous variants of the minor allele almost 5 times increase the risk of "dry" (OR = 4.96; 95.0 % CI 1.18-20.77) and "wet" (OR = 5.04; 95.0 % CI 1.15-21.98) forms of age-related macular degeneration The chances of developing "wet" AMD in individuals with GA genotype are 4.7 times higher compared to controls (OR = 4.74; 95.0 % CI 2.57-8.76), and for the "dry" form are 3.1 times (OR = 3.13; 95.0 % CI 1.70-5.74).

Therefore, due to the obtained results, it is possible to assert a significant effect of the rs1800629 polymorphism of the TNF gene on the development of age-related macular degeneration. Mutant genotypes show high statistical significance in heterozygous variants, and genotype AA can be considered a risk factor for age-related macular degeneration, regardless of form. Allele A is particularly closely associated with the "wet" form, which may indicate its important role in the progression of the pathology.

To further determine the probability of developing age-related macular degeneration, the Receiver Operating Characteristic Curve Analysis (ROC) method was used to determine the area under the ROC curve (AUC).

The prognostic significance of the rs1800629 TNF gene polymorphism was estimated using Figure 2 and the calculation of the area under the ROC curve. Thus, the GA genotype shows high statistical significance for the

Table 2. Results of logistic regression analysis of rs1800629 TNF gene polymorphism in patients with "dry" and "wet" forms of AMD.

Form of nosology	Genotypes / allelic variants	N subjects with pathology	N subjects from the control group	OR		χ^2	p
				value	95 % CI		
"Dry" form	GG	32	68				
	GA	50	34	3.125	1.699 - 5.74	14.144	<0.001
	AA	7	3	4.958	1.18 - 20.77	5.4562	<0.05
	G	114	170				
	A	64	40	3.4	1.9 - 6.07	18.138	<0.001
"Wet" form	GG	27	68				
	GA	64	34	4.74	2.566 - 8.76	26.995	<0.001
	AA	6	3	5.037	1.15 - 21.98	5.0976	<0.05
	G	118	170				
	A	76	40	4.78	2.65 - 8.64	29.53	<0.001

Notes: OR - odds ratio; 95 % CI - 95 % confidence interval; χ^2 - chi-square criterion; p - level of significance χ^2.

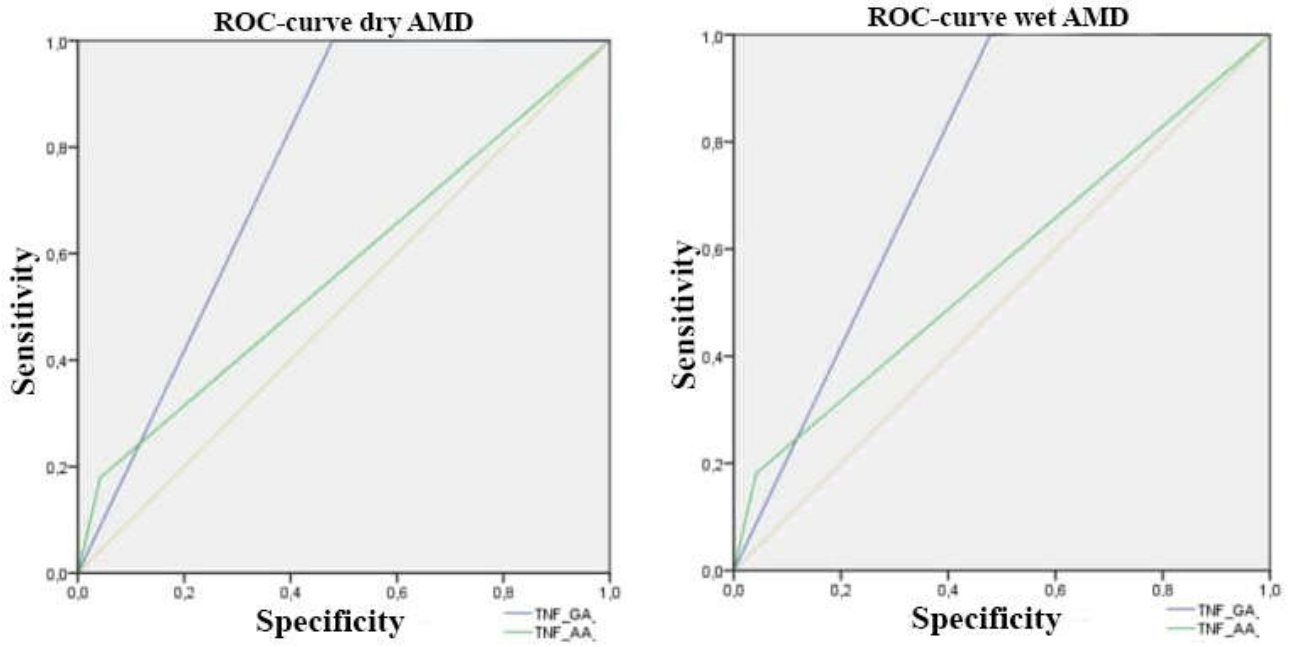

Fig. 2. ROC curves for "dry" and "wet" forms of age-related macular degeneration.

development of both "dry" (AUC = 0.761±0.044 at 95.0 % CI 0.67-0.85; p<0.001) and "wet" (AUC = 0.761±0.045 at 95.0 % CI 0.67-0.85; p<0.001) forms of AMD. In the study of homozygous genotypes for the minor allele, a reliable association was not established (p>0.05), which can be attributed to multifactorial pathology or the distribution of genotypes, which had a small number of representatives of the AA genotype among the control group and among patients (see table. 1).

Patients' results were presented in the form of categorical data, which did not allow to adequately assess the cut-off threshold formed by the ROC curve, so the specificity and sensitivity of the diagnostic test were analyzed using separate formulas using tables 2x2 (Table 3).

As can be seen from Table 3, in both forms of AMD the susceptibility of genotype AA, which according to logistic regression had the best prognostic value, but was inaccurate in estimating the ROC curve and AUC, was the worst and was 17.9 % in "dry" disease and 18.2 % - with "wet", while the specificity of this genotype for the minor allele was the highest in both forms of age-related macular degeneration and amounted to 95.8 %. Such ambiguous results of sensitivity and specificity can be attributed to the fact that age-related macular degeneration is a multifactorial disease, making it difficult to claim a single effect of this gene on the development and progression of pathology. Regarding the heterozygous variant of the rs1800629 polymorphism of the TNF gene, the sensitivity for it in the "dry" form was 61.0 %, and in the "wet" form - 70.3 %, while the specificity of its detection in both forms of the disease was 66.7 %.

Table 3. Sensitivity and specificity of rs1800629 TNF gene polymorphism in the development of "dry" and "wet" AMD.

	"Dry" form			"Wet" form		
	GG	GA	AA	GG	GA	AA
Sensitivity	-	61.0 %	17.9 %	-	70.3 %	18.2 %
Specificity	-	66.7 %	95.8 %	-	66.7 %	95.8 %

Thus, the results of the statistical methods indicate the high significance of the prognostic influence of the rs1800629 polymorphism of the TNF gene on the development of both forms of AMD, especially "wet", in the case of mutant genotypes. Indicators of specificity and sensitivity of SNP genotypes indicate a complex predisposition to the development of pathology with the involvement of other genetic factors, which in the study of their combination can significantly increase the sensitivity and specificity of the diagnostic test.

Discussion

The results of our study indicate a high statistical significance of the prognostic effect of the rs1800629 polymorphism of the TNF gene on the development of both forms of age-related macular degeneration, especially "wet" (p<0.05). When determining the distribution of genotypes, it was found that mutant genotypes are widely represented among patients from the cohorts of "dry" and "wet" forms of AMD, compared with the control group: 17.2 % and 22.0 % in the case of GA gene variant, respectively, and 2.4 % and 2.1 % for genotype AA, respectively. A significant difference in the distribution of mutant allelic variants between the two forms of AMD and control was confirmed by the Kruskal-Wallis method.

In the frequency of distribution of genotypes and alleles by Hardy-Weinberg equilibrium, the mutant variant AA and

allele A prevailed among people with "wet" form of the disease. Thus, the AA genotype was 4.3 times more common than the control, while the A allele was 2.0 times more common than the control. According to the results of logistic regression, it was found that the chances of developing "dry" form of AMD in patients with GA genotype, compared with the control group, were 3.1 times higher, while in the presence of allelic variant AA - 5.0 times. The same OR values were recorded when assessing the prognostic effect of this genotype on the development of the "wet" form of AMD, which indicates the effect of this allelic variant on both the occurrence and progression of the pathology. The analysis of the ROC curve and the determination of the area under it revealed a high statistical significance of the GA genotype for the development of both "dry" and "wet" forms of AMD, while no significant association was found in the study of homozygous genotype for minor allele. The specificity of determining the mutant genotype in the case of "wet" form of AMD was 95.8 %. The best sensitivity index was determined for the heterozygous genotype in the case of the "wet" form - 70.3 %.

In our work we tried to shed light on the most important links in the development of age-related macular degeneration, which can be modulated by modern pharmacogenetic methods. Numerous studies indicate the role of TNF-α in the pathogenesis of proliferative diabetic retinopathy and the wet form of age-related macular degeneration - such conclusions lead to information about the increase in the concentration of protein necrosis factor-alpha in the aqueous fluid of the eye among patients with such pathologies [20]. The gene expressing this biological agent contains one of the most studied polymorphisms that is likely to affect the expression of TNF-α, located in the promoter region of the gene in front of the transcription initiator, at 308 nucleotides, and known as G-308A (rs1800629) [1]. All allelic variations of this polymorphism have different ability to pathogenic activation, in particular: the wild genotype GG has a complex effect, without changing the risk of associated pathological processes. Heterozygotes (AG) and monozygotes by mutant allele (GG) increase the risk of compatible nosologies by 2.0 and 2.5 times, respectively. Sometimes in sources the rs1800629 allele (A) is referred to as 308.2 or TNF2, and the more common allele (G) is referred to as 308.1 or TNF1 [7, 17].

Aging, inflammation, and dysregulation of the complement system affect the retinal pigment epithelium, and evidence has been found to involve tumor necrosis factor alpha and complement component 3 (C3) as one of the key factors in the development of age-related macular degeneration [6]. The primary effects of TNF are related to the cytoplasmic domain TNF-R1, which sequentially recruits death domains in a number of key signaling proteins: primarily the death domain associated with the TNF-α receptor (tumor necrosis factor receptor type 1-associated via death domain protein, TRADD); Fas associated death domain (FADD); a starter of caspase-8 apoptosis (also known as FADD-like ICE, Fas-associated death domain-like IL-1β-converting enzyme, or FLICE), causing degeneration of numerous proteins [14]. The effects of TNF-α are not limited to this, the protein exerts stimulatory and inhibitory effects on signaling pathways regulating apoptosis, proliferation and differentiation, immune recognition and inflammatory response, for example: interaction with antiapoptotic receptor DCR1 (decoy receptor 1, also known as TRAIL receptor 3 (TRAILR3)), the levels of which are significantly lower in patients with AMD and almost indistinguishable in patients with dry and wet forms [2]. Issues of cross-regulation with VEGF, another potential determinant of AMD, remain important. The results suggest that VEGF secretion under inflammatory conditions depends on cell polarization, and TNF-α-induced VEGF suppression can lead to choroidal atrophy in polarized physiological cells of the retinal pigment epithelium. TNF-α-induced upward regulation of VEGF can cause neovascularization, which is considered a component of late age-related macular degeneration [16]. This is confirmed by the fact of successful application of biological agents of targeted action to VEGF and TNF-α in the context of slowing the progression of age-related macular degeneration [18]. Another point of application is considered to be a family of antioxidant systems that protect the cell from oxidative stress - their regulation also involves tumor necrosis factor, triggering not only downward effects, but also receiving feedback on their own expression. It actively interacts through cellular and molecular markers of inflammation and oxidative stress (eg, IL-1β, TGF-α, ABCG1, ABCA1, reduced glutathione), and almost all of them alter the metabolism of reactive oxygen species in retinal pigment epithelial cells, limiting oxidative stress for physiological functioning [13]. Additional evidence of an association between TNF and ROS is the ability of caspase inhibitors and fat-soluble free radical scavengers (eg, tocopherol) to reduce AMD-induced cytotoxicity, particularly in the treatment of TNF blockers [12].

In a study that looked at the potential cytoprotective and anti-inflammatory effects of carbon monoxide-releasing molecules, they markedly inhibited TNF. Moreover, CORMs have been shown to exert their inhibitory effects by blocking nuclear translocation of nuclear factor κB/p65 and IκBα degradation in retinal pigment epithelial cells under the influence of TNFα - this also echoes the information above [23].

Conclusions

1. The results of our study indicate the high statistical significance of the prognostic effect of the rs1800629 polymorphism of the TNF gene on the development of both forms of age-related macular degeneration, especially the wet nosological form.

2. Mutant variant AA and allele A of the rs1800629 polymorphism prevailed among individuals with a wet form of the disease, which suggests the association of this allele

with the development of pathology. Thus, the AA genotype was 4.3 times more common in people with age-related macular degeneration compared to the control, while the A allele was 2.0 times more common than the control. According to the results of logistic regression, it was found that the chances of developing dry AMD in patients with GA genotype, against the control group, were 3.1 times higher, while in the presence of allelic variant AA - 5.0 times, which is confirmed by literature data.

References

[1] Ahmed, R., Sharif, D., Jaf, M., & Amin, D.M. (2020). Effect of TNF-α 308G/A (rs1800629) Promoter Polymorphism on the Serum Level of TNF-α Among Iraqi Patients with Generalized Vitiligo. *Clin. Cosmet. Investig. Dermatol.*, 13, 825-835. doi: 10.2147/CCID.S272970

[2] Anand, A., Sharma, N.K., Singh, R., Gupta, A., Prabhakar, S., Jindal, N. … Gupta, P.K. (2014). Does DcR1 (TNF-related apoptosis-inducing-ligand Receptor 3) have any role in human AMD pathogenesis? *Sci. Rep.,* 4(4114), 1-5. doi: 10.1038/srep04114

[3] Colijn, J.M., Buitendijk, G.H.S., Prokofyeva, E., Alves, D., Cachulo, M.L., Khawaja, A.P. … Klaver, C.C.W. (2017). Prevalence of age-related macular degeneration in Europe. *Ophthalmology,* 124(12), 1753-1763. doi: 10.1016/j.ophtha.2017.05.035

[4] Cook, H.L., Patel, P.J., & Tufail, A. (2008). Age-related macular degeneration: diagnosis and management. *British Medical Bulletin,* 85(1), 127-149. doi: 10.1093/bmb/ldn012

[5] Domenech, E.B., & Marfany, G. (2020). The Relevance of Oxidative Stress in the Pathogenesis and Therapy of Retinal Dystrophies. *Antioxidants* (Basel), 9(4), 1-22. doi: 10.3390/antiox9040347

[6] Efstathiou, N.E., Moustafa, G.A., Maidana, D.E., Konstantinou, E.K., Notomi, S., Barbisan, P.R.T. … Vavvas, D.G. (2020). Acadesine suppresses TNF-α induced complement component 3 (C3), in retinal pigment epithelial (RPE) cells. *PLoS One,* 15(12), e0244307. doi: 10.1371/journal.pone.0244307

[7] El-Tahan, R. R., Ghoneim, A. M., & El-Mashad, N. (2016). TNF-α gene polymorphisms and expression. *SpringerPlus,* 5(1508), 1-7. doi: 10.1186/s40064-016-3197-y

[8] Falvo, J. V., Tsytsykova, A. V., & Goldfeld, A. E. (2010). Transcriptional Control of the TNF Gene. *Curr Dir Autoimmun,* 11, 27-60. doi: 10.1159/000289196

[9] Fischer, R., & Maier, O. (2015). Interrelation of Oxidative Stress and Inflammation in Neurodegenerative Disease: Role of TNF. *Oxid Med Cell Longev,* 2015(610813), 1-19. doi: 10.1155/2015/610813

[10] Garcia-Onrubia, L., Valentin-Bravo, F. J., Coco-Martin, R. M., Gonzalez-Sarmiento, R., Pastor, J. C., Usategui-Martin, R., & Pastor-Idoate, S. (2020). Matrix metalloproteinases in age-related macular degeneration (AMD). *Int J Mol Sci,* 21(16), 1-32. doi: 10.3390/ijms21165934

[11] Kaarniranta, K., Kajdanek, J., Morawiec, J., Pawlowska, E., & Blasiak, J. (2018). PGC-1α Protects RPE Cells of the Aging Retina against Oxidative Stress-Induced Degeneration through the Regulation of Senescence and Mitochondrial Quality Control. The Significance for AMD Pathogenesis. *Int J Mol Sci,* 19(8), 1-20. doi: 10.3390/ijms19082317

[12] Lu, J., Miyakawa, K., Roth, R.A., & Ganey, P.E. (2013). Tumor necrosis factor-alpha potentiates the cytotoxicity of amiodarone in Hepa1c1c7 cells: roles of caspase activation and oxidative stress. *Toxicol. Sci.,* 131(1), 164-78. doi: 10.1093/toxsci/kfs289

[13] Promsote, W., Veeranan-Karmegam, R., Ananth, S., Shen, D., Chan, C., Lambert, N.A. … Martin, P.M. (2014). L-2-oxothiazolidine-4-carboxylic acid attenuates oxidative stress and inflammation in retinal pigment epithelium. *Mol. Vis.,* 20, 73-88.

[14] Sethi, G., Sung, B., & Aggarwal, B.B. (2008). TNF: A master switch for inflammation to cancer. *Front. Biosci.,* 13, 5094-5107. doi: 10.2741/3066

[15] Shu, D. Y., Butcher, E., & Saint-Geniez, M. (2020). EMT and EndMT: Emerging Roles in Age-Related Macular Degeneration. *Int. J. Mol. Sci.,* 21(12), 1-26. doi: 10.3390/ijms21124271

[16] Terasaki, H., Kase, S., Shirasawa, M., Otsuka, H., Hisatomi, T., Sonoda, S., … & Sakamoto, T. (2013). TNF-α decreases VEGF secretion in highly polarized RPE cells but increases it in non-polarized RPE cells related to crosstalk between JNK and NF-κB pathways. *PLoS One,* 8(7), e69994. doi: 10.1371/journal.pone.0069994

[17] rs1800629. (2021, July 4). In SNPedia. https://www.snpedia.com/index.php/Rs1800629

[18] Wang, X., Ma, W., Han, S., Meng, Z., Zhao, L., Yin, Y., … Li, J. (2017). TGF-α participates choroid neovascularization through Smad2/3-VEGF/TNF-α signaling in mice with Laser-induced wet age-related macular degeneration. *Sci. Rep.,* 7(1), 1-13. doi: 10.1038/s41598-017-10124-4

[19] Wei, X., Chen, Y., Wu, L., Cui, L., Hu, D., & Zeng, X. (2016). Tumor necrosis factor-α G-308A (rs1800629) polymorphism and aggressive periodontitis susceptibility: a meta-analysis of 16 case-control studies. *Sci. Rep.,* 6(19099), 1-8. doi: 10.1038/srep19099

[20] Whitmore, H.A.B., Amarnani, D., O'Hare, M., Delgado-Tirado, S., Gonzalez-Buendia, L., An, M. … Kim, L.A. (2021). TNF-α signaling regulates RUNX1 function in endothelial cells. *FASEB J.,* 35(2), e21155. doi: 10.1096/fj.202001668R

[21] World Health Organization. (2019). World Report on Vision. https://www.who.int/publications/i/item/9789241516570

[22] World Medical Association. (2018). Ethical Principles for Medical Research Involving Human Subjects. WMA Declaration of Helsinki. https://www.wma.net/policies-post/wma-declaration-of-helsinki-ethical-principles-for-medical-research-involving-human-subjects/

[23] Yang, P., Cheng, K., Yuan, S., & Wung, B. (2020). Carbon monoxide-releasing molecules protect against blue light exposure and inflammation in retinal pigment epithelial cells. *Int. J. Mol. Med.,* 46(3), 1096-1106. doi: 10.3892/ijmm.2020.4656

[24] Zhang, Z., Bao, X., ong, Y., Fan, B., & Li, G. (2020). Autophagy in Age-Related Macular Degeneration: A Regulatory Mechanism of Oxidative Stress. *Oxid. Med. Cell. Longev.,* (2896036), 1-13. doi: 10.1155/2020/2896036

ДОСЛІДЖЕННЯ ВПЛИВУ TNF-α НА УШКОДЖЕННЯ КЛІТИН ПІГМЕНТНОГО ЕПІТЕЛІЮ СІТКІВКИ ПРИ ВІКОВІЙ МАКУЛОДИСТРОФІЇ

Малачкова Н. В., Мохаммад Машхур Мохаммад Маса'дех

Окисний стрес змінює клітинний гомеостаз і викликає клітинну відповідь, яка залежить від тяжкості та типу пошкодження: певна частина клітин активує захисні механізми, призначені для забезпечення виживання; інша ж, за умови гальмування

захисних механізмів, запускає альтернативні сигнальні шляхи, які призводять до апоптозу, некрозу, піроптозу, аутофагії тощо. Однак, точна причина такого пошкодження та індукції окисного стресу, включаючи пов'язані з цим окислювальні ефекти навколо клітин пігментного епітелію в контексті виникнення та прогресування вікової макулярної дегенерації - одного з найпоширеніших у світі захворювань ока із наслідками у вигляді сліпоти, залишаються недостатньо зрозумілими. Тому в процесі дослідження ми звернулися до ключових біогенетичних точок регуляції запалення та апоптозу, зокрема TNF. Мета роботи - освітлення ролі TNF як генетичної детермінанти, здатної ініціювати та впливати на перебіг вікової макулярної дегенерації. Для цього у 291 особи, які хворіли на вікову макулярну дегенерацію, та у 105 осіб без офтальмологічної патології були визначені основні патогномонічні маркери морфологічної структури макули, використовуючи оптичну когерентну томографію для підтвердження або виключення діагнозу захворювання. Для виявлення поліморфізму гена TNF використовували метод ПЛР-діагностики в режими реального часу на ампліфікаторі BioRad CFX 96, використовуючи реактиви ЛиТех. Статистичну обробку результатів проводили за допомогою рівноваги Харді-Вайнберга, методу Краскела-Уоллеса, логістичного регресійного аналізу та побудови ROC-кривої з визначенням області AUC і значень чутливості та специфічності. У результаті дослідження виявлено достовірну різницю у розподілі мутантних генотипів між пацієнтами з обома формами ВМД та контрольною групою. Також встановлено статистично високозначущий вплив мутантного алеля А на розвиток як "сухої" (OR = 3,40; 95,0 %; CI = 1,90-6,07, p<0,001), так і "вологої" форми ВМД (OR = 4,78; 95,0 % CI 2,65-8,64, p<0,001), а при аналізі мутантних генотипів виявлено, що генотип GA підвищує шанси виникнення "сухої" та "вологої" форм захворювання в 3,13 і 4,74 разів відповідно, тоді як AA - у 5 разів, незалежно від форми хвороби, що підтверджує вплив поліморфізму гена TNF на виникнення та прогресування вікової макулярної дегенерації. При аналізі ROC-кривих та областей AUC встановлено, що всі мутантні генотипи мають достовірний вплив на виникнення вікової макулярної дегенерації (p<0,05). Проте, отримані значення чутливості і специфічності, особливо при генотипі AA як при "сухій" (17,9 % і 95,8 % відповідно) так і при "вологій" (18,2 % і 95,8 % відповідно) формах вікової макулярної дегенерації свідчать про низький шанс безпомилкового підтвердження діагнозу захворювання, що може бути пов'язано з мультифакторіальністю захворювання і потребує подальших досліджень.

Ключові слова: *вікова макулярна дегенерація, TNF-α, ROS, NOS, ген.*

DOI: 10.31393/morphology-journal-2022-28(1)-06 Reports of Morphology, Vol. 28, №1, Pages 42-47

ISSN 1818-1295 eISSN 2616-6194

REPORTS OF MORPHOLOGY

Official Journal of the Scientific Society of Anatomists, Histologists, Embryologists and Topographic Anatomists of Ukraine

journal homepage: https://morphology-journal.com

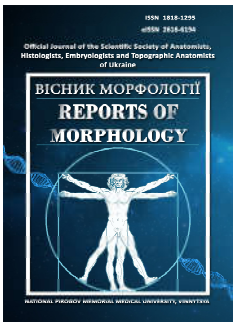

Densitometric assessment in the justification of rehabilitation of patients with atrophy of the bone tissue of the mandible, on the right side

Oshurko A. P.
Bukovinian State Medical University, Chernivtsi, Ukraine

ARTICLE INFO
Received: 28 November 2021
Accepted: 10 January 2022

UDC: 616.716.4-031-007.23-073.7-073.432.19-08

CORRESPONDING AUTHOR
e-mail: anatoliystudent@gmail.com
Oshurko A. P.

CONFLICT OF INTEREST
The authors have no conflicts of interest to declare.

FUNDING
Not applicable.

Densitometric methods for determining bone density are increasingly becoming fundamental in research and a priority in clinical applications in medical practice. Rehabilitation of patients with bone atrophy becomes impossible without assessing its density and, at the same time, is an important component in the diagnosis and planning of reconstructive surgery, in particular, prognosticity in the use of osteoplastic materials or osteointegration of dental implants. The aim of the study was to conduct a densitometric assessment to substantiate the rehabilitation of patients with atrophy of the mandible, on the right side, in the age groups of 25 to 75 years. Computed tomography digital scan scans obtained using the Vatech PaX-I 3D Green extra-oral radiography system and processed by the standardized X-ray diagnostic software Ez3D-I Original ver.5.1.9.0. Using the tools of the horizontal option panel, in particular the keys of the interface "profile", the density of bone tissue with interpretation in conventional units of grayness (CUG) in the projection of 4.6, 4.7 teeth was investigated. To obtain qualitatively homogeneous values, we used nonparametric methods of statistical analysis of comparison of age groups - using the multidimensional Kruskal-Wallis test as an alternative intergroup analysis of variance, for simultaneous comparison of three samples. It is proved that during the statistical analysis of bone density using the Mann-Whitney U test in the studied areas of the mandible on the right, the total average number of M experimental (E) groups compared to the average number of the control group (C), high reliability in vertical (VP) measurements and confirmed p<0.05. Thus, it is proved that the early loss of the masticatory group of teeth, in the first group of studies (25-45 years), leads to high rates, with increasing bone density in the direction of distalization of the final defect of the dentition. Conversely, the lack of functional action on bone tissue in the second (46-60 years) and third (61-75 years) groups of the study, leads to a decrease in its density, and, consequently, to the devastation of the trabecular layer, which contributes to the progression of atrophic processes.

Keywords: *mandible, computed tomography, densitometry, bone atrophy.*

Introduction

X-ray densitometry is one of the most advanced and diagnostic-informative method of studying bone density [1, 19, 28]. Widespread use [18, 32] and ranges of modifications regulate the possibilities in the study of complex morphological structures [9]. Dynamic observation is easily accessible thanks to digital methods of X-ray anatomical CT, which is much broader than conventional clinical radiology, provide a rapid result of the study of the dynamic bone system [13], which depends on metabolic processes and internal and external factors. environment, causing its pathological and morphological changes, including taking into account its structural topographic features. As a result of such implementations, densitometric determination of bone density, which is a depot of micro- and macroelements of the body, is becoming fundamental in various medical fields of clinical practice [5, 27].

The same assessment of bone mineral density can be performed using ultrasonic densitometry [14], but the difficulty in obtaining three-dimensional models sometimes limits its use.

To understand and assess the bone tissue of the jaws [7], the authors recommend a study of bone density with the

inclusion of cortical and trabecular layers [26], changes in which can be valuable indicators of its biomechanical potential, as described in these works [17, 22].

In direct proportion, the density of bone tissue is reflected in the success of the plan and subsequent surgical treatment of atrophy of the bone tissue of the jaws, with the possible use of osteoplastic materials and, in turn, osteointegration of dental implants. Therefore, rehabilitation of patients with bone atrophy becomes impossible without assessing its density, at the same time, an important component in the diagnosis and planning of reconstructive surgery and prediction of the desired results [26, 33].

X-ray densitometry remains an equally important early diagnostic criterion for detecting the effects of somatic pathology, in particular, endocrine, which leads to the devastation of the trabecular layer or, conversely, its corticalization [4, 23, 29].

The combination of methods for assessing the relationship between morphology, volume and density of bone tissue [4] prevents the possible consequences such as changes in occlusion and facial shape, speech disorders, difficulty in chewing food and social rehabilitation in general.

The available modern review of the literature provides a proper statement on the above issues, and has become an impetus for careful study and a fundamental support for this research.

The aim of the study was to conduct a densitometric assessment to substantiate the rehabilitation of patients with atrophy of the mandible, on the right side, in the age groups of 25 to 75 years.

Materials and methods

Using the Vatech PaX-I 3D Green extra-oral radiography system with a scan size range of 16x9 cm, minimizing the possibility of artifacts caused by patient movement, a 0.5 mm focal spot (IEC60336) on a 14-bit gray scale with a size of 0.2/0.3 voxel and due to the short scan time, high quality images are obtained. 68 scans have been selected that provide the best opportunities for diagnosis and are informative in achieving the goal of this work. The analysis of computed tomographic digital scans was performed using computer technology HEWLETT-SNCPUM1 with 16.0 GB of RAM, system software 10 Pro for Workstations, 2019: 00391-70000-00000-AA425 and standardized X-ray diagnostic software Ez3D-I Original ver.5.1.9.0, used for visualization of multimodal and multidimensional images. Using the tools of the horizontal option panel, in particular the keys of the interface "profile", the density of bone tissue with interpretation in conventional units of grayness (CUG) in the projection of 4.6, 4.7 teeth was studied (Fig. 1).

The material was divided according to the age of patients into four groups, namely: the first group (I) - 25-45 years, the second group (II) - 46-60 years, the third group (III) 61-75, the fourth group (IV) - 25-75 years old, persons with preserved dentition (control group).

All studies were performed after patients were informed and signed an informed consent to participate in studies in compliance with the basic provisions of the GSR (1996), the Council of Europe Convention on Human Rights and Biomedicine (04.04.1997), the Helsinki Declaration of the World Medical Association on Ethical Principles of Medical Research with human participation (1964-2013), orders of the Ministry of Health of Ukraine № 690 of 23.09.2009, № 616 of 03.08.2012 and approved by the decision of the **Commission on Biomedical Ethics** (Minutes № 2 of 21.10.2021).

The work is a fragment of the initiative research work of the Department of Histology, Cytology and Embryology of Bukovinian State Medical University "Structural and functional features of tissues and organs in ontogenesis, patterns of variant, constitutional, sex-age and comparative morphology of human", № state registration 0121U11012.

Digital statistical analysis was performed in StatSoft Statistica 10.0 software and presented as M±σ (mean and standard deviation). Using non-parametric methods of statistical analysis, the comparison of experimental groups with the control group was performed using the Mann-Whitney U-test. Comparison of age groups - using the multidimensional Kruskal-Wallis test as an alternative intergroup analysis of variance used to compare three or

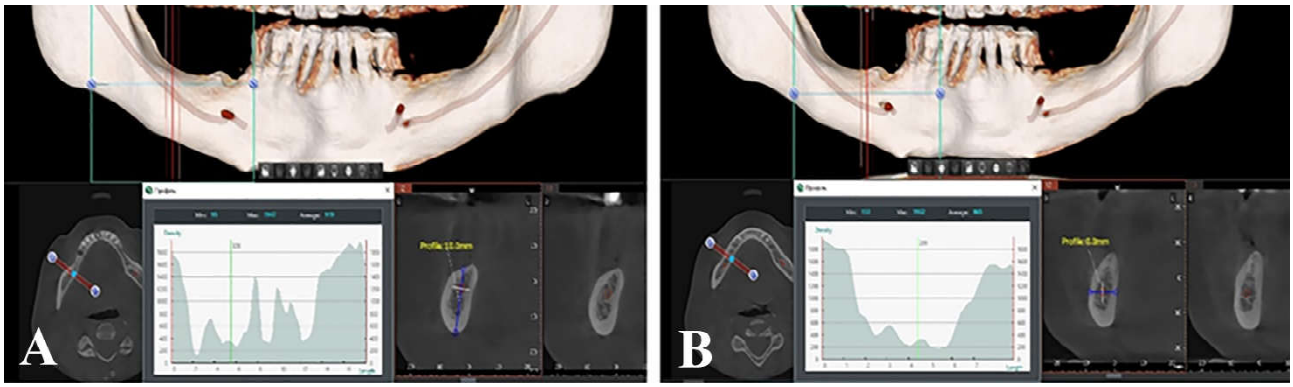

Fig. 1. Densitometric determination of bone density. A - distance, in the vertical plane on sagittal sections, from the edge of the pars alveolaris to the edge of the base of the mandible (VP); B - distance, in the horizontal plane on the sagittal sections, from the edge of the lingual surface to the edge of the buccal surface (HP).

more samples to test null hypotheses according to which different samples were taken from the same distribution with similar medians. Differences between groups were considered significant at a significance level of $p<0.05$.

Results

The obtained results of densitometric determination indicate a decrease in bone density, with the loss of the masticatory group of teeth, in all study groups. Detailed analysis shows a decrease in the mean value of M in the projections of missing 4.6 and 4.7 teeth in vertical (VP) and horizontal (HP) determinations in the three experimental groups (Table 1).

Table 1. Quantitative indicators of densitometric determination (CUG) of mandibular bone on the right side, on sagittal sections in vertical (VP) and horizontal (HP) planes due to loss of masticatory teeth in people aged 25-75 years (M±σ).

Research groups, years	Projection of 4.6 teeth		Projection of 4.7 teeth	
	VP	HP	VP	HP
I (25-45 p.) n=14	880.6±142.9	1159±176	980.1±144.4	1140±206
II (46-60 p.) n=20	812.9±242.4	1064±148	891.5±193.6	1042±148
III (61-75 p.) n=17	783.8±205.3	947.0±176.0	778.8±213.6	893.8±148.0
p	0.359	0.002	0.009	0.000

With increasing of age, bone density decreases in direct proportion to the loss of masticatory teeth, which is confirmed by high reliability, at a level of significance $p<0.05$, intergroup differences in values obtained, except VP in the projection of missing 4.6 teeth, where $p>0.05$ (Fig. 2).

This result is justified by the fact that the cortical layer of bone tissue of the buccal side is primarily affected by etiopathological factors, even with preserved dentition [6].

As well as the physiological process - bone remodeling, primarily occurs on endosteal surfaces, where the most localized osteoclasts and osteoblasts [10, 24].

By comparing the quantitative indicators of densitometric determination (CUG) of bone density, using the Mann-Whitney U-test, in the studied areas of the mandible, the total average number of M experimental (E) groups to the average number of control group (C), the reliability of such results in vertical definitions and is confirmed by $p<0.05$ (Table 2).

The VP value in projection 4.6 is characterized by a moderately high density in the experimental groups (E) and is 822.0±236.7 with a decrease in the control group (C) to 675.5±358.7 ($p<0.05$). The value of VP in the projection of missing 4.7 teeth indicates a decrease in bone density, both in the experimental groups (E) - 878.0±233.2 and in the control group (C) - 725.1±456.4 ($p<0.05$).

This analysis of the results of VP and HP, although confirms the hypothesis of dependence on the constitutional type of person, but its density is directly proportional to the

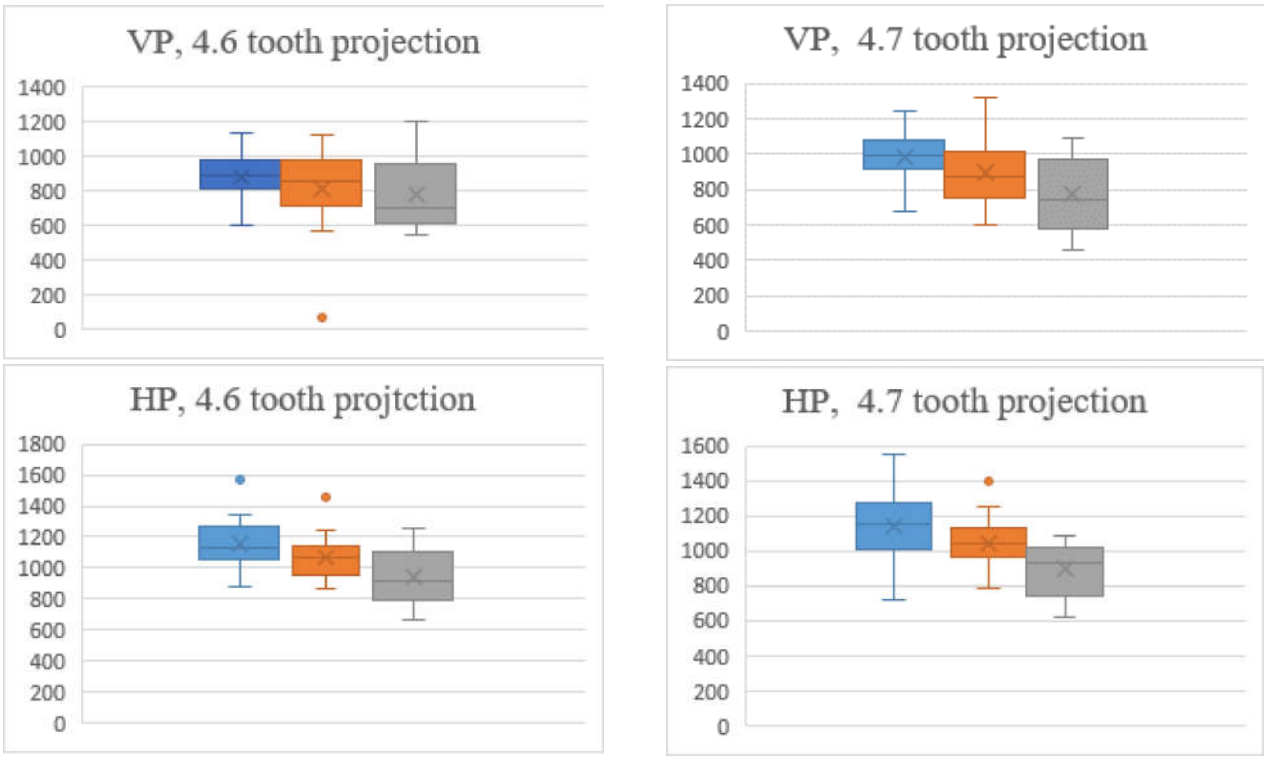

Fig. 2. The level of reliability (p) of the results of densitometric determination: - I research group (25-45 years), where n=14; - II research group (46-60 years), where n=20; - III research group (61-75 years), where n=17.

Table 2. Comparison of quantitative indicators of densitometric determination (CUG) of mandibular bone tissue on sagittal sections in vertical (VP) and horizontal (HP) planes due to loss of masticatory teeth in people aged 25-75 years (n=68).

Definition area		VP		HP	
		M±σ	p	M±σ	p
Projection of 4.6 teeth	E	822.0±236.7	0.004	1051±214	0.300
	C	675.5±358.7		977.4±388.4	
Projection of 4.7 teeth	E	878.0±233.2	0.023	1019±223	0.428
	C	725.1±456.4		959.3±446.1	

Notes: E - experiment; C - control.

The authors [8] point out that the rate of lower jaw bone remodeling is twice as high as in the upper jaw, and, hypothetically, may play a role in the development of osteonecrosis of the jaw, which occurs mainly in the mandibular pars alveolaris due to the pronounced density of cortical layers.

Significant densitometric differences are obtained in the analysis of functional or bone tissue "without activity". Bone mass is conditionally redistributed from one place to another, where force acts [2, 3, 12, 16]. Liquid trabeculation of the mandible (large intertrabecular spaces and thin trabeculae)

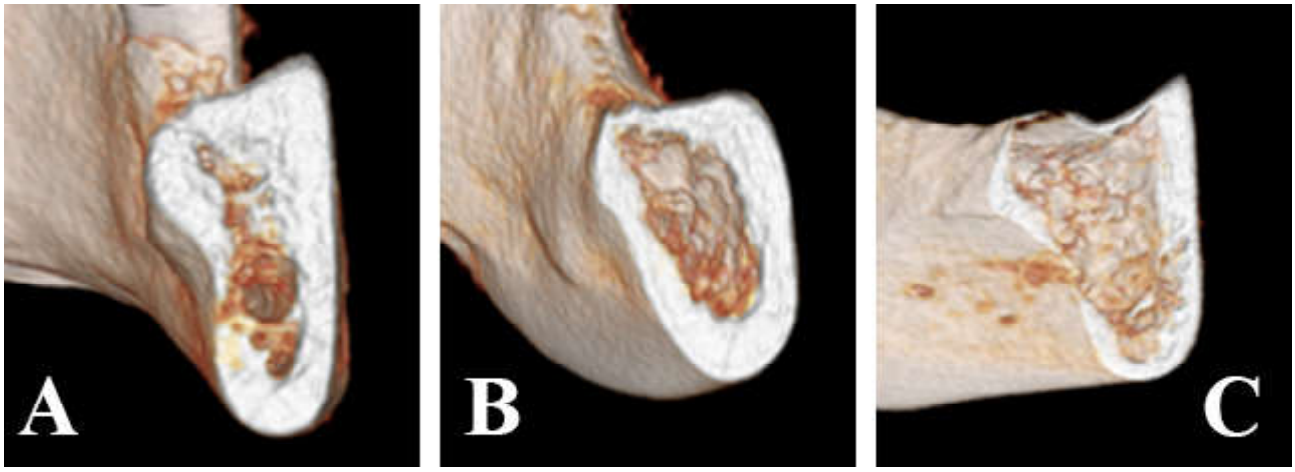

Fig. 3. 3D reconstruction models of coronal (frontal) sections of the mandible, with atrophy of bone tissue due to loss of masticatory teeth. A - the first age group (I, 25-45 years); B - the second age group (II, 46-60 years); C - the third age group (III, 61-75 years).

time of tooth loss. After all, we found that the early loss of the masticatory group of teeth, the first group of studies (25-45 years), leads to high rates, with increasing bone density in the direction of distalization of the final defect of the dentition. Conversely, the lack of functional effect on bone tissue, the second (46-60 years) and third (61-75 years) of the study group, leads to a decrease in its density, and consequently the devastation of the trabecular layer, which contributes to the progression of atrophic processes (Fig. 3).

Discussion

The study of bone density is one of the priority diagnostic methods in the rehabilitation protocol of patients with acquired atrophy of bone tissue with secondary defects of the dentition. After all, bone tissue, in particular lower jaw pars alveolaris, is characterized by pronounced morphological variability and has a unique ability to rearrange in the direction of vertical movement of the teeth [30].

Low bone density is characterized by rapid metabolic metabolism, which leads to increased manifestations of pathological changes. Dense trabeculation in the periapical mandibular molars, with well-mineralized trabeculae and small intertrabecular spaces, is a reliable sign of normal skeletal bone density, while sparse trabecular pattern indicates osteopenic manifestations and difficulty in selecting treatment.

is a reliable sign of osteopenia [22, 25]. Decreases in osteoblast-osteocyte-forming cells, which maintain the level of ionic concentration in the bone interstitial fluid, directly reflect the osteon structure and its volume.

In our previous studies [20], as well as the authors [31] focused on the fact that the lack of indirect "constant pressure" leads bone tissue to a state of relative metabolic rest, but also to its devastation, which we confirm in the interpretation of the results II and III experimental groups of this work, presented above.

Having an understanding of bone density, even with severe atrophy of the cell process, or even its complete resorption, the clinical prognosis becomes clear and receptive to the choice of methods of clinical rehabilitation [11]. Loss of bone width and depth can affect implantation success. Directed (controlled) regeneration (DCR) techniques are often used to restore sufficient bone volume for dental implants, but correct implementation of a modern clinical protocol without densitometric analysis becomes impossible and risky [15]. In previous scientific works, the clinical results of rehabilitation of a patient with dentition defects are clearly presented, in particular, on the example of the mandibular segment [21], which became the basis for further research and writing a scientific paper.

Of course, we, like every researcher, sought to compare the results obtained with acquired atrophy of bone tissue

due to loss of the masticatory group of teeth with age, however, the search for similar studies was not effective. Therefore, the prospects for further research include a detailed analysis of age densitometric assessment of bone tissue, as an interdependent diagnostic criterion in the rehabilitation of patients with early loss of the masticatory group of teeth.

Conclusions

1. The cortical layer of bone tissue on the buccal side is primarily affected by etiopathological factors, even with preserved dentition. Bone remodeling primarily occurs on endosteal surfaces.

2. The density of bone tissue is directly proportional to the time of tooth loss and manifests its variability in the age periods of ontogenetic development. With increasing of age, the bone density of the mandible decreases with end defects of the dentition, which is confirmed by the high intergroup difference of the obtained values, except for the study area in the projection of missing 4.6 teeth in the vertical plane as the area of this definition borders on functionally loaded and is provided with relatively proper mineralization.

References

[1] Abdelmohsen, A. M. (2017). Comparsion of central and peripheral bone mineral density measurements in postmenopausal women. *Journal of Chiropractic Medicine,* 16(3), 199-203. doi: 10.1016/j.jcm.2017.08.001

[2] Bouchard, A. L., Dsouza, Ch., Julien, C., Rummler, M., Gaumond, M-H., Cermakian, N., & Willie, B. M. (2022). Bone adaptation to mechanical loading in mice is affected by circadian rhythms. *Bone,* (154), 116218. doi: 10.1016/j.bone.2021.116218

[3] Evensen, E., Skeie, G., Wilsgaard, T., Christoffersen, T., Dennison, E., Furberg, A.-S., … & Emaus, N. (2018). How is adolescent bone mass and density influenced by early life body size and growth? The Tromsø Study: Fit Futures - A longitudinal cohort study from Norway. *JBMR,* 2(5), 268-280. doi: 10.1002/jbm4.10049

[4] Farzanegan, F., Zarch, S. H. H., Mobasheri, M. F., & Rangrazi, A. (2019). Evaluation of the Relationship Between Morphology, Volume, and Density of the Mandible and Dentofacial Vertical Dimension Using Cone Beam Computed Tomography. *Pesqui. Bras. Odontopediatria Clin. Integr.,* 19(1), 1-8. doi: 10.4034/PBOCI.2019.191.128

[5] He, J., Xu, S., Zhang, B., Xiao, Ch., Chen, Z., Si, F., … Chen, J. (2020). Gut microbiota and metabolite alterations associated with reduced bone mineral density or bone metabolic indexes in postmenopausal osteoporosis. *Aging* (Albany NY), 12(9), 8583-8604. doi: 10.18632/aging.103168

[6] Heimes, D., Schiegnitz, E., Kuchen, R., Kämmerer, P. W., & Al-Nawas, B. (2021). Buccal Bone Thickness in Anterior and Posterior Teeth-A Systematic Review. *Healthcare* (Basel), 9(12), 1-33. doi: 10.3390/healthcare 9121663

[7] Hutchinson, E. F., Farella, M., Hoffman, J., & Kramer, B. (2017). Variation in bone density across the body of the immature human mandible. *Journal of Anatomy*, 230(5), 679-688. doi: 10.1111/joa.12591

[8] Ihnatiev, O. M., Ermolenko, T. O., Turchyn, M. I., Paniuta, O. I., & Prutiian, T. L. (2020). Маркери метаболізму кісткової тканини: лекції [Markers of bone metabolism: lectures]. *Вісник морської медицини - Bulletin of Marine Medicine,* 2(87), 127-148. doi: 10.5281/zenodo.3976574

[9] Jankowski, L. G., Warner, S., Gaither, K., Lenchik. L., Fan, B., Lu, Y., & Shepherd, J. J. (2019). Cross-calibration, Least Significant Change and Quality Assurance in Multiple Dual-Energy X-ray Absorptiometry Scanner Environments: 2019 ISCD Official Position. *Clin. Densitom.,* 22(4), 472-483. doi: 10.1016/j.jocd.2019.09.001

[10] Kawata, K., Narita, K., Washio, A., Kitamura, Ch., Nishihara, T., Kubota, S., & Takeda, S. (2021). Odontoblast differentiation is regulated by an interplay between primary cilia and the canonical Wnt pathway. *Bone,* (150), 116001. doi: 10.1016/j.bone.2021.116001

[11] Khuder, T., Yunus, N., Sulaiman, E., Ibrahim, N., Khalid, T., & Masood, M. (2017). Association between occlusal force distribution in implant overdenture prostheses and residual ridge resorption. *Journal of Oral Rehabilitatiom*, 44(5), 398-404. doi: 10.1111/joor.12504

[12] Kralick, A. E., & Zemel, B. S. (2020). Evolutionary perspectives on the developing skeleton and implications for lifelong health. *Front. Endocrinol,* (Lausanne), (11), 1-11. doi: 10.3389/fendo.2020.00099

[13] Kuroiedova, V. D., Vyzhenko, Ye. Ye., Stasiuk, A. A., Halych, L. B., & Petrova, A. V. (2020). Оптична щільність різних відділів щелеп ортодонтичних пацієнтів в період формування зубощелепної системи [Optical density of different parts of jaws in orthodontic patients during dentofacial development]. *Актуальні проблеми сучасної медицини: Вісник Української медичної стоматологічної академії - Actual Problems of the Modern Medicine: Bulletin of Ukrainian Medical Stomatological Academy,* 3(71), 60-64. doi: 10.31718/2077-1096.20.3.60

[14] Lukyanets, E. Yu. (2021). Оцінка мінеральної щільності кісткової тканини та алгоритмів 10-річного ризику остеопоротичних переломів у жінок [Estimation of bone mineral density and algorithms of 10-year risk of osteoporotic fractures in women]. *Ліки України - Medicines of Ukraine,* 5(251), 31-34. doi: 10.37987/1997-9894.2021.5(251).238139

[15] Malo, P., de Araujo Nobre, M., Lopes, A., Ferro, A., & Botto, J. (2019). The All on 4 treatment concept for the rehabilitation of the completely edentulous mandible: A longitudinal study with 10 to 18 years of follow-up. *Clin. Implant. Dent. Relat. Res.,* 21(4), 565-577. doi: 10.1111/cid.12769

[16] Martinez-Rodriguez, A., Sanchez-Sanchez, J., Vicente-Martinez, M., Martinez-Olcina, M., Miralles-Amoros, L., & Sanchez-Saez, J. A. (2021). Anthropometric dimensions and bone quality in international male beach handball players: junior vs. senior comparison. *Nutrients,* 13(6), 1817. doi: 10.3390/nu13061817

[17] Morgan, E. F., Unnikrisnan, G. U., & Hussein, A. I. (2018). Bone mechanical properties in healthy and diseased states. *Ann. Rev. Biomed. Eng.,* (20), 119-143. doi: 10.1146/annurev-bioeng-062117-121139

[18] Morse, L. R., Biering-Soerensen, F., Carbone, L. D., Cervinka, T., Cirnigliaro, C. M., Johnston, T. E., & … Craven, B. C. (2019). bone mineral density testing in spinal cord injury: ISCD official position. *J. Clin. Densitom.,* 22(4), 554-566. doi: 10.1016/j.jocd.2019.07.012

[19] Ohiomoba, H., Sonis, A., Yansane, A., & Friedland, B. (2017). Quantitative evaluation of maxillary alveolar cortical bone thickness and density using computed tomography imaging. *American Journal of Orthodontics and Dentofacial Orthopedics*, 151(1), 82-91. doi: 10.1016/j.ajodo.2016.05.015

[20] Oshurko, A. P. (2021). Прогресивність вітчизняних та світових наукових обгрунтувань у реабілітації пацієнтів із атрофією кісткової тканини, ускладненої топографо-анатомічною особливістю каналу нижньої щелепи [Progressiveness of domestic and international scientific researches on patient rehabilitation with bone atrophy complicated by the topographical and anatomical peculiarity of the mandibular canal]. *Вісник проблем біології і медицини - Bulletin of Problems Biology and Medicine*, 162(4), 55-60. doi: 10.29254/2077-4214-2021-4-162-55-60

[21] Oshurko, A. P., Oliinyk, I. Yu., Yaremchuk, N. I., & Makarchuk, I. S. (2021). Morphological features of bone tissue in "disuse atrophy" on the example of a segment of the human lower jaw: clinical experience of treatment. *Biomedical and Biosocial Anthropology*, (42), 5-11. doi: 10.31393/bba42-2021-01

[22] Owen, R., & Reilly, G. C. (2018). In vitro models of bone remodelling and associated disorders. *Front. Bioeng. Biotechnol.,* (6), 1-22. https://doi.org/10.3389/fbioe.2018. 00134

[23] Ramanauskaite, A., Becker, K., Kassira, H. C., Becker, J., Sader, R., & Schwarz, F. (2020). The dimensions of the facial alveolar bone at tooth sites with local pathologies: A retrospective cone-beam CT analysis. *Clin. Oral. Investig.*, 24(4), 1551-1560. doi: 10.1007/s00784-019-03057-x

[24] Remmers, S. J. A., de Wildt, B. W. M., Vis, M. A. M., Spaander, E. S. R., de Vries, R. B. M., Ito, K., & Hofmann, S. (2021). Osteoblast-osteoclast co-cultures: A systematic review and map of available literature. *National Library of Medicine,* 16(11), e0257724. doi: 10.1371/journal.pone.0257724

[25] Rodionova, S. S., & Khakimov, U. R. (2018). Факторы риска дефицита минеральной плотности костной ткани и низкоэнергетического перелома при первичных формах остеопороза у мужчин [Risk factors of bone mineral density deficit and low-energy fractures in primary osteoporosis in men]. *Вестник травматологии и ортопедии имени Н.Н. Приорова - Bulletin of traumatology and orthopedics named after N. N. Priorov,* (1), 22-29. doi: 10.32414/0869-8678-2018-1-22-29

[26] Rossi, M., Bruno, G., de Stefani, A., Perri, A., & Gracco, A., (2017). Quantitative CBCT evaluation of maxillary and mandibular cortical bone thickness and density variability for orthodontic miniplate placement. *International Orthodontics,* 15(4), 610-624. doi: 10.1016/j.ortho.2017.09.003

[27] Schafmeyer, L., Linden, T., Sill, H., Rehberg, M., Schoenau, E., & Duran, I. (2022). Pediatric Reference Centiles of Bone Mineral Density and Body Composition of Lower Limbs. *Journal of Clinical Densitometry,* 25(1), 73-80. doi: 10.1016/j.jocd.2021.07.013

[28] The International Society for Clinical Densitometry (Adult) Official Positions. (2019). 1-35. https://www.iscd.org/official-positions/2019-iscd-official-positions-adult

[29] Tian, L., Yang, R., Wei, L., Liu, J., Yang, Y., Shao, F., … & Guo T. (2017). Prevalence of osteoporosis and related lifestyle and metabolic factors of postmenopausal women and elderly men: A cross-sectional study in Gansu province, Northwestern of China. *Medicine* (Baltimore), 96(43), e8294. doi: 10.1097/MD.0000000000008294

[30] Tsepkolenko, V. O., Pshenychnyi, T. Y., Holiuk, Ye. L., Tymochuk, V. V., & Derkach, R. V. (2021). Використання аутомезоконцентрату тромбоцитів у пацієнтів з патологією опорно-рухового апарату [The Platelet Automesoconcentrate in Patients with Orthopedical Pathology]. *Український журнал медицини, біології та спорту - Ukrainian Journal of Medicine, Biology and Sport,* 29(1), 160-167. doi: 10.26693/jmbs06.01.160

[31] Whitney, D. G., Hurvitz, E. A., & Caird, M. S. (2021). Critical periods of bone health across the lifespan for individuals with cerebral palsy: Informing clinical guidelines for fracture prevention and monitoring. *Bone,* (150), 116009. doi: 10.1016/j.bone.2021.116009

[32] Williams, K. M., Darukhanavala, A., Hicks, R., & Kelly, A. (2022). An Update on Methods for Assessing Bone Quality and Health in Cystic Fibrosis. *Journal of Clinical & Translational Endocrinology*, (27), 100281. doi: 10.1016/j.jcte.2021.100281

[33] Wismeijer, D., & Chen, S. T. (2018). Proceedings of the Sixth ITI Consensus Conference. *Clin. Oral. Impl. Res.*, 29(Suppl. 16), 5-7. doi: 10.1111/clr.13301

ДЕНСИТОМЕТРИЧНА ОЦІНКА В ОБҐРУНТУВАННІ РЕАБІЛІТАЦІЇ ПАЦІЄНТІВ ІЗ АТРОФІЄЮ КІСТКОВОЇ ТКАНИНИ НИЖНЬОЇ ЩЕЛЕПИ, З ПРАВОЇ СТОРОНИ

Ошурко А. П.

Методи денситометричного визначення щільності кісткової тканини дедалі частіше стають фундаментальними у наукових дослідженнях та пріоритетними у клінічному застосуванні в медичній практиці. Реабілітація пацієнтів з атрофією кісткової тканини стає неможливою без оцінки її щільності та, водночас, є важливою складовою при діагностиці та плануванні реконструктивного хірургічного втручання, зокрема, прогностичності у використанні остеопластичних матеріалів чи остеоінтеграції дентальних імплантатів. Метою роботи було проведення денситометричної оцінки для обґрунтування реабілітації пацієнтів з атрофією кісткової тканини нижньої щелепи з правої сторони у вікових групах людей від 25 до 75 років. Отримані з використанням системи екстра-оральної рентгенографії Vatech PaX-I 3D Green комп'ютерно-томографічні цифрові сканування опрацьовано стандартизованим рентгенодіагностичним програмним забезпеченням Ez3D-I Original ver.5.1.9.0. Використовуючи інструменти горизонтальної опційної панелі, зокрема клавіші інтерфейсу "профіль", досліджено щільність кісткової тканини з інтерпретацією в умовних одиницях сірості (УОС) у проекції 4.6 та 4.7 зубів. Для отримання якісно однорідних значень нами застосовано непараметричні методи статистичного аналізу порівняння груп за віком - із використанням багатовимірного критерію Краскела-Уолліса як альтернативного міжгрупового дисперсного аналізу для одночасного порівняння трьох вибірок. Під час статистичного аналізу отриманих показників щільності кісткової тканини з використанням U-критерію Манна-Уїтні в досліджуваних ділянках нижньої щелепи справа, за загальним середнім числом М дослідних (Д) груп у порівнянні із середнім числом групи контролю (К), отримано високу достовірність результатів у вертикальних (VP) замірах і підтверджено p<0,05. Таким чином, доведено, що рання втрата жувальної групи зубів, у першій групі дослідження (25-45 років), призводить до високих показників з наростанням щільності кісткової тканини в бік дисталізації кінцевого дефекту зубних рядів. І, навпаки, відсутність функціональної дії на кісткову тканину, у другій (46-60 років) та третій (61-75 років) групах дослідження, призводить до зниження її щільності, а, відповідно, і до спустошення трабекулярного шару, що сприяє прогресуванню атрофічних процесів.

Ключові слова: *нижня щелепа, комп'ютерна томографія, денситометрія, атрофія кісткової тканини.*

DOI: 10.31393/morphology-journal-2022-28(1)-07 Reports of Morphology, Vol. 28, №1, Pages 48-53

ISSN 1818-1295 eISSN 2616-6194

REPORTS OF MORPHOLOGY

Official Journal of the Scientific Society of Anatomists, Histologists, Embryologists and Topographic Anatomists of Ukraine

journal homepage: https://morphology-journal.com

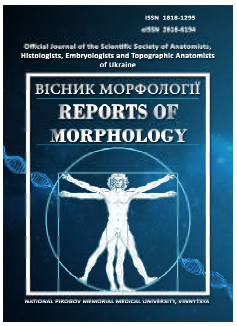

The results of morphological studies in women of reproductive age with hyperproliferative diseases of the endometrium

Abdullaiev V. E.
National Pirogov Memorial Medical University, Vinnytsya, Ukraine

ARTICLE INFO
Received: 29 November 2021
Accepted: 11 January 2022

UDC: 618.14-002.2-007.61

CORRESPONDING AUTHOR
e-mail: vahif.abdullaiev@gmail.com
Abdullaiev V. E.

CONFLICT OF INTEREST
The authors have no conflicts of interest to declare.

FUNDING
Not applicable.

Hyperproliferative processes of the endometrium, remaining one of the most common gynecological pathologies, still have imperfections in the diagnostic stages, both invasive and non-invasive. There is still controversy about the need to differentiate between hyperplasia and endometrial polyps. And the improvement of the method of pathomorphological research and the invention of immunohistochemical markers for the endometrium, opened new opportunities for better diagnosis of hyperproliferative processes of the endometrium. Also, an important component of the diagnosis of endometrial pathology are invasive methods, namely hysteroscopy, which has eliminated most of the shortcomings associated with the classic scraping of the uterine cavity. The definition of markers of chronic endometritis has opened new questions about the origin of chronic inflammation in the uterine cavity, its course and the relationship with the biocenosis of the lower genital tract. The aim of this study was to determine the role of pathomorphological immunohistochemical cytological methods of examination and microscopy in patients of reproductive age with hyperproliferative processes of the endometrium. In order to achieve this goal, we analyzed 161 women, of whom 58 women had verified diagnoses of endometrial hyperproliferative processes, 71 women were morphologically verified diagnoses of hyperproliferative processes in combination with chronic endometritis. The control group consisted of 32 women without evidence of hyperproliferative processes of the endometrium and chronic endometritis. The age of women ranged from 18 to 53 years. Also, all women underwent cytological examination of the cervix and microscopy of vaginal swabs. According to the data obtained, the percentage ratio between the number of diagnosed endometrial polyps and endometrial hyperplasia was equal, with a slight advantage towards endometrial polyps. Other gynecological diseases such as uterine fibroids, external endometriosis and cervical polyps accounted for a total of 0.8 to 3.9 %. Cytological examination of the cervix indicated the predominance of type 2 cytology in the group of women with chronic endometritis. Analysis of microscopic data of vaginal secretions indicates an increased level of inflammation in the group of women with a combination of hyperplastic processes of the endometrium and chronic endometritis. In conclusion, it is possible to claim a slightly higher level of chronic endometritis in the group of women with endometrial polyps, compared with endometrial hyperplasia. There is also a clear link between the diagnosis of chronic endometritis and inflammatory changes in cytological examination of the cervix and microscopy of vaginal discharge. Comparison of the results of the above diagnostic methods can improve the diagnosis of hyperproliferative processes of the endometrium and chronic endometritis, with the further development of effective treatment methods.

Keywords: *endometrial hyperplasia, endometrial polyps, endometrial hyperproliferative processes, pathomorphological study, immunohistochemical study, cytological examination.*

Introduction

Hyperproliferative diseases of the endometrium (HE) attract the attention of scientists and practitioners because they have a high risk of progression to neoproliferative processes [1, 2]. At the same time, there are many differences in the interpretation of the etiopathogenetic aspects of these processes, their classification and

methods of treatment. The issue of endometrial polyps (PE) is debatable, most authors consider them a special form of proliferative process, and distinguish it from endometrial hyperplasia [2, 3, 5]. At the same time, some authors believe that endometrial polyps are a local form of endometrial hyperplasia, and polyps larger than 15 mm in diameter are generally considered a manifestation of diffuse endometrial hyperplasia [7, 10]. The WHO has adopted a classification of proliferative processes - hyperplasia in two forms: without atypia and with atypia. Despite the large amount of research on various aspects of endometrial hyperplastic processes, the role of inflammatory processes in the pathogenesis of endometrial hyperplasia and polyps remains controversial, the possibility of using anti-inflammatory therapy in conservative treatment of hyperplastic processes and prevention of malignancy is unclear [10, 12].

In addition to the study of anamnesis, the use of laboratory and non-invasive methods of endometrial examination, invasive diagnostic techniques with subsequent morphological examination have become widely used [11, 15]. According to endometrial biopsy, we have the opportunity to obtain sufficiently informative material for diagnosis, while some authors point to its lack of information due to possible technical errors, such as the inability to remove polyps in this way. However, the combination of this method with hysteroscopy allows for better diagnosis of hyperproliferative processes of the endometrium [13, 18, 21].

Hysteroscopy is now considered the most reliable method for diagnosing hyperproliferative processes of the endometrium, and the doctor has the opportunity not only to assess visually pathological changes, but also to conduct targeted surgery, to assess its effectiveness. The informativeness of hysteroscopy is estimated by various authors in 84-96 % [16, 17]. Some authors point out the disadvantages of this method, the presence of individual errors caused by the peculiarities of changes in the endometrium.

Finally, the diagnosis of hyperproliferative processes of the endometrium can be established as a result of histological examination of the surgical material [19]. Histological examination makes it possible to assess not only the form of hyperproliferative processes of the endometrium, but also the presence of signs of neoproliferative process in the studied material. The main question to be answered by histological diagnosis is the presence or absence of signs of atypia.

Different authors determine the different effectiveness of hysteroscopy in chronic endometritis (CE), and differences in estimates are quite polar: from 16 to 93 % of cases [19, 20]. At the same time, the presence of such signs as uneven endometrial thickness, focal hypertrophy of the mucous membrane, the presence of polypoid growths, hyperemia or uneven coloration of the mucous membrane suggest the presence of chronic endometritis [20].

Immunohistochemical method detects markers characteristic of chronic endometritis: CD68+, CD45+, CD56+, CD20+, CD16+, rarely CD4+, CD8+. For autoimmune chronic endometritis is characterized by an increase in CD56+ in the amount of 25-60 in the field of view. Most authors point out that the most important sign of chronic endometritis is the presence of markers of plasma CD138+ cells in lymphoid infiltrates of the endometrial stroma [19, 20, 21].

The final point in the diagnosis of chronic endometritis makes it possible to put a morphological examination of the endometrium. In the presence of inflammatory infiltrates in the endometrium, which consist mainly of lymphoid elements located around the glands and blood vessels; especially in the presence of plasma cells in these infiltrates, the presence of fibrosis of the endometrial stroma and sclerotic changes in the walls of the spiral arteries of the uterus, we have the opportunity to diagnose chronic endometritis.

The aim of the study is to compare the results of pathomorphological and immunohistochemical methods of endometrial examination with methods of diagnosing the biocenosis of the lower parts of the female genital tract.

Materials and methods

According to the conclusion of the **Committee on Bioethics** of the National Pirogov Memorial Medical University, Vinnytsya № 2 dated 10.02.2022, the research methods described in the publication were applied in compliance with human rights in accordance with current legislation in Ukraine, meet international ethical requirements and do not violate ethical norms and standards. conducting biomedical research.

In connection with the objectives of the study analyzed the results of laboratory studies of 161 women, of whom 58 had verified diagnoses of endometrial hyperplastic processes (group 1), and 71 were found morphologically verified hyperplastic processes in combination with chronic endometritis registered in 2018 until 2020 (group 2). The control group consisted of 32 women without signs of hyperplastic processes and chronic endometritis.

In verifying the diagnosis used common morphological signs of chronic endometritis [6]:

- the presence in the endometrium of inflammatory infiltrates, which consist mainly of lymphoid elements with the inclusion of macrophages and eosinophils and are located more often around the glands and blood vessels, rarely diffuse;
- the presence of plasma cells in infiltrates;
- focal stroma fibrosis;
- sclerotic changes in the walls of the spiral arteries of the endometrium.

In all cases, the so-called "complete symptom complex of chronic endometritis" was verified, ie the presence of not one but all morphological signs of the disease from the above list.

Vaginal smear microscopy and determination of the degree of purity of secretions were used to assess the state of the biocenosis of the lower genital tract of the examined women.

For the purpose of early diagnosis of oncological diseases and determination of the condition of the cervical epithelium, we performed a cytological examination of the cervix in women.

Statistical data processing was performed on a personal computer using Microsoft Excel spreadsheets and the application package Statistica for Windows V.7.0, StatSoft Inc. (USA). All obtained quantitative data were processed by the method of variation statistics. Percentages were determined for each relative parameter. For nonparametric data, the φ-Fisher angular transformation method was used (for 2 groups) for unrelated sets.

Results

After careful collection of anamnestic data, detection of clinical manifestations, gynecological examination, performed pathomorphological and immunohistochemical examination of endometrial samples. Pathomorphological examination of the endometrium to verify the diagnosis of chronic endometritis and hyperplastic processes of the endometrium was performed in all patients. The results of the morphological study are presented in table 1.

According to our data, in patients of the studied groups in 44.2 % of cases there was endometrial hyperplasia without atypia, in 55.8 % local endometrial hyperplasia (polyp), in 55.0 % of women signs of chronic endometritis, in 55.8 % - CD138 expression, in addition to isolated fibroids cases (1.6 %), endometrioid cyst (3.1 %), endometrial rejection disorders (3.9 %), cervical polyps (0.8 %).

The results of cytological examination of the cervix are presented in table 2 and figure 1.

According to the results of our study, the 2nd grade of cervical cytology prevailed in both study groups (63.8 % in the group of women with hyperplastic endometrial processes, and 81.7 % in the group of women with a combination of endometrial hyperplastic processes and chronic endometritis, $p<0.05$). For other grades (1st and 3rd) we did not find statistically significant differences for the indicators of the studied groups.

In the studied groups, the highest rate was set for grade 2 cytology of the cervix, which indicates the presence of elements of inflammation. This parameter was statistically significantly higher than the same indicator of the control group (73.6 % vs. 46.9 %, respectively, $p<0.05$). It should be noted that in the control group the highest was the indicator of the 1st grade of cytology (corresponding to the norm), which was significantly higher than the studied groups of women with pathology (50.0 % vs. 11.6 %, respectively, $p<0.01$). The significant advantage of the 3rd grade of cytology (focal changes without atypia) in the studied women (14.8 % vs. 3.1 % in the control group, $p<0.05$) is noteworthy.

We note a tendency for a slightly higher rate of cytology grade 2 in women with chronic endometritis, compared with endometrial hyperplastic processes (71.9 vs. 53.8 %, respectively) and the predominance of cytology grade 3 in women with HE over PE (34.8 vs. 12.5 %, respectively), but they are not statistically significant ($p>0.05$).

The results of determining the degree of purity of secretions in women of the study groups are presented in table 3.

In women of the studied groups there is a predominance of 2 degrees of purity (65.1 %), less (33.3 %) - 3 degrees of

Table 1. The results of morphological examination in patients of the studied groups.

Nosology	Group 1 (n=58)		Group 2 (n=71)		Fisher's ratio	Total (n=129)	
	n	%	n	%	φ	n	%
Endometrial hyperplasia without atypia	26	44.8	31	43.7	0.125	57	44.2
Endometrial polyp	32	55.2	40	56.3	0.124	72	55.8
Chronic endometritis	0	0	71	100	17.75**	71	55.0
Progesterone receptor expression	1	1.7	1	1.4	0.137	2	1.6
Expression of CD138	1	1.7	71	100	16.27**	72	55.8
Fibroids	1	1.7	1	1.4	0.137	2	1.6
Endometrioid cyst	0	0	4	5.6	2.700**	4	3.1
Disorders of endometrial rejection	1	1.7	4	5.6	1.222	5	3.9
Cervical polyp	0	0	1	1.4	1.340	1	0.8

Notes: * - p<0.05; ** - p<0.01.

Table 2. The results of cytological examination of the cervix in patients of the studied groups.

Nosology	Group 1 (n=58)		Group 2 (n=71)		Fisher's ratio	Total (n=129)	
	n	%	n	%	φ	n	%
Grade 1	9	15.5	6	8.5	1.229	15	11.6
Grade 2	37	63.8	58	81.7	2.300*	95	73.6
Grade 3	12	20.7	7	9.9	1.720	19	14.8

Notes: * - p<0.05; ** - p<0.01.

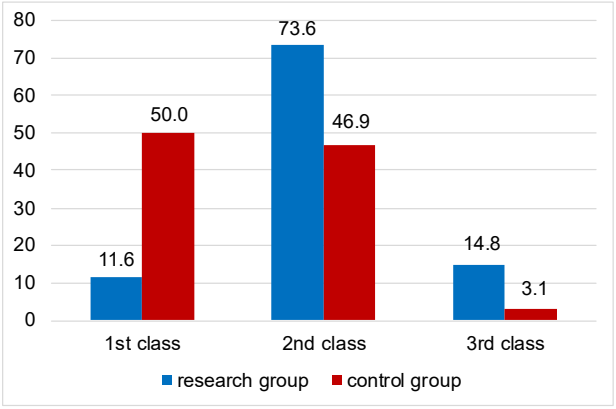

Fig. 1. Comparative diagrams of the results of cytological examination of the cervix in women from control and study groups.

Table 3. The degree of purity of secretions in women of the study groups.

Nosology	Group 1 (n=58)		Group 2 (n=71)		Fisher's ratio	Total (n=129)	
	n	%	n	%	φ	n	%
1 degree	0	0	1	1.4	1.340	1	0.8
2 degree	47	81.0	37	52.1	3.541**	84	65.1
3 degree	11	19.0	32	45.1	3.224**	43	33.3
4 degree	0	0	1	1.4	1.340	1	0.8

Notes: * - p<0.05; ** - p<0.01.

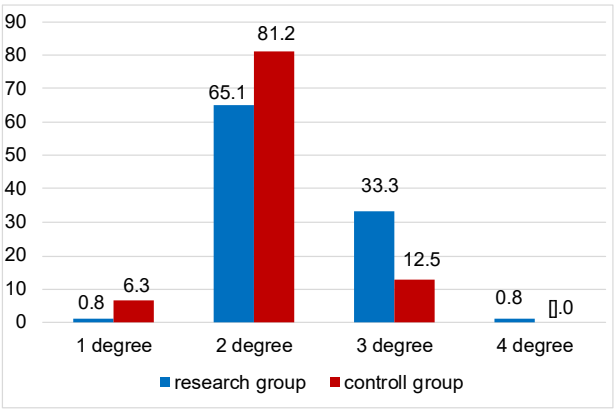

Fig. 2. Comparative diagrams of the microscopy results of vaginal swabs in women from control and study groups.

purity, with a small amount (0.8 %) of 1 degree and 4 degrees of purity (Fig. 2).

Comparing the data of studies of discharges between patients in the study groups, our attention was drawn to the fact that the group of women with HE significantly dominated by smears of 2 degrees of purity with leukocytes up to 10, a large number of lactobacilli, moderate microflora (81.0 % vs. 52.1 % in women with HE and CE, p<0.01). Also in this group the indicator of 3 degrees of purity of smears was significantly lower (19.0 % against 45.1 %, respectively, p<0.01). Thus, in the 2nd group smears with the number of leukocytes 10-30, a small number of lactobacilli, moderate mixed microflora predominates. Thus, the group of women with HE is dominated by smears typical of healthy women who are already having sex, and in the group of women with a combination of HE and CE a high percentage of respondents at high risk of developing inflammatory diseases (vulvovaginitis, etc.).

According to our data, the control group is dominated by women with normal microflora (1 and 2 degrees of purity) - 87.5 % against 65.9 % of women in the study groups (p<0.05). Among women in the study groups, in particular, respondents with a combination of HE and CE, indicators with a high risk of infectious diseases (3-4 degrees of purity) prevail - 34.1 % vs. 12.5 %, respectively.

Discussion

The distribution of the structure of endometrial hyperproliferative processes into polyps and endometrial hyperplasia, according to our data, is uniform, with a slight advantage towards endometrial polyps, which is consistent with the authors Chen Y. Q. and co-authors [3] and Fang R. L. and co-authors [8]. In addition, according to Cicinelli E. co-authors [5] and Cheung W. and Cheung V. [4], the presence of patients with a confirmed diagnosis of endometrial hyperproliferative processes does not exclude the presence of concomitant gynecological diseases such as uterine fibroids, external endometriosis and cervical polyps. The presence of pathomorphologically confirmed diagnosis of hyperproliferative processes of the endometrium significantly increases the risk of a positive immunohistochemical marker of chronic endometritis, especially in the group of endometrial polyps [4, 5].

In turn, chronic endometritis, as a possible risk factor for hyperproliferative processes of the endometrium requires both immunohistochemical verification and pathomorphological confirmation using multiple criteria, such as the presence of plasma cells, inflammatory infiltration, stroma fibrosis, sclerotic changes [7, 9, 11]. It should be noted that patients with hyperproliferative processes of the endometrium and chronic endometritis with a higher frequency have type 2 cytological examination of the cervix with inflammation and increased inflammation according to microscopy of vaginal discharge [11, 14]. According to Clark T.J. and Stevenson H. [6], endometrial polyps increase the risk of developing chronic endometritis compared to other types of endometrial hyperproliferative processes, which is comparable to the results of our study. It is an indisputable fact that chronic endometritis may be the basis for the development of hyperproliferative processes of the endometrium, which may under certain conditions progress to atypical endometrial hyperplasia and endometrial adenocarcinoma.

The attention of scientists is also drawn to the interaction of the infectious agent with the protective systems of the female body. Thus, the presence of a large number of lactobacilli is considered an indicator of normal microflora, which counteracts the development of other groups of potentially dangerous microorganisms. Thus, Fang R. L. and co-authors [8] indicated a fairly high level of lactobacilli in patients with endometrial polyps (38.6 %). The data of these authors are slightly lower than ours, but it should be borne in mind that in this study we took into account only the degree of bacterial purity. At the same time, these data are refined by Kimura F. and co-authors [13], who indicate that the study on CD138 did not reveal statistically significant differences between women with and without chronic endometritis. According to researchers, this suggests that the interaction between the infectious agent and endometrial immunity is important in the development of chronic inflammation.

Another topical issue that is widely studied in the context of endometrial hyperproliferative processes associated with chronic endometritis is the problem of fertilization of the ovum and pregnancy, which makes the problem of

combining hyperproliferative processes of the endometrium and chronic endometritis multidisciplinary, relevant for obstetricians and gynecologists, as well as for oncogynecologists and reproductive specialists [9, 21]. Today, there are a small number of published studies that describe the relationship between chronic endometritis and the microflora of the lower female genitalia. Studying such relationships may be key to discovering the pathogenesis of chronic endometritis. Authors Cheung W. and Cheung V. [4] compared the origins of chronic inflammatory processes of the fallopian tubes and uterine cavity, which in our opinion is a very promising area. An important aspect in studying the origin of chronic endometritis is the use of modern diagnostic techniques. In our opinion, the combination of classical diagnostic techniques such as microscopy and cytology with modern immunohistochemical markers is optimal, which may be the optimal solution to the treatment of chronic endometritis [16, 18].

The above diagnostic techniques do not allow to decide on the appointment of etiopathogenetic treatment, but only to state the fact of diagnosis of chronic endometritis. In this case, it may be useful to use PCR to determine the pathogen and bacterial load in the test material. At this stage, before the invention and widespread implementation of unified diagnostic and therapeutic approaches to the treatment of chronic endometritis, diagnosis requires an extended approach using many different techniques and comparing their results [3, 5, 9, 15].

Conclusions

1. Patients with endometrial polyps have a higher risk of developing chronic endometritis compared with patients with endometrial hyperplasia.

2. To detect chronic endometritis as a cause of hyperproliferative processes of the endometrium, it is advisable to use a combined diagnostic approach using pathomorphological examination with many criteria, immunohistochemical marker CD138, cytological examination of the cervix and microscopy of vaginal secretions.

3. The obtained results confirm the common origin of chronic inflammation of different parts of the female genital tract and indicate its connection with the occurrence of hyperproliferative processes of the endometrium.

4. PCR diagnosis of endometrial samples can be considered a promising area for the diagnosis of etiological factors of chronic endometritis in patients with hyperproliferative processes of the endometrium.

References

[1] Akeda, K., An, H. S., Okuma, M., Attawia, M., Miyamoto, K., Thonar, E. J.-M. A., … Masuda, K. (2016). Platelet-rich plasma stimulates porcine articular chondrocyte proliferation and matrix biosynthesis. *Osteoarthritis Cartilage*, 14(12), 1272-1280. doi: 10.1016/j.joca.2006.05.008

[2] Benyuk, V. O., Goncharenko, V. M., Zabudskiy, O. V., & Yarmak, V. S. (2015). Роль хронічного ендометриту в генезі гіперпластичних процесів ендометрію [The role of chronic endometritis in the genesis of hyperplastic endometrial processes]. *Здоровье женщины - Woman's Health,* 102(6), 16-21.

[3] Chen, Y. Q., Fang, R. L., Luo, Y. N., & Luo, C. Q. (2016). Analysis of the diagnostic value of CD138 for chronic endometritis, the risk factors for the pathogenesis of chronic endometritis and the effect of chronic endometritis on pregnancy: a cohort study. *BMC Womens Health,* 16(1), 60. doi: 10.1186/s12905-016-0341-3

[4] Cheung, W., & Cheung, V. (2017). Coexisting Endosalpingiosis and Subserous Adenomyosis. *J. Min. Invasive Gyn.,* (22), 315-316. doi: 10.1016/j.jmig.2014.07.012

[5] Cicinelli, E., Matteo, M., Tinelli, R., Lepera, A., Alfonso, R., Indraccolo, U., … Resta, L. (2015). Prevalence of chronic endometritis in repeated unexplained implantation failure and the IVF success rate after antibiotic therapy. *Hum. Reprod. Oxf. Engl.,* 30(2), 323-330. doi: 10.1093/humrep/deu292

[6] Clark, T. J., & Stevenson, H. (2017). Endometrial Polyps and Abnormal Uterine Bleeding (AUB-P): What is the relationship, how are they diagnosed and how are they treated? *Best Pract. Res. Clin. Obstet. Gynaecol.,* (40), 89-104. doi: 10.1016/j.bpobgyn.2016.09.005

[7] Committee on Gynecologic Practice, Society of Gynecologic Oncology. (2015). Committee on Gynecologic Practice, Society of Gynecologic Oncology Committee opinion № 631. Endometrial intraepithelial neoplasia. *Obstetrics & Gynecology,* 125(5), 1272-1278. doi: 10.1097/01.AOG.0000465189.50026.20

[8] Fang, R. L., Chen, L. X., Shu, W. S., Yao, S. Z., Wang, S. W., & Chen, Y. Q. (2016). Barcoded sequencing reveals diverse intrauterine microbiomes in patients suffering with endometrial polyps. *American Journal of Translational Research*, 8(3), 1581-1592.

[9] Gombolevskaya, N. A., & Marchenko, L. A. (2012). Современные критерии диагностики хронического эндометрита (обзор литературы) [Modern criteria for the diagnosis of chronic endometritis (literature review)]. *Проблемы репродукции - Reproduction Problems,* 18(1), 42-46.

[10] Horban, N. Y., Vovk, I. B., Lysiana, T. O., Ponomariova, I. H., & Zhulkevych, I. V. (2019). Peculiarities of uterine cavity biocenosis in patients with different types of endometrial hyperproliferative pathology. *Journal of Medicine and Life,* 12(3), 266-270. doi: 10.25122/jml-2019-0074

[11] Huchon, C., Koskas, M., Agostini, A., Akladios, C., Alouini, S., Bauville, E., ... Fauconnier, A. (2015). Operative hysteroscopy versus vacuum aspiration for incomplete spontaneous abortion (HY-PER): study protocol for a randomized controlled trial. *Trials,* 16, 363. doi: 10.1186/s13063-015-0900-1

[12] Khmil, S. V., Khmil, M. S., Drozdovska, Yu. B., & Chudiiovych, N. Ya. (2018). Ефективність гістероскопії у жінок з безпліддям на фоні лейоміоми матки в програмах допоміжних репродуктивних технологій [Efficiency of hysteroresectoscopy in women with infertility in the background of uterine leiomyomas in the programs of assisted reproductive technologies]. *Вісник соціальної гігієни та організації охорони здоров'я України - Bulletin of Social Hygiene and Health Protection Organization of Ukraine,* 78(4), 51-55. doi: 10.11603/1681-2786.2018.4

[13] Kimura, F., Takebayashi, A., Ishida, M., Nakamura, A., Kitazawa, J., … Murakami, T. (2019). Review: Chronic endometritis and

its effect on reproduction. *J. Obstet. Gynaecol. Res.,* 45(5), 951-960. doi: 10.1111/jog.13937

[14] Kitaya, K., Tada, Y., Hayashi, T., Taguchi, S., Funabiki, M., & Nakamura, Y. (2014). Comprehensive endometrial immunoglobulin subclass analysis in infertile women suffering from repeated implantation failure with or without chronic endometritis. *Am. J. Reprod. Immunol.,* 72(4), 386-391. doi: 10.1111/aji.12277

[15] Kitaya, K., Yasuo, T., Tada, Y., Hayashi, T., Iwaki, Y., Karita, M., … Yamada, H. (2014). Unusual inflammation in gynecologic pathology associated with defective endometrial receptivity. *Histol. Histopathol.,* 29(9), 1113-1127. doi: 10.14670/hh-29.1113

[16] Moreno, I., Cicinelli, E., Garcia-Grau, I., Gonzalez-Monfort, M., Bau, D., Vilella, F., … Simon, C. (2018). The diagnosis of chronic endometritis in infertile asymptomatic women: a comparative study of histology, microbial cultures, hysteroscopy, and molecular microbiology. *AJOG,* 218(6), 602. doi: 10.1016/j.ajog.2018.02.012

[17] Nijkang, N. P., Anderson, L., Markham, R., & Manconi, F. (2019). Endometrial polyps: Pathogenesis, sequelae and treatment. *SAGE Open Med.,* 7, 1-12. doi: 10.1177/2050312119848247

[18] Puente, E., Alonso, L., Lagana, A. S., Ghezzi, F., Casarin, J., & Carugno, J. (2020). Chronic endometritis: Old problem, novel insights and future challenges. *Int. J. Fertil. Steril.,* 13(4), 250-256. doi: 10.22074/ijfs.2020.5779

[19] Resta, L., Palumbo, M., Piscitelli, D., Grazia Fiore, M., & Cicinelli, E. (2012). Histology of micro polyps in chronic endometritis. *Histopathology,* 60(4), 670-674. doi: 10.1111/j.1365-2559.2011.04099.x

[20] Sfakianoudis, K., Simopoulou, M., Nitsos, N., Lazaros, L., Rapani, A., Pantou, A., … Pantos, K. (2019). Successful Implantation and Live Birth Following Autologous Platelet-rich Plasma Treatment for a Patient with Recurrent Implantation Failure and Chronic Endometritis. *In Vivo,* 33(2), 515-521. doi: 10.21873/invivo.11504

[21] Vaskkivuo, T., Stenback, F., & Tapanainen, J. (2012). Apoptosis and apoptosisrelated factors Bcl-2, Bax, tumor necrosis factor-alpha, and NFkappaB in human endometrial hyperplasia and carcinoma. *Cancer,* 95(7), 1463-1471. doi: 10.1002/cncr.10876

[22] Wu, D., Kimura, F., Zheng, L., Ishida, M., Niwa, Y., Hirata K., ... Murakami, T. (2017). Chronic endometritis modifies decidualization in human endometrial stromal cells. *Reprod. Biol. Endocrinol.,* 15(1), 16. doi: 10.1186/s12958-017-0233-x

РЕЗУЛЬТАТИ МОРФОЛОГІЧНОГО ДОСЛІДЖЕННЯ У ЖІНОК РЕПРОДУКТИВНОГО ВІКУ З ГІПЕРПРОЛІФЕРАТИВНИМИ ЗАХВОРЮВАННЯМИ ЕНДОМЕТРІЯ

Абдуллаєв В. Е.

Гіперпроліферативні процеси ендометрія, залишаючись однією з найбільш розповсюджених гінекологічних патологій, усе ще мають недосконалості на етапах діагностики як інвазивної, так і неінвазивної. Досі існують суперечності у необхідності диференціації між гіперплазією та поліпами ендометрія. Удосконалення методики патоморфологічного дослідження та винайдення імуногістохімічних маркерів для ендометрія відкрило нові можливості для більш досконалої діагностики його гіперпроліферативних процесів. Важливою складовою діагностики патології ендометрія є гістероскопія, котра дозволила усунути більшість недоліків, пов'язаних із класичним вишкрібанням порожнини матки. Визначення маркерів хронічного ендометриту відкрило нові запитання про походження хронічного запального процесу в порожнині матки, його перебіг та взаємозв'язок з біоценозом нижчих відділів статевого тракту. Метою даного дослідження стало порівняння результатів патоморфологічного та імуногістохімічного дослідження ендометрія з методами діагностики біоценозу нижніх відділів жіночого статевого тракту. З метою виконання встановленої мети нами було проведено аналіз результатів лабораторних досліджень у 161 жінки, з яких 58 жінок мали верифіковані діагнози гіперпроліферативних процесів ендометрія, 71 жінці було встановлено морфологічно верифіковані діагнози гіперпроліферативних процесів у поєднанні з хронічним ендометритом. Контрольну групу становили 32 жінки без ознак гіперпроліферативних процесів ендометрія та хронічого ендометриту. Вік жінок становив від 18 до 53 років. Усім жінкам було проведено цитологічне дослідження шийки матки та мікроскопія вагінальних мазків. За отриманими даними відсоткове співвідношення між кількістю діагностованих поліпів ендометрія та гіперплазії ендометрія виявилось однаковим із незначною перевагою кількості поліпів. Інші гінекологічні захворювання (міома матки, зовнішній ендометріоз та поліпи шийки матки) становили від 0,8 до 3,9 %. Цитологічне дослідження шийки матки вказало на перевагу 2 типу цитології у групі жінок з хронічним ендометритом. Аналіз даних мікроскопії вагінальних виділень вказує на підвищений рівень запальних показників у групі жінок з поєднанням гіперпластичних процесів ендометрію та хронічного ендометриту. Таким чином, можливо стверджувати про незначно вищий рівень хронічного ендометриту у групі жінок з поліпами ендометрія порівняно з гіперплазією ендометрія. Встановлено прямий взаємозв'язок між діагностикою хронічного ендометриту та запальними змінами у цитологічному дослідженні шийки матки з мікроскопією вагінальних виділень. Порівняння результатів вище перелічених діагностичних методів дозволяє покращити діагностику гіперпроліферативних процесів ендометрія та хронічного ендометриту.

Ключові слова: *гіперплазія ендометрія, поліпи ендометрія, гіперпроліферативні процеси ендометрія, патоморфологічне дослідження, імуногістохімічне дослідження, цитологічне дослідження.*

DOI: 10.31393/morphology-journal-2022-28(1)-08 Reports of Morphology, Vol. 28, №1, Pages 54-58

ISSN 1818-1295 eISSN 2616-6194

REPORTS OF MORPHOLOGY

Official Journal of the Scientific Society of Anatomists, Histologists, Embryologists and Topographic Anatomists of Ukraine

journal homepage: https://morphology-journal.com

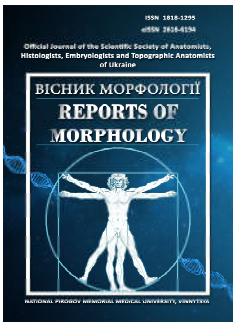

Morphological features of the respiratory part in guinea pigs lung in dynamics of experimental allergic inflammatory process

Popko S. S.
Zaporizhzhia State Medical University, Zaporizhzhia, Ukraine

ARTICLE INFO
Received: 30 November 2021
Accepted: 13 January 2022

UDC: 611.24-018:616-056.3-036]-092.9:599.324.7

CORRESPONDING AUTHOR
e-mail: kluchkosv@gmail.com
Popko S. S.

CONFLICT OF INTEREST
The authors have no conflicts of interest to declare.

FUNDING
The work was financially supported by the Zaporizhzhia State Medical University, Ministry of Health of Ukraine (No state registration: 0118U004250)

The main function of the components of the respiratory tract is gas exchange while maintaining homeostasis in lung, given the pathogenic and non-pathogenic elements of the environment contained in the inhaled air. Morphological changes of the components of the respiratory part in lung of human and animals of adaptive nature under the influence of various factors on the body today remain insufficiently studied. The aim of the study was to investigate the morphological changes of the components of the respiratory part of guinea pigs lung in the dynamics of experimental ovalbumin-induced allergic inflammation. We used histological and electron microscopic methods to study the lungs of 48 male guinea pigs in experimental ovalbumin-induced allergic inflammation, simulated by subcutaneous sensitization and subsequent intranasal inhalation with ovalbumin. Morphological changes of the components of the respiratory tract of the lungs were determined in the early and late phases of allergic inflammatory process at the optical and submicroscopic levels. The early phase (23rd and 30th days of the experiment) was characterized by a predominance of alterative and destructive changes, consisted in the desquamation of the alveolar epithelium with a violation of the blood-gas barrier and hemomicrocirculatory bed. Type II alveolar cells had lesions of varying severity in the form of the absence of lamellar bodies or disturbances in the formation of their contents, vacuolization of the cytoplasm, mitochondrial damage. In the late phase of the development of the allergic inflammatory process (36th and 44th days of the experiment) in the respiratory part of lung were dominated adaptive and restorative changes. In addition, we observed dilation of the lung alveoli and thinning of the interalveolar septa, which is a consequence of the cascade of reactions of the local neuroendocrine and immune systems of lung as a result of allergen action. Thus, experimental ovalbumin-induced allergic inflammatory process of the respiratory tract is accompanied by structural and functional changes in the components of the respiratory part in lung of guinea pigs in stages depending on the duration of the experiment.

Key words: *alveolar epithelium, surfactant, allergic inflammation, ovalbumin, guinea pig.*

Introduction

The components of the respiratory part of lung provide gas exchange and are important for reducing the surface tension at the air-liquid interface in the alveoli, as well as for regulating the local immune response [3, 8, 13]. Type II alveolar cells synthesize, store and secrete surfactant, including lipid and protein molecules (SP). Type II alveolar cells, in turn, have unique organelles for storing lipids and hydrophobic proteins - lamellar bodies (LB), which at the ultrastructural level correlate with the intracellular surfactant pool [2]. LB are modified lysosomes surrounded by a membrane and filled with densely packed membranes of surfactant lipids and hydrophobic proteins. LB undergo exocytosis and release surfactant components into the aqueous hypophase between the alveolar cells and the gaseous phase [20]. After exocytosis, phospholipids form a double layer of phospholipids and glycoproteins, filled the surface of alveolar cells at the air-liquid interface with surface-active components [4]. SP-B and SP-C are associated with LB. In contrast, SP-A and SP-D are secreted by type II alveolar cells in a LB-independent pathway [20]. SP-A and SP-D are also secreted by bronchiolar exocrine cells in the distal airways - terminal bronchioles and

respiratory bronchioles [14]. After reuptake by type II alveolar cells, inactive surfactant aggregates are either catabolized or recycled by re-incorporation into the metabolic pathway [19]. A small part of surfactant is phagocytosed and cleaved by alveolar macrophages or eliminated through the respiratory tract using mucociliary clearance.

Soluble SP bind and regulate a number of effector immune cells in allergic airway inflammation. Both SP-A and SP-D inhibit the activity of the allergic inflammatory process, made them interesting molecules for the treatment of bronchial asthma [10]. The anti-inflammatory properties of alveolar macrophages are being actively studied nowadays [8, 19]. However, most of the scientific works, focused on the study of the components of the respiratory part of lung in allergic inflammation are immunological studies [2, 3, 4, 9]. The above indicates the need to clarify this urgent problem from a morphological point of view in the early and late phases of the experimental allergic inflammatory process.

The aim of this work is to study the morphological changes of the components of the respiratory part of guinea pig lung in the dynamics of experimental ovalbumin-induced allergic inflammation.

Materials and methods

Forty-eight sexually mature male guinea pigs (450 - 600 gram) were weighed and kept at vivarium of Zaporizhzhya State Medical University, with free access to OVA-free food and water. The experimental protocol was followed the published guidelines (Strasbourg, 1986; Kiev, 2006).

The study protocol was approved by the institutional review board of the Bioethics Committee of Zaporizhzhia State Medical University (Protocol № 8 of 11 Juny 2019).

Induction of airway allergic inflammatory process was performed by subcutaneous sensitization and airway challenge through nasal inhalation with OVA (0,5 mg/mL per animal) mixed with aluminum hydroxide (10 mg/mL in saline per animal) on days 0, 7 and 14. From 21 to 28 days animals were exposed for 15 min to an aerosol of OVA (10 mg/mL in saline) using a nebulizer (Little Doctor International, Singapore, LD-211C) attached to a plastic chamber [14]. Animals were assigned equally into six experimental groups of 8 guinea pigs each. Group I - IV are guinea pigs sensitized and challenged with ovalbumin (OVA) (Sigma Aldrich, USA) with alum as an adjuvant (AlumVax Hydroxide vaccine adjuvant, OZ Biosciences, France), dropped out the experiment respectively on the 23rd, 30th, 36th and 44th days after its start. Group V: guinea pigs sensitized and exposed to saline, served as control. Group VI: intact animals (norm).

Lungs removed and fixed in 10 % neutral buffered formalin. Formalin fixed, paraffin wax embedded lung specimens were selected for histological preparation, prepared as 5-μm-thick sections and stained with hematoxylin and eosin. Histological study was carried out on Carl Zeiss Primo Star microscope equipped with the Axiocam digital microphoto attachment using the ZEISS ZEN 2011 software, using the oil immersion technique (x1000).

Electron microscopy was performed on glutaraldehyde-fixed 1x1 mm specimens of lung tissue followed by processing in a 1 % solution of osmium tetroxide. Subsequently, the pieces were dehydrated in a series of graded ethanol up to 100 % according to histological standards, acetone with additional contrasting for two hours in 2.5 % uranyl acetate at 700°C. Pouring into the block was carried out by gradual impregnation of the material with acetone oxide with Eponym (2:1, 1:1, 1:2) and poured into pure Epon. The resin polymerization was carried out in two stages at 36°C (12:00) and 56°C (24 hours). Ultra-thin (55-65 nm) sections were obtained on a "PowerTome RMC Boeckeler" ultratom and contrasted with Reynolds lead citrate for 25 minutes at room temperature. Ultrathin sections viewed on a PEM-100-01 electron microscope.

Results

In the control group of animals in the morphological view of the respiratory part of lung, we showed that the walls of the alveoli are lined by flattened type I alveolar cells, among which type II alveolar cells are localized. We also found single alveolar macrophages and eosinophilic granulocytes in the alveoli lumen. Septal cells, fibroblasts, plasma cells and eosinophilic granulocytes occupied the pulmonary interstitium in respiratory portion of lung (fig. 1a).

We have shown short microvilli and a small number of LB at the apical pole of type II alveolar cells in the control group at the submicroscopic level. Alveolar macrophages had an underdeveloped cytoplasmic membrane, formed single cell processes. There were rare secondary lysosomes in their cytoplasm. Type I alveolar cells had a more expanded nucleus-containing part protruded into the alveoli lumen and thin peripheral part of the cytoplasm. There single pinocytic vesicles in the endotheliocytes of blood capillaries in the peripheral part of their cytoplasm.

We have found local destruction and desquamation of alveolar epithelium, interalveolar septa, exposure of the basal membrane of the endothelium in blood capillaries in the early manifestation of the allergic inflammatory process on the 23rd day after the experiment in the respiratory portion of guinea pigs lung. There were abundant alveolar macrophages in the alveoli lumen with signs of increased phagocytic activity. The count of eosinophilic granulocytes was increased. In addition, we observed some microcirculatory disorders, such as plethora and stasis of blood capillaries and postcapillary venules, numerous foci of erythrocyte diapedesis in the alveoli lumen and in the pulmonary interstitium (fig. 1b).

On the 30th day after the start of the experiment morphological changes in the respiratory part of lung became less pronounced, although microcirculatory disorders in the form of plethora and stasis of blood

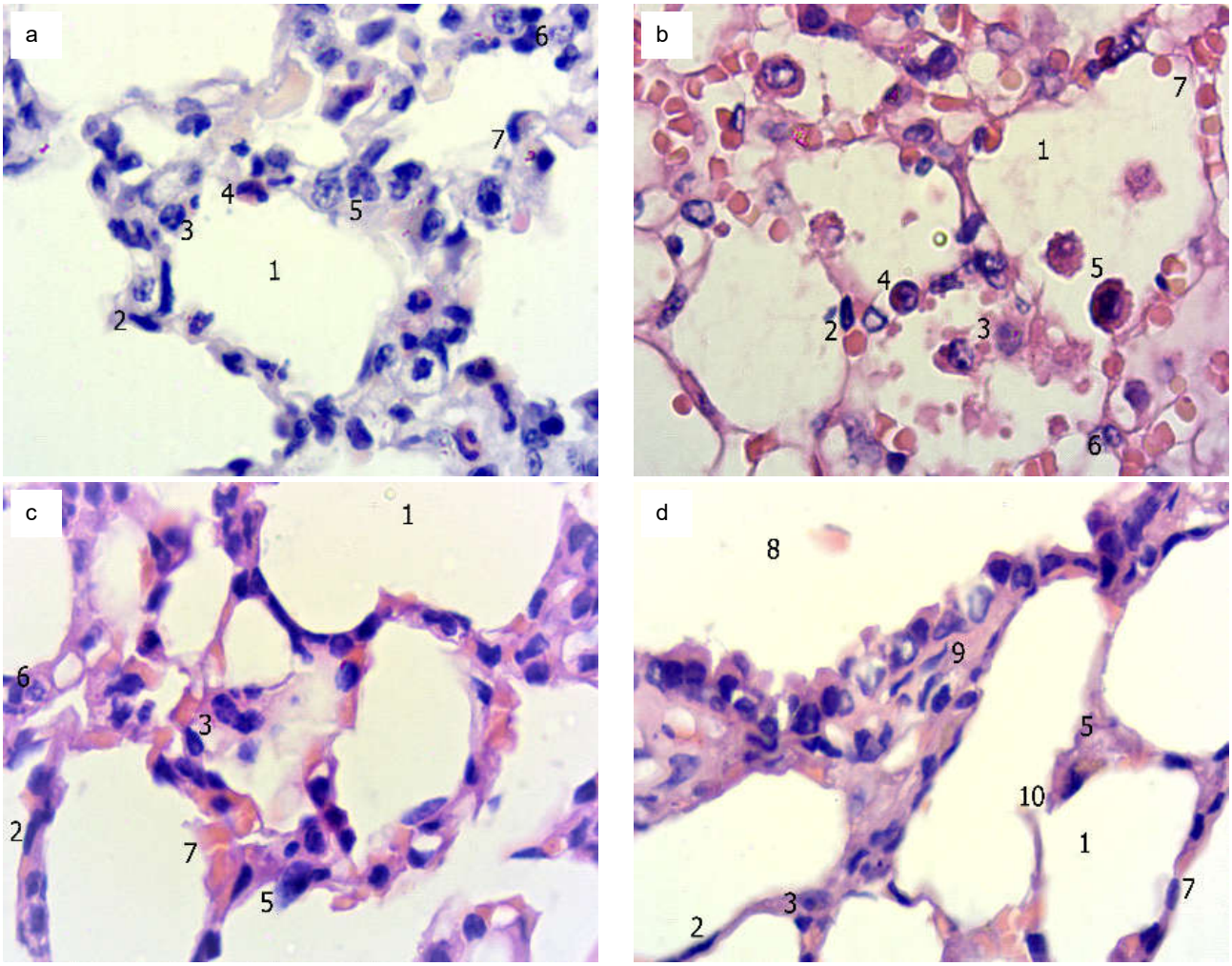

Fig. 1. Microscopic changes in the respiratory portion of the guinea pigs lung after sensitization and aeroallergization with ovalbumin on days 23 (1b), 30 (1c) and 44 (1d) after the start of the experiment compared with the control group (1a). 1 - alveoli lumen; 2 - type I alveolar cell; 3 - type II alveolar cell; 4 - eosinophilic granulocyte; 5 - alveolar macrophage; 6 - plasma cell; 7 - blood capillary; 8 - lumen of the terminal bronchiole; 9 - smooth myocyte in the wall of the terminal bronchiole; 10 - interalveolar pore. Stain: hematoxylin and eosin. x1000.

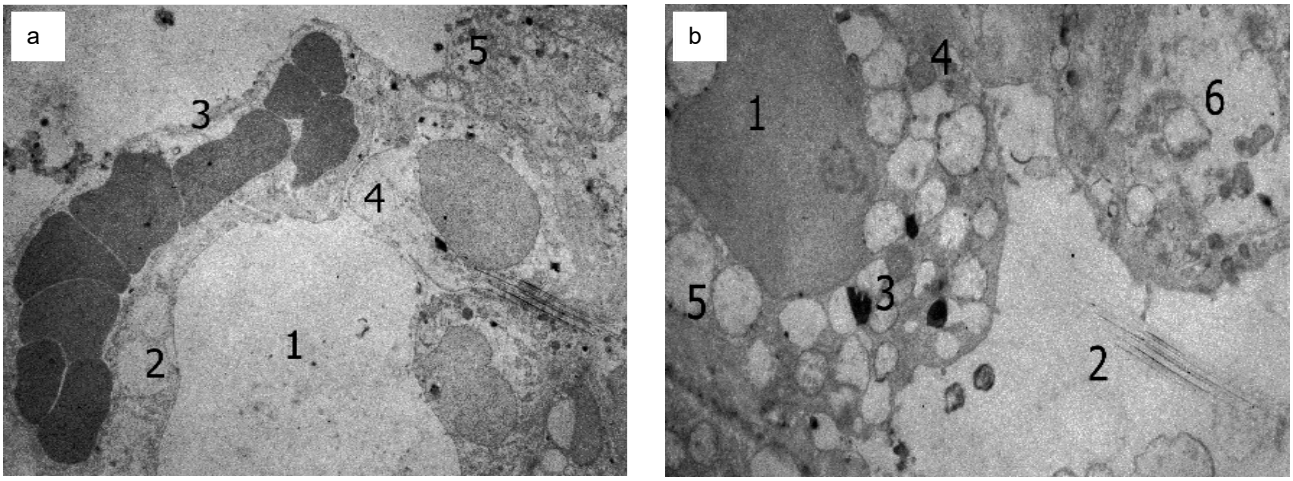

Fig. 2. Ultrastructural changes in the respiratory portion of the guinea pigs lung after sensitization and aeroallergization with ovalbumin on days 23 (2a) and 30 (2b) after the start of the experiment. 2a: 1 - alveoli lumen; 2 - type I alveolar cell; 3 - blood capillary; 4 - type II alveolar cell; 5 - alveolar macrophage. 2b: 1 - type II alveolar cell nucleus; 2 - alveoli lumen; 3 - lamellar body; 4 - mitochondria; 5 - cytoplasm vacuolization; 6 - fragment of the cytoplasm of alveolar macrophage. Transmission electron microphotos. 2a) x6000. 2b) x6800.

capillaries persisted (fig. 1c). In some places, the intercellular septa were thickened due to edema. We observed a trend towards renewal of the alveolar epithelium.

The morphological changes detected at the optical level are confirmed by the results of electron microscopic examination. Swelling and thickening of the peripheral portion of cytoplasm of type I alveolar cells, stasis, plethora and deformation of erythrocytes of blood capillaries were demonstrated (fig. 2a). Type II alveolar cells had lesions of varying severity. Absence of LB or disturbances in the formation of their content, cytoplasm vacuolization, mitochondria damage. Less frequently we observed destruction and necrosis of type II alveolar cells. Abundant lysosomes and heterophagosomes, residual bodies were found in the cytoplasm of alveolar macrophages (fig. 2b).

In the late phases of the allergic inflammatory process on the 36th and 44th days after the start of the experiment in the respiratory portion of the guinea pigs lung, we have shown thinning of the interalveolar septa and, at the same time, alveoli expansion (fig. 1d), correlated with emphysematous lesions. In local places, plethora and stasis of blood capillaries were noticeable, although less pronounced, compared with the early phases of the allergic inflammatory process.

Discussion

Morphological analysis of the respiratory part of guinea pigs lung made it possible to identify the phases of the allergic inflammatory process. The early manifestations (23rd and 30th days of the experiment) were characterized by the predominance of destructive changes. We demonstrated desquamation of the alveolar epithelium with a violation of the air-blood barrier on the background of a violation of hemomicrocirculatory bed in the early phases of the allergic inflammatory process. Similar changes in the lungs under the influence of various pathological factors were found by other scientists [6, 7, 11]. The revealed changes can be explained by the rapid degranulation of mastocytes with the release of histamine and leukotrienes, which, in addition to bronchospasm and mucus hyperproduction, caused alterative-exudative changes in the components of the respiratory part of the lungs [1]. Damage to type II alveolar cells is especially significant, since it is known that they ensure the regeneration of both their population and type I alveolar cells [10, 17]. However, their severe disorders in the form of necrosis were rarely observed, more often signs of damage to their mitochondria and LB were revealed. Accordingly, it can be assumed that there was a disturbance in the surfactant system, in turn, its enhanced exocytosis as a manifestation of the innate resistance of the lungs to damage caused by allergen, which is in agreement with other scientists [20]. We have also assumed that type II alveolar cells, after the action of the allergen, were involved in the regeneration of the alveolar epithelium, respectively, their secretory function decreased, and the proliferative function prevailed. Alterative changes in the alveolar epithelium were accompanied by elevated number and phagocytic activity of alveolar macrophages, which confirmed their anti-inflammatory properties in conditions of the allergic inflammatory process [3, 9]. In the late phases of the experimental allergic inflammatory process in the respiratory part of the lungs adaptive-renewal changes prevailed. Despite the renewal of the alveolar epithelium, we observed expansion of the alveoli and thinning of the interalveolar septa, which was a consequence of a cascade of reactions of the local neuroendocrine and immune systems in lung [5, 12, 15]. Latest lead to remodeling of the airways and the hemomicrocirculatory bed of lung, which was confirmed by other scientists [16, 18].

We are going to study electron microscopic changes in the elements of the hemomicrocirculatory bed of guinea pigs lung in the early and late phases of allergic inflammatory process.

Conclusions

Experimental ovalbumin-induced allergic inflammatory process was accompanied by structural and functional changes in the components of the respiratory part of the guinea pigs lungs, which were different in the early and late phases of the inflammatory process, depending on the duration of the experiment.

References

[1] Amin, K. (2012). The role of mast cells in allergic inflammation. *Respiratory Medicine,* 106(1), 9-14. doi: 10.1016/j.rmed.2011.09.007

[2] Bissonnette, E. Y., Lauzon-Joset, J.-F., Debley, J. S., & Ziegler, S. F. (2020). Cross-Talk Between Alveolar Macrophages and Lung Epithelial Cells is Essential to Maintain Lung Homeostasis. *Frontiers in Immunology,* 11. doi: 10.3389/fimmu.2020.583042

[3] Coleman, M. M., Ruane, D., Moran, B., Dunne, P. J., Keane, J., & Mills, K. H. G. (2013). Alveolar Macrophages Contribute to Respiratory Tolerance by Inducing FoxP3 Expression in Naive T Cells. *American Journal of Respiratory Cell and Molecular Biology,* 48(6), 773-780. doi: 10.1165/rcmb.2012-0263oc

[4] Faffe, D. S., & Zin, W. A. (2009). Lung Parenchymal Mechanics in Health and Disease. *Physiological Reviews,* 89(3), 759-775. doi: 10.1152/physrev.00019.2007

[5] Ha, E. H., Choi, J.-P., Kwon, H.-S., Park, H. J., Lah, S.J., Moon, K.-A., … Cho, Y.S. (2019). Endothelial Sox17 promotes allergic airway inflammation. *Journal of Allergy and Clinical Immunology,* 144(2), 561-573. doi: 10.1016/j.jaci.2019.02.034

[6] Herasymiuk, I. E., & Vatsyk, M. O. (2018). Features of reorganization of blood vessels of lungs of rats at various degrees of total dehydration. *Morphologia,* 12(3), 44-50. doi: 10.26641/1997-9665.2018.3.44-50

[7] Herasymiuk, I. E., & Vatsyk, M. O. (2019). Features of remodeling of blood vessels of rat lungs in applying different methods of fluid resuscitation after general dehydration. *Bulletin of Problems Biology and Medicine,* 1(2), 272. doi: 10.29254/2077-4214-2019-1-2-149-272-276

[8] Hussell, T., & Bell, T. J. (2014). Alveolar macrophages: plasticity in a tissue-specific context. *Nature Reviews Immunology,*

14(2), 81-93. doi: 10.1038/nri3600
[9] Joshi, N., Walter, J. M., & Misharin, A. V. (2018). Alveolar Macrophages. *Cellular Immunology,* 330, 86-90. doi: 10.1016/j.cellimm.2018.01.005
[10] Knudsen, L., & Ochs, M. (2018). The micromechanics of lung alveoli: structure and function of surfactant and tissue components. *Histochemistry and Cell Biology,* 150(6), 661-676. doi: 10.1007/s00418-018-1747-9
[11] Koptev, M. M., Vynnyk, N. I., Kokovska, O. V., Filenko, B. M., & Bilash, S. M. (2018). The use of semi-thin section method in the study of stress-induced structural changes in lungs. *World of Medicine and Biology,* 64(14), 153. doi: 10.26724/2079-8334-2018-2-64-153-156
[12] Lambrecht, B. N., & Hammad, H. (2014). The immunology of asthma. Nature Immunology, 16(1), 45-56. doi: 10.1038/ni.3049
[13] McKenzie, A. N. J. (2014). Type-2 Innate Lymphoid Cells in Asthma and Allergy. *Annals of the American Thoracic Society,* 11(Suppl. 5), S263-S270. doi: 10.1513/annalsats.201403-097aw
[14] Popko, S. S. (2021). Changes in the cellular composition of guinea pig's distal airways epithelium in the dynamics of experimental ovalbumin-induced allergic inflammation. *Reports of Morphology,* 27(3), 55-60. doi: 10.31393/morphology-journal-2021-27(3)-08
[15] Popko, S. S., Evtushenko, V. M., & Syrtsov, V. K. (2020). Influence of pulmonary neuroendocrine cells on lung homeostasis. *Zaporozhye Medical Journal,* 22(4), 568-575. doi: 10.14739/2310-1210.4.208411
[16] Pronina, O. M., Koptev, M. M., Bilash, S. M., & Yeroshenko, G. A. (2018). Response of hemomicrocirculatory bed of internal organs on various external factors exposure based on the morphological research data. *World of Medicine and Biology,* 63(1), 153-157. doi: 10.26.724 / 2079-8334-2018-1-63-153-157
[17] Stegemann-Koniszewski, S., Jeron, A., Gereke, M., Geffers, R., Kroger, A., Gunzer, M., & Bruder, D. (2016). Alveolar Type II Epithelial Cells Contribute to the Anti-Influenza A Virus Response in the Lung by Integrating Pathogen- and Microenvironment-Derived Signals. *MBio,* 7(3). doi: 10.1128/mbio.00276-16
[18] Sui, P., Wiesner, D. L., Xu, J., Zhang, Y., Lee, J., Van Dyken, S., … Sun, X. (2018). Pulmonary neuroendocrine cells amplify allergic asthma responses. *Science,* 360(6393), eaan8546. https://doi.org/10.1126/science.aan8546
[19] Westphalen, K., Gusarova, G. A., Islam, M. N., Subramanian, M., Cohen, T. S., Prince, A. S., & Bhattacharya, J. (2014). Sessile alveolar macrophages communicate with alveolar epithelium to modulate immunity. *Nature,* 506(7489), 503-506. doi: 10.1038/nature12902
[20] Winkler, C., & Hohlfeld, J. M. (2013). Surfactant and allergic airway inflammation. *Swiss Med. Wkly.,* 143, w13818. doi: 10.4414/smw.2013.13818

МОРФОЛОГІЧНІ ОСОБЛИВОСТІ РЕСПІРАТОРНОГО ВІДДІЛУ ЛЕГЕНЬ МОРСЬКИХ СВИНОК В ДИНАМІЦІ ЕКСПЕРИМЕНТАЛЬНОГО АЛЕРГІЧНОГО ЗАПАЛЬНОГО ПРОЦЕСУ

Попко С. С.

Основна функція компонентів респіраторного відділу легень полягає в газообміні та забезпеченню гомеостазу в легенях, враховуючи патогенні та непатогенні елементи навколишнього середовища, які містяться у повітрі, що вдихається. Морфологічні зміни компонентів респіраторного відділу легень людини і тварин адаптаційного характеру при дії на організм різноманітних чинників на сьогоднішній день залишаються недостатньо дослідженими. Мета роботи - дослідити морфологічні зміни компонентів респіраторного відділу легень морських свинок в динаміці експериментального овальбумін-індукованого алергічного запалення. За допомогою гістологічного та електронно-мікроскопічного методів вивчили легені 48 самців морської свинки в умовах експериментального овальбумін-індукованого алергічного запалення, яке моделювали шляхом підшкірної сенсибілізації та наступної інтраназальної інгаляції овальбуміном. На світлооптичному та субмікроскопічному рівнях визначали морфологічні зміни компонентів респіраторного відділу легень в ранньому та пізньому періодах алергічного запального процесу. Ранні стадії (23 та 30 доба експерименту) характеризувались переважанням альтеративних і деструктивних змін, котрі полягали в десквамації коміркового епітелію з порушенням аерогематичного бар'єру й гемомікроциркуляції. Альвеолоцити II типу мали ушкодження різного ступеня тяжкості у вигляді відсутності пластинчастих тілець або порушення у формуванні їх вмісту, вакуолізації цитоплазми, пошкодження мітохондрій. У пізні стадії розвитку алергічного запального процесу (36 і 44 доба експерименту) в респіраторному відділі легень переважали адаптаційно-відновні зміни. Крім того, ми спостерігали розширення легеневих комірок та витончення міжкоміркових перегородок, що є наслідком каскаду реакцій локальної нейроендокринної та імунної систем легень в результаті дії антигену. Таким чином, експериментальний овальбумін-індукований алергічний запальний процес супроводжувався структурно-функціональними змінами компонентів респіраторного відділу легень морських свинок, які відрізнялися у ранній та пізній фазах запального процесу залежно від тривалості експерименту.

Ключові слова: *коміркoвий епітелій, сурфактант, алергічне запалення, овальбумін, морська свинка.*

DOI: 10.31393/morphology-journal-2022-28(1)-09 Reports of Morphology, Vol. 28, №1, Pages 59-63

ISSN 1818-1295 eISSN 2616-6194

REPORTS OF MORPHOLOGY

Official Journal of the Scientific Society of Anatomists, Histologists, Embryologists and Topographic Anatomists of Ukraine

journal homepage: https://morphology-journal.com

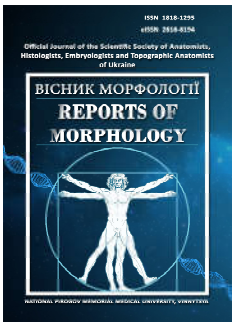

Histological structure of intercellular fluid circulation pathways

Kondor Yu. Yu., Tykholaz V. O., Guminskyi Yu. Yo.
National Pirogov Memorial Medical University, Vinnytsia, Ukraine

ARTICLE INFO
Received: 10 December 2021
Accepted: 14 January 2022

UDC: 611.811.018

CORRESPONDING AUTHOR
e-mail: kondorgeorg@gmail.com
Kondor Yu. Yu.

CONFLICT OF INTEREST
The authors have no conflicts of interest to declare.

FUNDING
Not applicable.

Studies of the nervous system today are quite relevant and important. There are a large number of methods of studying and researching the brain, among which the histological method is widely used. Despite the variety of methods, in the possible practical application of histological examination of the central nervous system and brain in particular there are problems encountered by researchers: the complexity of the method, a large number of conventions to consider when working with nerve tissue, methods of fixation. Among other research methods, there is a group of histological methods, united by a common feature - in vivo staining of the nervous system, among which there is also a method of in vivo staining with methylene blue. The aim of the study was to establish the morphological features of the structure of the intercellular fluid circulation of the brain in experimental animals. The article describes a new method of injectable in vivo staining of the brains of laboratory animals with methylene blue. It is relevant for studying the morphology of the intercellular fluid circulation of the brain and the study of the structure of the microcirculatory tract. In our work it is offered to combine already known methods of perfusion fixation and a technique of supravital staining with methylene blue. Since most scientific studies of the brain use conventional research methods without a comprehensive study of the entire microcirculatory tract and intercellular fluid circulation, there is a need for more detailed study of the histological structure and topography of microcirculatory brain complexes to establish their normal structure. The results of the study confirm the researchers' observation that methylene blue has a high affinity for nerve fibers in the brain. In addition, it is obvious that the additional use of formalin as a solvent increases the resistance of methylene blue to leaching and the ability to stain the structures of the microcirculatory tract. In addition, the lifetime application of this technique allows you to visualize the morphological features of the microcirculation pathways of the intercellular fluid of the brain, Virchow-Robin space and capillary walls.

Keywords: *nervous system, glymphatic system, methylene blue, in vivo staining technique.*

Introduction

In modern science, the study of the nervous system has a special place. In recent decades, research on the brain, nervous tissue, and neurophysiology has advanced significantly. However, together with progressive studies of the properties of proteins, gene expression and the effects of neurotransmitters, morphohistological methods of studying the nervous system are still relevant.

To study the structure of nervous tissue, there are methods that are used to satisfy certain tasks set by the researcher. Despite the variety of methods, in the possible practical application of histological examination of the central nervous system in general and the brain in particular, there are problems encountered by researchers: the complexity of the method, the large number of conventions to consider when working with nerve tissue, methods of fixation [15].

Among the known methods of histological examination, which are recommended for work with nervous tissue, are: the method of staining with toluidine blue (blue) according to Nissl, the "gold standard" of histology - staining with hematoxylin-eosin and methods of impregnation [15]. The above techniques have one characteristic feature - they are associated with long-term fixation with formalin, alcohol and xylene, which are certainly necessary measures to preserve the samples. Among other research methods, there is a group of histological methods, united by a

common feature - in vivo staining of the nervous system, among which is a method of in vivo staining with methylene blue.

The method of using methylene blue in vivo is not new, its use was described by Ehrlich in 1886, and the method was improved and refined by Dogiel and Cajal (1896-97) [14]. The advantages of this technique are the staining of still living tissues, especially when it comes to a vital way of staining. According to Ehrlich- Dogiel, a sequence of actions has been formulated to ensure the optimal staining of cells of the nervous system, which consists in the lifelong introduction or shortly after euthanasia into the bloodstream or directly into the parenchyma of the organ. The peculiarity is that this method of staining is used not only in the study of the central nervous system, but more to detect neurons, neuroglia, nerve endings and axons of the peripheral nervous system, which is considered the primary goal of the method and has more advantages than CNS [14]. In addition, the substance used for staining is selectively specific in three respects: first, methylene blue is a specific dye for cells of the nervous system and is relatively non-toxic to cells of the nervous system; secondly, as a nitrogen-containing compound, it reacts with nitric oxide, which leads to a heterogeneous distribution of the dye in the tissue due to the fact that living cells break down methylene blue, and non-living - accumulate dye; third, methylene blue is a substance that crosses the blood-brain barrier. The above-mentioned phenomena are a consequence of the chemical structure and properties of both the substance and the biochemistry of cells [11]. This question remains open today [14].

At the electron microscopic level in supravital research, researchers have developed a method of visualization of dye accumulation sites in neurons. However, their techniques include complex fixation after brain sampling, when after sampling the stained organ requires additional fixation with special chemical compounds (eg ammonium picrate, osmium compounds, molybdenum). These compounds are primarily toxic and are used to prevent methylene blue leaching during fixation in aldehydes or alcohols [11, 14, 15].

When studying the structure of the brain, scientists widely use the method of perfusion fixation. Given the size of the samples, the purpose of fixation is to quickly and evenly preserve the tissue in an unchanged state [8, 9]. Often, changes in response to hypoxia begin before the tissue can be preserved [17]. The advantage of direct fixation through the circulatory system is that the chemical can quickly reach all parts of the body through the natural vascular network. Using this method of fixation, it is necessary to take into account the parameters of the circulatory system, such as pressure, pH, temperature, which significantly improves the result [6]. The main advantage of this method (compared to volumetric methods) is that the circulatory system is used most efficiently [4].

In our work it is offered to combine already known methods of perfusion fixation and a technique of supravital staining with methylene blue. Since most scientific studies of the brain use conventional research methods without a comprehensive study of the entire microcirculatory tract and intercellular fluid circulation, there is a need for more detailed study of the histological structure and topography of microcirculatory brain complexes to establish their normal structure.

The aim of the study was to establish the morphological features of the structure of the intercellular fluid circulation of the brain in experimental animals.

Materials and methods

Humane principles of animal care were applied in the work, and all procedures complied with the current law on animal protection.

The following methods were used: methylene blue (pure for analysis), previously diluted to a concentration of 1 % (1 g per 100 ml) with 10 % formalin solution in phosphate buffer (pH=7.35) and filtered before use; heparin; 0.9 % sodium chloride for exsanguination; 5 % glucose to prevent gliolysis; systems for intra-arterial infusion; G26 Vasafix catheters; sodium thiopental for anesthesia; sucrose solutions 15 % and 30 % for cryoprotection.

5 male Oryctolagus cuniculus rabbits weighing 1 to 1.5 kg were selected. The animals were kept in good condition with free access to food and water. All conditions of detention and all procedures with animals were carried out in compliance with bioethics (Protocol of the **Commission on Bioethics** № 2 of 09.03.2021) and in compliance with the ethical principles of the European Convention for the Protection of Vertebrate Animals.

Animals were anesthetized with sodium thiopental (1 mg/kg administered intraperitoneally), and the common carotid artery was isolated and catheterized with a Vasafix G26 catheter. The vascular bed was bled and washed with 0.9 % sodium chloride solution up to 4 ml. To prevent gliosis, up to 1 ml of 5 % glucose solution was administered. After rinsing the vascular bed with a syringe, a system with a vial of 1 % filtered solution of methylene blue in 10 % buffer solution of formalin preheated (t =37°C, pH=7.34-7.45, V=15-20 ml) was connected to common carotid artery drip (60 drops/min). Adjustment of the solution injection pressure was provided by raising the vial on a tripod to a height of 100-120 cm, which corresponded to the design pressure of 120 mm Hg. Methylene blue was continued until the animal's skin and mucous membranes turned blue. Euthanasia of the animal was performed by overdose of sodium thiopental.

The brain was isolated and removed by decapitation and dissection of the skull vault. After removal, the brain sample was immersed in a cooled buffer solution of 10 % formalin (t =4°C, pH=7.34-7.45) for one day, followed by cryoprotection in 15 % and 30 % buffer solutions of sucrose (chemically pure) in each solution at t =0-4°C for two days.

After pre-fixation and cryoprotection, sections 10-15 μm thick were made using a freezing microtome (t =-15-20 C). Subsequently, micropreparations made on slides were examined under a light microscope (SCOPE S/N EU1960762). Surveys were performed using a sCMEX Euromex Microscopen B.V. DC.1359 F100.

Results

Macroscopic examination of brain samples reveals a change in tissue color from pale pink to blue. Contrast-filled vessels are well traced: vessels of the circle of Willis, middle cerebral arteries, ocular artery (Fig. 1). The meninges have acquired a stable blue color. The stem tissue of the brain is well stained. In the cross-section of the brain there is a clear demarcation of gray, white matter, nuclei and conductive pathways of the brain. With a more saturated shade of blue, the gray matter is clearly visualized (Fig. 2, 3).

Capillaries with erythrocytes were well visualized on micropreparations of cryosection of rabbit brain 10-15 m in the frontal and horizontal planes. The capillary wall is painted blue, around which the so-called Virchow-Robin space is clearly visible, bounded on the outside by a layer of glia cells, painted in deep blue [1]. The accumulation of methylene blue contrast accompanies capillaries and clusters of glia, located in the form of tangentially directed "strands", presumably along the paraaxonal outflow path of the intercellular fluid of the brain (see Fig. 2, 3). The above picture is heterogeneous and depends primarily on the layer of bark, the direction of axon fibers in the white matter, the location of the capillary network, radial glia, and so on. This pattern can be well seen in the direction from the meninges, where the dye enters the brain parenchyma with capillaries, accumulates in the gray matter, where the capillaries, neuroglia accumulation or axon location spreads to the white matter, reaching the basal nuclei of the brain. to other structures (Fig. 2, 3, 4, 5).

This type of distribution of methylene blue in brain tissue can be seen in the comparison of sections of different thickness and when changing the plane of the sections

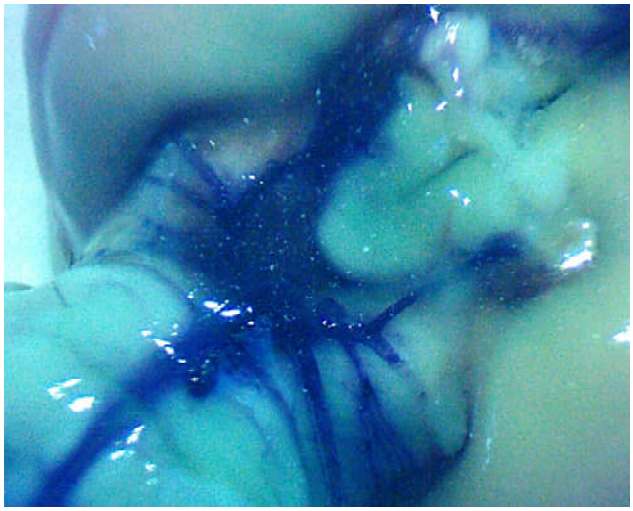

Fig. 1. The vessels of the rabbit's basis cerebri are filled with methylene blue. The change in color of a parenchyma of a brain is well visible.

Fig. 2. Morphology of paravasal spaces of the cerebral cortex using light microscopy. Horizontal section of the rabbit brain. Method of lifelong staining with methylene blue. x10.

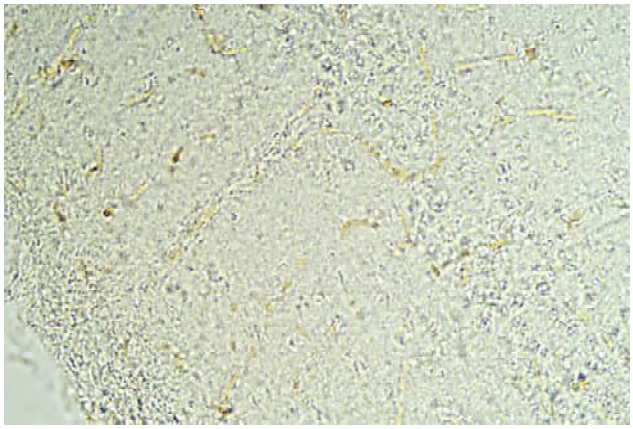

Fig. 3. The structure of the microcirculatory tract, glia cells, paravasal spaces, cerebral cortex. Method of lifelong staining with methylene blue. x40, 10-15 μm.

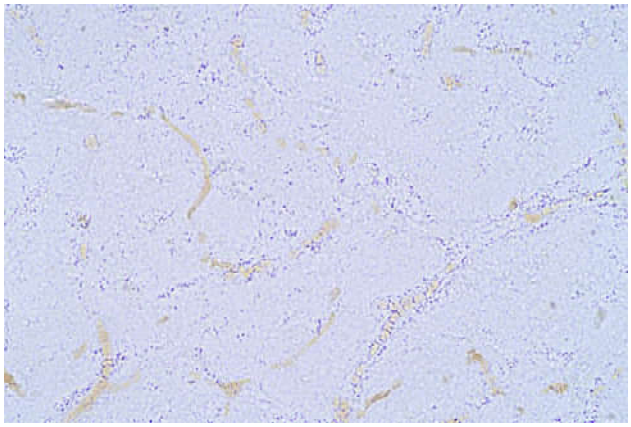

Fig. 4. The structure of the microcirculatory tract, the white matter. Method of lifelong staining with methylene blue. x10, 10-15 μm.

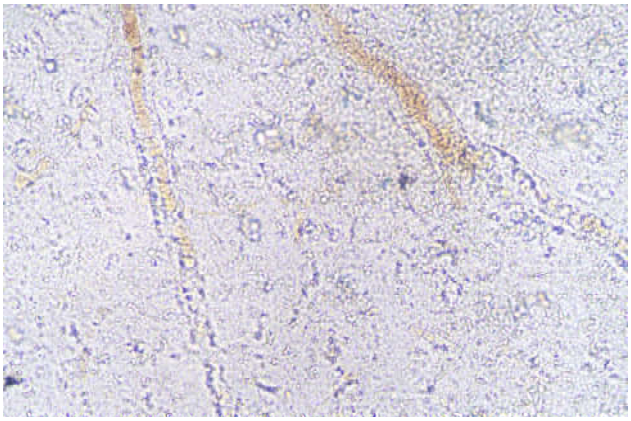

Fig. 5. The structure of the microcirculatory tract, the white matter. Method of lifelong staining with methylene blue. x40, 10-15 μm.

from frontal to horizontal (Fig. 4, 5).

In contrast to the well-known Nissl method, in this case the neurons were not stained, as methylene blue accumulated only in neuroglia cells, capillary endotheliocytes and intercellular space. We assume that this occurs due to the biochemical properties of methylene blue and the conditions of lifelong staining [11].

Discussion

This method of in vivo injection of intra-arterial staining and fixation of the brain with methylene blue provides a better study of the microcirculatory tract and the circulation of intercellular fluid of the brain [10].

The morphological characteristics of the studied material primarily describe the distribution of methylene blue in brain tissue. The latter repeats the path of intercellular fluid circulation: from the capillaries to the Virchow-Robin space, then into the intercellular space by transglial and paraaxonal pathways towards the venous system [1, 2]. This pathway of intercellular fluid circulation by some authors, such as Maiken Nedergaard [7, 10], is defined as a system of purification and regulation of fluid balance in the brain and is called "glymphatic system" [13].

First of all, it should be noted that the main substance in this technique, methylene blue, is commonly used as an inhibitor of cytosolic guanylyl cyclase, a physiological receptor for nitric oxide [5, 11, 14].

Methylene blue is a thiazide dye that selectively stains the nuclei of neurons, endothelium, glia, axons, and others. In addition, due to the interaction with nitric oxide receptors, blocking them, it does not stain living neurons in the brain, selectively staining neuroglia, meninges and capillary wall. Although Cajal (1897) described the ability of methylene blue to stain perineuronal networks around neurons [3, 14].

In contrast to the above characteristics of the aqueous solution of methylene blue, we used a solution of formalin 10 % in buffer solution. The main physicochemical characteristics of the microcirculatory tract were also taken into account, in particular: pressure, temperature, pH, etc.

All the above actions for the methylene blue solution are explained by the following observations. Changing the base for the methylene blue solution slightly increased the resistance of methylene blue to leaching and allowed simultaneous fixation and staining while the nerve tissue remained alive. Also taken into account the characteristics of the solution were close to the characteristics of the microcirculatory tract (t =37°C, pH=7.34-7.45, V=5-10 ml, P=100/120 mm Hg), which in turn reduced the negative impact on the nervous tissue.

It should also be noted that the use in this study of the formalin base for the solution is considered a valid option for its use as a fixative, because there are similar methods of fixing the brain in rodents. The latter is widely used in immunohistochemical studies and electron microscopy [4, 12, 16].

Further studies are planned to link the supravital use of methylene blue directly to biochemical and electrophysiological experiments; which would give more insights into the extra- and intracellular metabolic pathways of the dye. It is also planned to supplement the method with other substances specific to the nervous system, and to apply the method of injectable in vivo staining of the brains of laboratory animals with methylene blue for other organs and systems.

Conclusions

1. The results of the study confirm the observations of Ehrlich and other researchers that methylene blue has a high affinity for nerve fibers in the brain. It is obvious that the additional use of formalin as a solvent increases the resistance of methylene blue to leaching and the ability to stain the structures of the microcirculatory tract. Lifetime application of this technique allows to visualize the morphological features of the microcirculation pathways of the intercellular fluid of the brain, Virchow-Robin space and capillary walls. Therefore, the demonstrated fixation technique should be considered a significant improvement of the modern method.

2. Due to its simplicity and high specificity to nervous tissue, the described technique is a useful addition to other histological methods, especially those that visualize other types of nerve fibers, such as myelin staining methods.

3. Due to the ability to visualize the morphological features of the microcirculation pathways of the intercellular fluid of the brain, this method is a useful addition to neuroanatomy.

References

[1] Abbott, N. J., Pizzo, M. E., Preston, J. E., Janigro, D., & Thorne, R. G. (2018). The role of brain barriers in fluid movement in the CNS: is there a 'glymphatic'system?. *Acta Neuropathologica,* 135(3), 387-407. doi: 10.1007/s00401-018-1812-4

[2] Benveniste, H., Liu, X., Koundal, S., Sanggaard, S., Lee, H., & Wardlaw, J. (2019). The glymphatic system and waste clearance with brain aging: a review. *Gerontology,* 65(2), 106-119. doi: 10.1159/000490349

[3] Fawcett, J. W., Oohashi, T., & Pizzorusso, T. (2019). The roles of perineuronal nets and the perinodal extracellular matrix in neuronal function. Nature Reviews. *Neuroscience,* 20(8), 451-465. doi: 10.1038/s41583-019-0196-3

[4] Gage, G. J., Kipke, D. R., & Shain, W. (2012). Whole animal perfusion fixation for rodents. *JoVE (Journal of Visualized Experiments),* (65), e3564. doi: 10.3791/3564

[5] IARC Working Group on the Evaluation of Carcinogenic Risks to Humans. (2016). *Methylene blue.* In: Some drugs and Herbal Products. Lyon: International Agency for Research on Cancer.

[6] Ikeda, K., Nara, Y., & Yamori, Y. (1991). Indirect systolic and mean blood pressure determination by a new tail cuff method in spontaneously hypertensive rats. *Laboratory Animals,* 25(1), 26-29. doi: 10.1258/002367791780808176

[7] Iliff, J. J., & Nedergaard, M. (2013). Is there a cerebral lymphatic system?. *Stroke,* 44(6, Suppl. 1), S93-S95. doi: 10.1161/STROKEAHA.112.678698

[8] Jonkers, B. W., Sterk, J. C., & Wouterlood, F. G. (1984). Transcardial perfusion fixation of the CNS by means of a compressed-air-driven device. *Journal of neuroscience methods*, 12(2), 141-149. doi: 10.1016/0165-0270(84)90013-X

[9] Kasukurthi, R., Brenner, M. J., Moore, A. M., Moradzadeh, A., Ray, W. Z., Santosa, K. B., ... & Hunter, D. A. (2009). Transcardial perfusion versus immersion fixation for assessment of peripheral nerve regeneration. *Journal of Neuroscience Methods*, 184(2), 303-309. doi: 10.1016/j.jneumeth.2009.08.019

[10] Kondor, Y., Tykholaz, V., & Huminskyi, Y. (2019). Morphology of the pathways of intracellular circulation in the brain. *Pain Medicine,* 4(4), 61-70. doi: 10.31636/pmjua.v4i4.4

[11] Mayer, B., Brunner, F., & Schmidt, K. (1993). Inhibition of nitric oxide synthesis by methylene blue. *Biochem. Pharmacol.,* (45), 367-374. doi: 10.1016/0006-2952(93)90072-5

[12] McFadden, W. C., Walsh, H., Richter, F., Soudant, C., Bryce, C. H., Hof, P. R., … & McKenzie, A. T. (2019). Perfusion fixation in brain banking: a systematic review. *Acta Neuropathologica Communications,* 7(1), 146. doi: 10.1186/s40478-019-0799-y

[13] Mestre, H., Mori, Y., & Nedergaard, M. (2020). The Brain's Glymphatic System: Current Controversies. *Trends in neurosciences,* 43(7), 458-466. doi: 10.1016/j.tins.2020.04.003

[14] Mueller, T. (1998). Methylene blue supravital staining: an evaluation of its applicability to the mammalian brain and pineal gland. *Histology and histopathology,* 13(4), 1019-1026. doi: 10.14670/HH-13.1019

[15] Mulisch, M. (2015). *Fixierungen fur Licht-und Elektronenmikroskopie.* In: Romeis-Mikroskopische Technik (pp. 87-98). Springer Spektrum, Berlin, Heidelberg. doi: 10.1007/978-3-642-55190-1

[16] Yankova, G., Bogomyakova, O., & Tulupov, A. (2021). The glymphatic system and meningeal lymphatics of the brain: new understanding of brain clearance. *Reviews in the neurosciences*, 32(7), 693-705. doi: 10.1515/revneuro-2020-0106

[17] Zwienenberg, M., Gong, Q. Z., Lee, L. L., Berman, R. F., & Lyeth, B. G. (1999). ICP monitoring in the rat: comparison of monitoring in the ventricle, brain parenchyma, and cisterna magna. *Journal of neurotrauma,* 16(11), 1095-1102. doi: 10.1089/neu.1999.16.1095

ГІСТОЛОГІЧНА СТРУКТУРА ШЛЯХІВ ЦИРКУЛЯЦІЇ МІЖКЛІТИННОЇ РІДИНИ

Кондор Ю. Ю., Тихолаз В. О., Гумінський Ю. Й.

Дослідження нервової системи на сьогоднішній день є досить актуальними і важливими. Існує велика кількість методів вивчення та дослідження головного мозку, серед яких широко використовується гістологічний метод. Попри різноманіття методик, у можливому практичному застосуванні гістологічного дослідження центральної нервової системи та головного мозку зокрема виникають проблеми, з якими зустрічаються дослідники: складність виконання методики, велика кількість умовностей, які потрібно враховувати при роботі з нервовою тканиною, способи фіксації. Серед інших методів дослідження виокремлюється група методів гістологічного дослідження, об'єднаних спільною рисою - прижиттєве забарвлення нервової системи, серед яких до того ж є спосіб прижиттєвого забарвлення метиленовим синім. Метою дослідження було встановлення морфологічних особливостей будови шляхів циркуляції міжклітинної рідини головного мозку експериментальних тварин. У статті описана нова методика ін'єкційного прижиттєвого забарвлення головного мозку лабораторних тварин метиленовим синім. Вона є актуальною для вивчення морфології шляхів циркуляції міжклітинної рідини головного мозку та дослідження структури мікроциркуляторного русла. У нашій роботі пропонується поєднати уже відомі методи перфузійної фіксації та методику суправітального забарвлення метиленовим синім. Оскільки більшість наукових праць, в яких досліджували головний мозок, використовують звичайні методи дослідження без комплексного дослідження всього мікроциркуляторного русла та шляхів циркуляції міжклітинної рідини, то виникає потреба у більш детальному дослідженні гістологічної структури та топографії мікроциркуляторних комплексів головного мозку для встановлення їх нормальної будови. Отримані результати дослідження підтверджують спостереження дослідників про те, що метиленовий синій має високу спорідненість до нервових волокон головного мозку. Крім того, очевидно, що додаткове застосування формаліну, як розчинника, підвищує стійкість метиленового синього до вимивання та здатність до забарвлення структур мікроциркуляторного русла. До того ж, прижиттєве застосування даної методики дозволяє візуалізувати морфологічні особливості шляхів мікроциркуляції міжклітинної рідини головного мозку, простори Вірхова-Робінсона та стінки капілярів.

Ключові слова: *нервова система, глімфатична система, метиленовий синій, прижиттєва методика забарвлення.*

DOI: 10.31393/morphology-journal-2022-28(1)-10 Reports of Morphology, Vol. 28, №1, Pages 64-69

ISSN 1818-1295 eISSN 2616-6194

REPORTS OF MORPHOLOGY

Official Journal of the Scientific Society of Anatomists, Histologists, Embryologists and Topographic Anatomists of Ukraine

journal homepage: https://morphology-journal.com

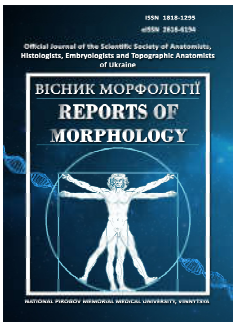

Morphometric indicators for selection of dual endobronchial tube in thoracic anesthesiology

Usenko O. Yu., Sydiuk A. V., Sydiuk O. Ye., Klimas A. S., Savenko G. Yu., Teslia O. T.
Shalimov National Institute of Surgery and Tranplantology, National Academy of Medical Sciences of Ukraine, Kyiv, Ukraine

ARTICLE INFO
Received: 15 December 2021
Accepted: 20 January 2022

UDC: 617.54-089.5:616.24-06-089.163

CORRESPONDING AUTHOR
e-mail: oleh.teslya95@gmail.com
Teslia O.T.

CONFLICT OF INTEREST
The authors have no conflicts of interest to declare.

FUNDING
Not applicable.

For the purpose of single-lung ventilation, various methods of lung isolation are used in the world, which is a prerequisite for many thoracic, cardiac and esophageal surgeries. Numerous studies have reported various methods for determining the optimal suitability between the diameter of the tube and the diameter of the left main bronchus for adequate ventilation and gas exchange during operations on the thoracic cavity. However, there is no consensus among anesthesiologists on the choice of tube size for effective lung ventilation and isolation. We have developed a new mathematical formula for determining the appropriate size of the left bilateral luminal endobronchial tube (LDT). The aim of the study was to determine the effectiveness of the developed standardized mathematical formula for determining the appropriate size of LDT for use in thoracic anesthesiology. The study was performed on 192 patients with diseases of the thoracic cavity (esophagus, lungs, mediastinum), operated on in the thoracoabdominal department of the Shalimov National Institute of Surgery and Tranplantology. A retrospective comparison group - 96 patients after thoracic surgery, which used the choice of LDT size according to the well-known Slinger method "according to the patient's height". The study group consisted of 96 patients after thoracic surgery, in which the choice of the size of the bifurcated endobronchial tube was used according to the developed method (according to the formula that evaluates morphometric indicators of height, sex and diameter of the left main bronchus). The application of the proposed method reduces (p = 0.001) the risk of pulmonary complications, HR = 0.39 (95 % CI 0.22-0.70) compared to traditional methods. The risk decreased 2.5 times.

Key words: *morphometric parameters, formula for determining the size of the bifurcated endobronchial tube.*

Introduction

For the purpose of single-lung ventilation, various methods of lung isolation are used in the world, which is a prerequisite for many thoracic, cardiac and esophageal surgeries. Left dual luminal endobronchial tubes (LDT) are most often used in thoracic anesthesia for lung isolation [1]. Numerous studies have reported various methods for determining the optimal suitability between the diameter of the tube and the diameter of the left main bronchus for adequate ventilation and gas exchange during operations on the thoracic cavity [18, 19]. However, there is no consensus among anesthesiologists on the choice of tube size for effective ventilation and lung isolation [2, 3, 16, 20]. Therefore, each thoracic surgery clinic uses different methods to determine the appropriate tube size (according to the patient's height, tracheal diameter and diameter of the left main bronchus) [4, 5, 6, 7]. It is important that these indicators were not studied or compared together. Thus, when using formulas and methods based on individual anthropometric data, many authors (including the authors of this study) are faced with the possibility of incorrect choice of left bilateral luminal endobronchial tube, for example, when tall patients have small bronchial diameters and vice versa [8, 17, 21]. There is still no standardized approach to this issue. We have developed a new mathematical formula for determining the appropriate size of LDT [9].

The aim of the study was to determine the effectiveness of the developed standardized mathematical formula for determining the appropriate size of the left bilateral luminal endobronchial tube for use in thoracic anesthesiology.

Materials and methods

According to the conclusion of the **Committee on**

Bioethics of the State Institution "National Institute of Surgery and Transplantology named after O.O. Shalimov" NAMS of Ukraine Protocol №12 of January 12, 2018, the research methods described in the publication were applied in compliance with human rights in accordance with current legislation in Ukraine, meet international ethical requirements and do not violate ethical norms in science and standards of biomedical research. The study was performed on 192 patients with diseases of the thoracic cavity (esophagus, lungs, mediastinum), operated on in the thoracoabdominal department of the Shalimov National Institute of Surgery and Tranplantology. A retrospective comparison group - 96 patients after thoracic surgery, which used the choice of LDT size according to the well-known Slinger method "according to the patient's height" [2]. The study group consisted of 96 patients after thoracic surgery, in which the choice of the size of the bifurcated endobronchial tube was used according to the developed method (according to the formula that evaluates morphometric indicators of growth, sex and diameter of the left main bronchus (DLMB)).

Inclusion criteria were: a patient assigned to open thoracic or video-assisted thoracoscopic surgery under general anesthesia requiring single pulmonary ventilation (excluding emergency surgery); BMI<35 kg / m^2; age> 18 years; planned lung isolation with LDT;

Exclusion criteria were: grade 3 and 4 chronic obstructive pulmonary disease, pulmonary fibrosis, documented bullae, severe pulmonary emphysema, pneumothorax; uncontrolled asthma; grade 3 and 4 coronary heart disease; previous lung surgery; documented pulmonary arterial hypertension>40 mm Hg (ultrasound assessment); bilateral procedures; isolation of the lungs by a method other than LDT;

Table 1. Demographic profile of patients in the study and control groups. Comparison Me (QI - QIII).

Indicator	Control group, n=96	Research group, n=96	The level of significance of the difference, p
Height	174.5 (168 - 176)	172 (168 - 176)	0.406
Weight	76 (69.5 - 82.5)	76 (70 - 86)	0.312
DLMB	1.295 (1.2 - 1.34)	1.29 (1.2 - 1.34)	0.738
Age	60 (56 - 65)	58 (56 - 64)	0.265
Ppeak	26 (24 - 28)	10 (9 - 11)	<0.001
Pplat	23 (20 - 25)	22 (20 - 24)	0.75
Pmean	12 (10 - 12.5)	19 (17 - 22)	<0.001
Lung_Compliance	22 (21 - 24)	24 (23 - 26.5)	<0.001
CVP	40 (40 - 50)	50 (40 - 50)	0.022
PAo2_Fio2	220 (2 - 230)	240 (230 - 260)	<0.001
PAco2_kPa_	43.5 (40 - 45)	38 (36 - 40)	<0.001
Po2	130 (114 - 140)	140 (132.5 - 150)	<0.001
FEV1. %	78 (76 - 86)	82 (78 - 86.5)	0.061
tOLV	120 (90 - 140)	100 (90 - 120)	0.007
T body	36.1 (35.8 - 36.5)	36 (36 - 36.3)	0.528

Note: The Mann-Whitney test was used in the comparison.

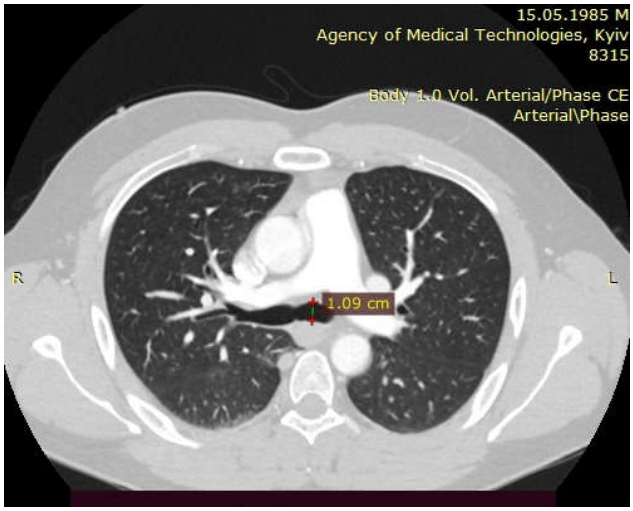

Fig. 1. The diameter of the left main bronchus on the CT image in the axial section.

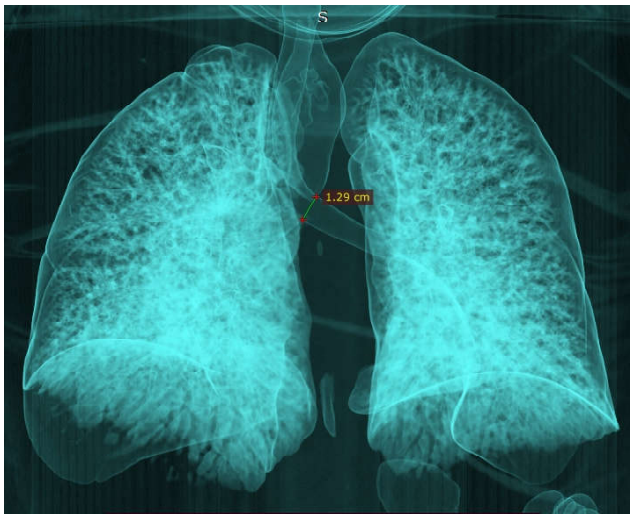

Fig. 2. The diameter of the left main bronchus in the CT image in the 3D model.

Written informed consent was obtained from all patients.

Patients in both groups were comparable in age, sex, ASA scale, weight, height, duration of surgery (Table 1), p>0.05 in all indicators.

The diameter of the left main bronchus was measured by computed tomography (CT) at a distance of 1-2 mm from the bifurcation of the trachea. To do this, it is better to use the construction of a 3D model with the help of computer programs (Horos, Radiant), which allow you to get clearer images of the airways and accurately measure their diameters. Here is a clinical example. Figure 1 shows the measurement of the diameter of the left main bronchus on the image of the CT in the axial section.

In Fig. 2 shows a 3D model of the same patient where

you can see that the size of the left main bronchus is larger than the axial section.

Such differences are noted by many authors [8, 11, 12], who point to the need to measure several sizes of the left main bronchus, or compare the diameters of cricket cartilage, trachea and bronchi to compare these indicators with the choice of endobronchial tube size.

To study the effectiveness of single lung ventilation, we investigated the following parameters: the number of postoperative pulmonary complications, which are reported to be directly correlated with inadequate single lung ventilation.

EZR v.1.54 statistical software was used for statistical calculations (graphical user interface for statistical software R version 4.0.3, R Foundation for Statistical Computing, Vienna, Austria) [10].

Results

According to the distribution by number of the left bilateral luminal endobronchial tube, the patients of the study and control groups did not differ from each other, p = 0.752 (Table 2).

The main indicator of the effectiveness of using the developed standardized mathematical formula to determine the appropriate size of LDT is the number of pulmonary complications after thoracic surgery. In this study, pulmonary complications developed in 33 (34.4 %) patients of the control group and in 13 (13.5 %) patients of the study group, a statistically significant difference was found at p = 0.001 (Fig. 3).

Table 2. Distribution of patients on the left bilateral endobronchial tube.

Indicator		Control group, n=96	Research group, n=96	The level of significance of the difference, p
№ Tube	35	21 (21.9)	21 (21.9)	0.752
	37	18 (18.8)	20 (20.8)	
	39	44 (45.8)	34 (35.4)	
	41	13 (13.5)	21 (21.9)	

Note: Fisher's exact test or chi-square test is used in the comparison.

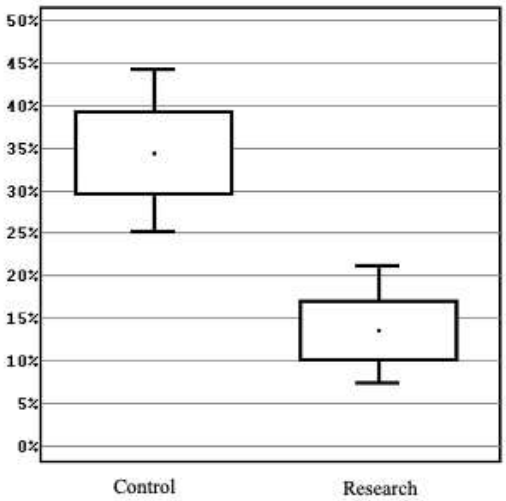

Fig. 3. The number of postoperative pulmonary complications in patients of the study group and control group.

This is evidence of effective perioperative management of patients with thoracic diseases and shows that clear and consistent use of simple, innovative methods of prevention of postoperative pulmonary complications (such as accurate selection of LDT by several morphometric parameters) in thoracic patients significantly reduces these complications.

Thus, the application of the proposed technique reduces (p = 0.001) the risk of pulmonary complications, HR = 0.39 (95 % CI 0.22-0.70) compared to traditional methods. The risk decreased 2.5 times.

Discussion

One of the difficulties most anesthesiologists encounter in performing lung ventilation is choosing the optimal size of the left bilateral luminal endobronchial tube for each patient [22]. At our institute, this selection is usually based on the method recommended by Slinger [2]. It involves calculating the required number based on the average height and sex of patients. However, this recommendation may not be acceptable to all patients, especially those with tall stature and narrow airways. Therefore, we decided to use an assessment methodology that included not only the sex and height of patients, but also integrated LDT as an indicator. This allowed us to more accurately predict the appropriate size for left-sided LDT.

Different research groups have used different methods to select a bilateral endobronchial tube based on individual anthropometric parameters (eg, sex and height, DLMB) [11, 12, 13, 14, 15]. Based on our review of available sources, no studies have compared the full range of these indicators, and there are no standardized formulas for endobronchial tube selection.

A previous study reported that the use of a method based on gender and height gives an accuracy of 58.3 % [11]. However, when the transverse diameter of the annular cartilage was measured by ultrasound and CT, the accuracy of intubation in the groups of ultrasound and CT was 90.2 % and 94.1 %, respectively (p>0.05). Thus, the authors concluded that the measurement of the transverse diameter of the annular cartilage led to much greater accuracy in choosing the size of LDT than traditional methods. In addition, they reported that this method can significantly reduce postoperative complications. Given that there is no significant difference between the accuracy of ultrasound and CT, their results showed that both of these methods for tube selection can be safely used before intubation in thoracic surgery [23].

A prospective study was conducted to test the hypothesis that a previously developed formula based on height (0.25 x 0.916 height) could predict the exact depth of LDT administration in 66 patients who underwent breast

surgery. The formula led to optimal LDT positioning without additional adjustments in 45 patients (70 %) [12].

In our study, we used a new approach to compare the set of indicators (sex, height, DLMB), which allowed us to develop a standardized formula for choosing the size of left-sided LDT. Although we used the sex and height of patients to choose the size of LDT, not taking into account DLMB. The advantages of this method are that it is simple and easy to use. However, it has shortcomings that can significantly worsen the prognosis of the postoperative period. These include: the predicted result by this method is average, and the chosen LDT size is not suitable for all patients due to the large individual variation in airway size in patients with the same growth range. Therefore, the specificity of this method is low, and the positive predictive value is low. Thus, we have developed a formula that includes all three features [9].

In our study, using the method of selection of LDT only by sex and height, its size corresponded to the calculations of the formula, only 81.77 %, while in 18.23 % of patients the size was either overestimated or underestimated. This once again confirmed the discrepancy between gender and height, as well as airway diameters.

Conclusions

Thus, the application of the proposed method of LDT selection reduces (p = 0.001) the risk of pulmonary complications by 2.5 times, BP = 0.39 (95 % CI 0.22-0.70) compared to traditional methods.

References

[1] Arndt, G. A., Kranner, P. W., Rusy, D. A., & Love, R. (1999). Single-lung ventilation in a critically ill patient using a fiberoptically directed wire-guided endobronchial blocker. *Anesthesiology,* 90(5), 1484-1486. https://doi.org/10.1097/00000542-199905000-00037

[2] Bernasconi, F., & Piccioni, F. (2017). One-lung ventilation for thoracic surgery: current perspectives. *Tumori,* 103(6), 495-503. https://doi.org/10.5301/tj.5000638

[3] Campos, J. H. (2002). Current techniques for perioperative lung isolation in adults. *Anesthesiology,* 97(5), 1295-1301. https://doi.org/10.1097/00000542-200211000-000362.

[4] Cohen, E. (2005). The Cohen flexitip endobronchial blocker: an alternative to a double lumen tube. *Anesthesia and Analgesia,* 101(6), 1877-1879. https://doi.org/10.1213/01.ANE.0000184116.86888.D9

[5] Chen, A., Lai, H. Y., Lin, P. C., Chen, T. Y., & Shyr, M. H. (2008). GlideScope-assisted double-lumen endobronchial tube placement in a patient with an unanticipated difficult airway. *Journal of Cardiothoracic and Vascular Anesthesia,* 22(1), 170-172. https://doi.org/10.1053/j.jvca.2007.04.0063

[6] Cheng, Y. J., Chan, K. C., Chien, C. T., Sun, W. Z., & Lin, C. J. (2006). Oxidative stress during 1-lung ventilation. *The Journal of Thoracic and Cardiovascular Surgery,* 132(3), 513-518. https://doi.org/10.1016/j.jtcvs.2006.03.060

[7] Clayton-Smith, A., Bennett, K., Alston, R. P., Adams, G., Brown, G., Hawthorne, T. … Tan, J. (2015). A Comparison of the Efficacy and Adverse Effects of Double-Lumen Endobronchial Tubes and Bronchial Blockers in Thoracic Surgery: A Systematic Review and Meta-analysis of Randomized Controlled Trials. *Journal of Cardiothoracic and Vascular Anesthesia*, 29(4), 955-966. https://doi.org/10.1053/j.jvca.2014.11.017

[8] Culver, B. H. (2001). Preoperative assessment of the thoracic surgery patient: pulmonary function testing. *Seminars in Thoracic and Cardiovascular Surgery,* 13(2), 92-104. https://doi.org/10.1053/stcs.2001.25041

[9] Eldawlatly, A. A., El Tahan, M. R., Kanchi, N. U., Al Qatari, A., & Ahmad, A. E. (2020). Efficacy of height-based formula to predict insertion depth of left-sided double lumen tube: A prospective observational study. *Anaesthesia and Intensive care,* 48(5), 354-357. https://doi.org/10.1177/0310057X209460516

[10] Falzon, D., Alston, R. P., Coley, E., & Montgomery, K. (2017). Lung Isolation for Thoracic Surgery: From Inception to Evidence-Based. *Journal of Cardiothoracic and Vascular Anesthesia,* 31(2), 678-693. https://doi.org/10.1053/j.jvca.2016.05.032

[11] Ideris, S. S., Che Hassan, M. R., Abdul Rahman, M. R., & Ooi, J. S. (2017). Selection of an appropriate left-sided double-lumen tube size for one-lung ventilation among Asians. *Annals of Cardiac Anaesthesia,* 20(1), 28-32. https://doi.org/10.4103/0971-9784.197824

[12] Ishikawa, S., & Lohser, J. (2011). One-lung ventilation and arterial oxygenation. *Current Opinion in Anaesthesiology,* 24(1), 24-31. https://doi.org/10.1097/ACO.0b013e3283415659

[13] Lohser, J., & Slinger, P. (2015). Lung Injury After One-Lung Ventilation: A Review of the Pathophysiologic Mechanisms Affecting the Ventilated and the Collapsed Lung. *Anesthesia and Analgesia*, 121(2), 302-318. https://doi.org/10.1213/ANE.0000000000000808

[14] Narayanaswamy, M., McRae, K., Slinger, P., Dugas, G., Kanellakos, G. W., Roscoe, A., & Lacroix, M. (2009). Choosing a lung isolation device for thoracic surgery: a randomized trial of three bronchial blockers versus double-lumen tubes. *Anesthesia and Analgesia,* 108(4), 1097-1101. https://doi.org/10.1213/ane.0b013e3181999339

[15] Nieman, G. F., Satalin, J., Andrews, P., Aiash, H., Habashi, N. M., & Gatto, L. A. (2017). Personalizing mechanical ventilation according to physiologic parameters to stabilize alveoli and minimize ventilator induced lung injury (VILI). *Intensive Care Medicine Experimental,* 5(1), 8. https://doi.org/10.1186/s40635-017-0121-x

[16] Kanda, Y. (2013). Investigation of the freely available easy-to-use software 'EZR' for medical statistics. *Bone Marrow Transplantation,* 48(3), 452-458. https://doi.org/10.1038/bmt.2012.244

[17] Seo, J. H., Cho, C. W., Hong, D. M., Jeon, Y., & Bahk, J. H. (2016). The effects of thermal softening of double-lumen endobronchial tubes on postoperative sore throat, hoarseness and vocal cord injuries: a prospective double-blind randomized trial. *British Journal of Anaesthesia,* 116(2), 282-288. https://doi.org/10.1093/bja/aev414

[18] Silva, P. L., Moraes, L., Santos, R. S., Samary, C., Ornellas, D. S., Maron-Gutierrez, T. … Pelosi P (2011). Impact of pressure profile and duration of recruitment maneuvers on morphofunctional and biochemical variables in experimental lung injury. *Critical Care Medicine,* 39(5), 1074-1081. https://doi.org/10.1097/CCM.0b013e318206d69a

[19] Sinclair, S. E., Kregenow, D. A., Lamm, W. J., Starr, I. R., Chi, E. Y., & Hlastala, M. P. (2002). Hypercapnic acidosis is protective in an in vivo model of ventilator-induced lung injury. American *Journal of Respiratory and Critical Care Medicine,* 166(3), 403-408. https://doi.org/10.1164/rccm.200112-117OC

[20] Slinger, P. (2003). A view of and through double-lumen tubes. *Journal of Cardiothoracic and Vascular Anesthesia*, 17(3), 287-288. https://doi.org/10.1016/s1053-0770(03)00058-2

[21] Slinger, P. (2001). Lung isolation in thoracic anesthesia, state of the art. *Canadian Journal of Anaesthesia = Journal Canadien d'Anesthesie*, 48(1), R13-R15. https://doi.org/10.1007/BF03028172

[22] Sydiuk, A., & Sydiuk, O. (2021).New formula for selection of an appropriate left-sided double-lumen tube size in thoracic anaesthesiology. *Perioperative Care and Operating Room Management,* 25, 100219. https://doi.org/10.1016/j.pcorm.2021.100219

[23] Zhang, C., Qin, X., Zhou, W., He, S., Liu, A., Zhang, Y., Dai, Z., & Yin, J. (2021). Prediction of Left Double-Lumen Tube Size by Measurement of Cricoid Cartilage Transverse Diameter by Ultrasound and CT Multi-Planar Reconstruction. *Frontiers in Medicine,* 8, 657-612. https://doi.org/10.3389/fmed.2021.657612

МОРФОМЕТРИЧНІ ПОКАЗНИКИ ДЛЯ ВИБОРУ ДВОПРОСВІТНОЇ ЕНДОБРОНХІАЛЬНОЇ ТРУБКИ В ТОРАКАЛЬНІЙ АНЕСТЕЗІОЛОГІЇ

Усенко О. Ю., Сидюк А. В., Сидюк О. Є., Клімас А. С., Савенко Г. Ю., Тесля О. Т.

З метою однолегеневої вентиляції в світі використовують різноманітні методи ізоляції легень, яка є передумовою для багатьох грудних, серцевих та стравохідних хірургічних втручань. Численні дослідження повідомляють про різні методи визначення оптимальної придатності між діаметром трубки та діаметром лівого головного бронха для адекватної вентиляції та газообміну під час операцій на грудній порожнині. Однак серед анестезіологів немає єдиної думки щодо вибору розміру трубки для ефективної вентиляції та ізоляції легень. Нами була розроблена нова математична формула для визначення відповідного розміру лівосторонньої двопросвітної ендобронхіальної трубки (ЛДТ). Метою дослідження стало визначити ефективність розробленої стандартизованої математичної формули для визначення відповідного розміру ЛДТ для використання в торакальній анестезіології. Дослідження виконано на 192 хворих із захворюваннями грудної порожнини (стравоходу, легень, середостіння), оперованих в торакоабдомінальному відділі Національного інституту хірургії та трансплантології ім. О.О.Шалімова. Ретроспективну групу порівняння становили 96 пацієнтів після торакальних операцій, у котрих використаний вибір розміру ЛДТ за загальновідомою методикою Slinger "за зростом хворого". Групу дослідження становили 96 пацієнтів після торакальних операцій, для котрих був використаний вибір розміру двопросвітної ендобронхіальної трубки за розробленою методикою (за формулою, завдяки якій можна оцінити морфометричні показники зросту, статі та діаметра лівого головного бронха). Застосування запропонованої методики дозволяє знизити (p = 0,001) ризик розвитку легеневих ускладнень, ВР = 0,39 (95 % ВІ 0,22-0,70). У порівнянні з традиційною методикою: ризик знизився у 2,5 рази.

Ключові слова: *морфометричні показники, формула визначення розміру двопросвітної ендобронхіальної трубки.*

REQUIREMENTS FOR ARTICLES

For publication, scientific articles are accepted only in English only with translation on Ukrainian, which contain the following necessary elements: UDC code; title of the article (in English and Ukrainian); surname, name and patronymic of the authors (in English and Ukrainian); the official name of the organization (institution) (in English and Ukrainian); city, country (in English and Ukrainian); structured annotations (in English and Ukrainian); keywords (in English and Ukrainian); introduction; purpose; materials and methods of research; research results; discussion; conclusions; bibliographic references.

The title of the article briefly reflects its contents and contains no more than 15 words.

Abstract. The volume of the annotation is 1800-2500 characters without spaces. The text of an annotation in one paragraph should not contain general phrases, display the main content of the article and be structured. The abstract should contain an introductory sentence reflecting the relevance of the study, the purpose of the study, a brief description of the methods of conducting research (2-3 sentences with the mandatory provision of the applied statistical methods), a description of the main results (50-70% of the volume of the abstract) and a concise conclusion (1 sentence). The abstract should be clear without familiarizing the main content of the article. Use the following expressions: "Detected ...", "Installed ...", "Fixed ...", "Impact assessed ...", "Characterized by regularities ...", etc. In an annotation, use an active rather than passive state.

Keywords: 4-6 words (or phrases).

"Introduction"

The introduction reflects the state of research and the relevance of the problem according to the world scientific literature (at least 15 references to English articles in international journals over the past 5 years). At the end of the entry, the purpose of the article is formulated (contains no more than 2-3 sentences, in which the problem or hypothesis is addressed, which is solved by the author).

"Materials and methods"

The section should allow other researchers to perform similar studies and check the results obtained by the author. If necessary, this section may be divided into subdivisions. Depending on the research objects, the ethical principles of the European Convention for the protection of vertebrate animals must be observed; Helsinki Declaration; informed consent of the surveyed, etc. (for more details, see "Public Ethics and its Conflict"). At the end of this section, a "statistical processing of results" section is required, which specifies the program and methods for processing the results obtained by the automobile.

"Results"

Requirements for writing this section are general, as well as for all international scientific publications. The data is presented clearly, in the form of short descriptions, and must be illustrated by color graphics (no more than 4) or drawings (no more than 8) and tables (no more than 4), the information is not duplicated.

"Discussion"

In the discussion, it is necessary to summarize and analyze the results, as possible, compare them with the data of other researchers. It is necessary to highlight the novelty and possible theoretical or practical significance of the results of the research. You should not repeat the information already listed in the "Introduction" section. At the end of the discussion, a separate paragraph should reflect the prospects for using the results obtained by the author.

"Conclusion"

5-10 sentences that summarize the work done (in the form of paragraphs or solid text).

"Acknowlegements"

Submitted after conclusion before bibliographic references.

"References"

References in the text are indicated by Arabic numerals in square brackets according to the numerology in the list of references. The list of references (made without abbreviations) sorted by alphabet, in accordance with the requirements of APA Style (American Psychological Association Style): with the obligatory referencing of all authors, work titles, journal names, or books (with obligatory publication by the publishing house, and editors when they are available), therefore, numbers or releases and pages. In the Cyrillic alphabets references, give the author's surnames and initials in English (Cyrillic alphabet in brackets), the title of the article or book, and the name of the magazine or the publisher first to be submitted in the original language of the article, and then in square brackets in English. If available, doi indexes must be provided on www.crossref.org (at least 80% of the bibliographic references must have their own doi indexes). Links to online publications, abstracts and dissertations are not welcome.

After the list of references, it is necessary to provide information about all authors (in English, Ukrainian and Russian): last name, first name and patronymic of the author, degree, place of work and position, **ORCID number** (each of the authors of the ORCID personal number if absence - free creation on the official website http://www.orcid.org) to facilitate the readers of this article to refer to your publications in other scientific publications.

The last page of the text should include the surname, name and patronymic of the author, degree, postal address, telephone number and e-mail of the author, with which the editors will maintain contact.

Concluding remarks

The manuscript should be executed in such a way that the number of refinements and revisions during the editorial of the article was minimal.

When submitting the article, please observe the following requirements. The volume of the article - not less than 15 and not more than 25 pages, Times New Roman, 14 pt, line spacing - one and a half, fields - 2 cm, sheet A4. Text materials should be prepared in the MS Word editor (* .docx), without indentations. Math formulas and equations to prepare in the embedded editor; graphics - in MS Excel. Use the units of the International Measurement System. Tables and drawings must contain the name, be numbered, and references to them in the text should be presented as follows: (fig. 1), or (table 1). The drawings should be in the format "jpg" or "tif"; when scanned, the resolution should be at least 800 dpi; when scanning half-tone and color images, the resolution should be at least 300 dpi. All figures must be represented in the CMYK palette. The statistical and other details are given below the table in the notes. Table materials and drawings place at the end of the text of the manuscript. All elements of the text in images (charts, diagrams, diagrams) must have the Times New Roman headset.

Articles are sent to the editorial board only in electronic form (one file) at the e-mail address nila@vnmu.edu.ua

Responsible editor - Gunas Igor Valeryovich (phone number: + 38-067-121-00-05; e-mail: igor.v.gunas@gmail.com).

Signed for print 22.02.2022
Format 60x84/8. Printing offset. Order № 0634. Circulation 100.
Vinnytsia. Printing house “TVORY”, Nemyrivske shose St., 62a,
Vinnytsya, 21034
Phone: 0 (800) 33-00-90, (096) 97-30-934, (093) 89-13-852,
(098) 46-98-043
e-mail: tvory2009@gmail.com
http://www.tvoru.com.ua